

UNIVERSITY OF TURIN



*Doctoral School in Life and Health Sciences*

*Department of Clinical and Biological Sciences*

*29<sup>TH</sup> PHD PROGRAM IN EXPERIMENTAL MEDICIN AND THERAPY*

**Analysis of human renal angiomyolipoma  
cells: pharmacological modulation of growth  
and migration in vitro**

*Dott.ssa Francesca Bertolini*

Tutor: Prof.ssa Silvia Anna Racca

Co-tutor: Dott.ssa Barbara Mognetti

PhD Coordinator: Prof. Giuseppe Saglio

Academic Years: 2014-2018  
Scientific Field: Bio/14-Pharmacology



## ABSTRACT

**Introduction:** Renal angiomyolipomas (AMLs) are highly vascular masses variously composed by differentiated cells such as smooth muscle, adipose, and vascular endothelial cells. Pulmonary lymphangiomyomatosis (LAM) is an age and gender disease, which hits at first young women, characterized by smooth muscle infiltration of the lung alveolar walls, leading to cystic degeneration. While both can occur clinically as isolated conditions, AML and LAM are also common manifestations of tuberous sclerosis complex (TSC), an autosomal dominant disorder characterized by hamartomas involving the central nervous system, skin, liver, heart, and eyes. Individuals diagnosed with TSC develop AMLs by adulthood in 70–90% of cases, whereas LAM can occur in up to 30-40% of affected women. TSC arises from inactivating mutations of either TSC1 (chromosome locus 9q34.3) or TSC2 (16p13.3) genes that encode for hamartin and tuberin, respectively. These proteins regulate cell proliferation and differentiation, and are involved in the mTOR (mammalian target of rapamycin) signaling pathway. Mutations in TSC2 often result in more severe clinical profiles, including higher frequency and severity of renal angiomyolipomas. No pharmacological treatment for AMLs is available and the most common approach is still the surgical ablation in the case of symptomatic disease or for lesions greater than 4 cm. Although the molecular events responsible for AML development are not fully understood, mTOR inhibitor therapy with sirolimus and everolimus may delay the growth and progression of AML in patients with TSC. Trials with sirolimus suggest its efficacy in slowing the evolution of the pulmonary disease. In cases of severe functional respiratory or rapid evolution of the disease, the treatment of election is the pulmonary transplantation.

TSC-associated and sporadic AMLs and LAM are more common in female patients. Thus, some Authors have suggested a key role for the estrogen in their development. Nevertheless, it has not been fully clarified yet whether and how hormonal modulation is involved in the different occurrence in male and female patients.

The smooth muscle cells of patients affected by both AML and LAM are characterized by structural cytologic analogy and the same somatic mutations; furthermore, AML cells have been detected in donor lungs of patients who had lung transplantation. These observations support the hypothesis that LAM might occur because of the migration of cells from other sites, such as the kidney, lymphatic system, or uterus. Therefore a common cell progenitor originating in the kidney and a metastatic behavior have been suggested. Despite several publications describing AML and LAM, a very few is known about their triggering agents and an eventual correlation between the two pathologies. To date, only a small number of hypotheses have been formulated regarding a link between them, but no proof exists either for or against. In our opinion, the demonstration of a direct link between AML and LAM might be of paramount importance in foreseeing and preventing their evolution, especially in fertile-age women. It must be considered that AML and LAM have, at now, a very dramatic evolution and no definitive cure has been established yet.

The overall objectives of this study are: 1) to ascertain the migratory proprieties of AML cells, 2) to identify common characteristics that might bind AML and LAM, and 3) to define innovative potential pharmacological approaches able to interfere with proliferation and migration of AML cells.

**Material and Methods:** The study has been performed on two different models: 1) *ex vivo* experiments on cells isolated from AML, and 2) *in vitro* experiments on three stabilized AML cell lines. Human primary AMLs cells were isolated from two spontaneous angiomyolipomas, surgically excised from a male (AML3) and a female (AML4) patient, which had neither clinical signs and symptoms nor a family history of tuberous sclerosis. On the other hand, two of the stabilized cell lines were TSC mutated: 4004 male cells carry a mutation in the exon 33 of TSC2 gene (4083-4087 del AGTCG) and 621-101 female cells have biallelic mutations in the exon 16 of TSC2 gene (G1832A). The third cell line (621-103) derives from the 621-101 cell line by restoration of the TSC2 gene.

We tested, *in vitro*, different concentrations and exposure times of drugs employed for the treatment of LAM and AML patients (sirolimus and everolimus) as well as of alternative selected drugs

(simvastatin, zoledronic acid, estradiol, and tamoxifen) to evaluate whether they can modulate AML cells proliferation.

By means of 2D and 3D migration assays, we assessed if AML cells can migrate and if hormonal stimuli and drugs can modulate this property. Moreover, we evaluated the production of metalloproteases principally involved in malignant phenotype acquisition (MMP-2 and MMP-9) by zymography. Finally, by quantitative RT-PCR, we studied the expression of some genes crucial for the progression of these diseases.

**Results:** In the first part of the study, we isolated and grew cells from primary human spontaneous angiomyolipomas derived from male and female patients. To better understand which type of cells we isolated from fresh masses, we characterized the cellular composition of our cultures by means of immunofluorescence staining against HMB45, Melan-A, S-100,  $\alpha$ -Smooth-Muscle Actin, keratin 8/18 and vimentin. The different cellular positivity to the antibodies confirmed the heterogeneous nature of both AMLs.

Subsequently, we examined the expression of estrogen receptor genes; the analysis demonstrated that both primary cell cultures express significantly level of mRNA for GPR30 and ER $\alpha$ , but not for ER $\beta$ . Moreover, no significant differences in ER gene expressions have been detected between the male and female AMLs.

We evaluated if the treatments with 17- $\beta$ -estradiol, tamoxifen or the combination of both modulated the proliferation and migration of cells. Concentrations comprised between 0.1 and 100 nM of 17- $\beta$ -estradiol or between 0.2 and 20  $\mu$ M of tamoxifen did not modify cell proliferation. Through the analyses of 2D and 3D migration assays, we observed a different cell behavior. Treatment with estradiol (1 nM) for 2 hours induced a significant increase in 2D motility for both primary cell cultures; in 3D migration assay, only the female cells significantly responded to estrogen after 4 hours. Tamoxifen (2  $\mu$ M) had no influence on cell motility, but it was able to erase the effects of estradiol. Moreover, we performed a western blot analysis of Erk1/2 phosphorylation, demonstrating that estradiol incubation activates Erk1/2 pathways.

Finally, we evaluated if the migration of our cells was modulated by SDF-1 $\alpha$ , a chemokine associated with invasion and homing to specific organs. Both cells expressed, in basal condition, similar levels of mRNA for CXCR4, the receptor for SDF-1 $\alpha$ . The addition of SDF-1 $\alpha$  (100 ng/mL) to the culture medium stimulated the migration of both primary cells already after 4 hours of incubation; the stimulation was coherently abolished by the SDF-1 $\alpha$  -receptor antagonist plerixafor (100 nM). At last, we analyzed by zymography the activities of MMP2 and MMP9 on the supernatant collected after 3D migration assay; in both cells treatment with SDF-1 $\alpha$  significantly increased MMP-9 activity in both primary cultures.

Considering the limited number of primary AML cells available, we strengthened our results by studying the stabilized AML cell lines.

In these cells, we evaluated the expression level of specific genes involved in proliferation and migration in either basal condition or under specific drugs treatment. In basal condition, we observed significant expression level of antiapoptotic factors, enzymes involved in the metastatic process, and elements involved in dedifferentiation processes in all cell lines.

At the same concentrations and time tested for primary cells, the treatment with 17- $\beta$ -estradiol did not induce any significant modification on cell proliferation. Unexpectedly, the proliferation of cell lines was inhibited by 10  $\mu$ M tamoxifen already after 24 hours. In three-dimensional migration assay, incubation with estradiol, tamoxifen or both did not modify the migration ratio for male 4004 cells. On the other hand, 1 nM 17- $\beta$ -estradiol significantly increased the rate of female 621-101 and 621-103 cells migration; 2  $\mu$ M tamoxifen increased the migration of these cells also, even if less than compared with 17- $\beta$ -estradiol ( $P < 0.05$ ). The different behavior of male and female cells was also confirmed, after 4 hours of incubation with the same concentration of 17- $\beta$ -estradiol, by the increments in the expression level of several genes (such as MMPs, cMET, VEGF, FN1, and IGFR1) involved in motility and cellular adhesion.

Treatment with everolimus (1-100 nM), zoledronic acid, and simvastatin (1-100  $\mu$ M) had a direct toxic effect on AML cells, though at different concentrations and incubation time. Moreover, we

tested these drugs in association or alone in a 3D migration assay. For all cell lines, the combination of everolimus and zoledronic acid strongly inhibited the migration at low concentration. We also observed a decrease of migratory capacity induced by 10  $\mu$ M simvastatin, that inhibits cell migration already after 4 hours ( $P < 0.05$ ).

**Conclusion:** Our results suggest that significant differences between the analyzed AMLs are present for what concerns the response to the tested molecules. Both primary and stabilized cells have basic migratory properties. The migration of primary cells is likely modulated by agonists such as SDF-1 $\alpha$  and 17- $\beta$ -estradiol, as confirmed by the quenching effect of their blockers. Primary cells increase their migration under estrogen influences independently from their gender. This confirms the hypothesis of a potential involvement in propagation and colonization to lung or other organs. In stabilized cells, the female ones are more responsive to estrogenic stimulation in terms of three-dimensional and genetic modulation than the male cells. Drugs such as zoledronic acid and everolimus (alone or in association), can significantly inhibit the growth and migration of the stabilized cells. The AML cells present, in basal condition, expression patterns attributable to invasive behavior, modulation of apoptosis, modification of the microenvironment, and angiogenesis. This feature supports the plasticity and abnormal cell proliferation typical of AML disease. Furthermore, the selected drugs analyzed do not induce a statistically significant modification of the level expression genes so far analyzed. In conclusion, these results represent a starting point for the development of valid pharmacological therapies for AML pathology.

# TABLE OF CONTENTS

1. Introduction	1
1.1 Renal Angiomyolipoma	2
1.2 The “Benign Metastasis” hypothesis	4
1.3 Lymphangioliomyomatosis	6
1.4 Tuberous sclerosis	7
1.5 mTOR pathway	8
1.5.1 The PI3K/Akt and MAPK pathways	9
1.6 mTOR inhibitor: Everolimus	10
1.7 The role of estrogen in AML	11
1.8 Other approaches in AML treatment	13
1.8.1 Zoledronic acid	14
1.8.2 Simvastatin	15
2 Aim of the study	16
3 Material and methods	18
3.1 Angiomyolipoma cells, tissue and ethical approvals	19
3.2 Stabilized cell culture	19
3.3 Immunofluorescence	20
3.4 Proliferation assay	20
3.5 Two-dimensional migration assay-wound healing	21
3.6 Three dimensional migration assay	21
3.7 Western blot	23
3.8 Gelatin zymography	24
3.9 Quantitative real-time PCR (qRT-PCR)	25
3.10 Statistical analysis	26



4	Results	27
4.1	Immunohistochemistry to confirm the AML diagnoses	28
4.2	Cells characterization by immunofluorence	28
4.3	Estrogen and SDF-1 $\alpha$ receptor gene expression	29
4.4	Influence of estrogen on cell proliferation	30
4.5	Influence of estrogen on two- dimensional migration (wound healing)	31
4.6	Influence of estrogen on three-dimensional migration	32
4.7	ERK phosphorylation	33
4.8	Influence of SDF-1 $\alpha$ on two and three-dimensional migration	34
4.9	Metalloproteases activity in supernatant derived from 3D-migration test	35
4.10	Estrogen receptor expression	36
4.11	Influence of 17- $\beta$ -estradiol, tamoxifen and combination of both on cell proliferation	37
4.12	Influence of 17- $\beta$ -estradiol and tamoxifen on three-dimensional migration	38
4.13	ERK and AKT phosphorylation	39
4.14	Effect of 17- $\beta$ -estradiol and tamoxifen on adhesion/invasiveness gene expression	41
4.15	Influence of simvastatin, zoledronic acid and everolimus on cell proliferation	43
4.16	Three dimensional migration assay in presence of zoledronic acid, everolimus and Simvastatin	45
4.17	ERK and AKT phosphorylation	47
4.18	Effect of zoledronic acid, everolimus and simvastatin on adhesion/invasiveness gene expression	48
5	Discussion	52
6	Bibliography	60
7	Publications	74

Appendix

# **1. Introduction**

## **1.1 Renal angiomyolipoma**

Renal angiomyolipoma (AML) is a mesenchymal highly vascular mass composed by three different elements present in variable proportion: smooth muscle, fat, and thick-walled blood vessels [1].

Angiomyolipoma, together with lymphangiomyomatosis (LAM) and other clear cell tumor of different sites, belongs to a family of neoplasms characterized by the presence of perivascular epithelioid cell (PEC) and therefore named PEComas [2].

The perivascular epithelioid cell have morphologic, immunohistochemical, ultrastructural and genetic distinctive features such as an epithelioid appearance [3]. Different reports indicate that these cells are immunoreactive for melanocytic, such as HMB-45 and melan-A, and smooth muscle, such as actin, markers [2,4,5].

PEComas of the kidney include different type of angiomyolipoma: classic, cystic, epithelioid, oncocytoma-like AML and lymphangiomyomatosis of the renal sinus [2].

In general AML is a benign mass and represents the 2-6.4% of the renal tumors [6,7].

Renal AMLs can occur sporadically (80-90% of cases) or as part of tuberous sclerosis (TSC), an autosomal dominant syndrome characterized by hamartomas; and less commonly, can occur in association with sporadic lymphangiomyomatosis (LAM) [8,9].

Two main types of renal AML are recognized: the sporadic type, usually a unilateral and solitary neoplasm typically seen in middle-aged women, and the multifocal neoplasms, usually small and bilateral, diagnosed in patients with TSC [1]. The sporadic AMLs are asymptomatic and are incidentally discovered during radiographic procedures; in contrast, TSC-associated AML lesions are often symptomatic at presentation and have frequent involvement of both kidneys [10].

TSC-associated and sporadic AMLs are more common and occur at an earlier age than in male in female patients than male (ratio of 2:1) [11].

The most common approach for remove AMLs at present is still the surgical ablation in the case of symptomatic disease or for lesions greater than 4 cm. Although the molecular events responsible for

AML development are not fully understood, mTOR inhibitor therapy with sirolimus and everolimus may delay the growth and progression of AML in patients with TSC. Everolimus has been approved by the Food and Drug Administration (FDA) for the treatment of TSC-associated angiomyolipoma in adult patients [12,13].

The heterogeneity of renal angiomyolipoma cells make it difficult their isolation, identification and phenotype characterization [14]. In the past, several studies have been conducted to analyze AML and LAM behavior an in vivo murine model (Eker rat with TSC2 germline mutation occurring in one of its alleles) or in vitro on ELT3 cell line derived from uterine leiomyomas [15,16,17]. To better understand the nature and characteristics of AML cells different authors tried to isolate cells from human angiomyolipoma masses to create in vitro and in vivo models to study human AML pathogenesis.

In 2004 (Yu et al.) and in the 2005 (Lesma et al.) two human cell lines were successfully isolated from tissue obtained from patients with TSC associated angiomyolipoma [18,19]. These cells were positive for melanocytic and smooth muscle markers and the smooth muscle cells revealed TSC2 LOH and a lack of tuberin expression.

In 2009, Clements and colleagues isolated two cell line populations derived from angiomyolipoma: spindle-shaped cells and epithelioid-like cells. The cultured cells showed constitutive activation of S6K1 protein and strong expression of  $\alpha$ SMA, mRNA of gp100, and MART-1 [20].

These in vitro researches highlights the fact that the phenotype of AML cells depends on their microenvironment, exposure to cytokines, growth factors and interactions with other cells

Moreover, these studies allowed uncovering new molecules involved in processes of proliferation, vascularization, angiogenesis and differentiation such as VEGF, EGF, IGF-1, TGFB1 and TGFB1 that can become a new therapeutic targets for the AML cells [14].

## 1.2 The “Benign Metastasis” hypothesis

Although the histological characteristics of AML cells are benign, a hypothesis was formulated in which smooth muscle cells with mutations in TSC1 or TSC2 gene could travel to the lungs from renal angiomyolipomas [21,22].

Identical somatic mutations of TSC2 have been described in abnormal lung and kidney cells, but not in healthy cells, in the 60% of women with sporadic LAM and renal AML [23].

Spread of angiomyolipoma smooth muscle cells to the lungs could explain the occasional recurrences of LAM in the donor lung after lung transplantation [23].

This hypothesis is supported by the finding that TSC2-deficient smooth muscle cells have higher migration potential than normal cells in vitro, and different patients with tuberous-sclerosis-associated pulmonary lymphangiomyomatosis have large, potentially metastatogenic renal angiomyolipomas [22,24]. The genetic analyses reveal that the metastatic mechanism was related to the presence of mutations in TSC1 or TSC2 gene [25].

The molecular mechanisms underlying the presumed metastatic properties of AML have not still clarified, but the identification, reported in several studies in the literature [26,27,28], of molecules involved in migration, invasion, proliferation and angiogenesis in the cells and tissues of LAM and AML patients supports this unusual disease mechanism.

A recent in vivo and in vitro study discovered that PPAR $\gamma$  (peroxisome proliferator-activated receptor gamma) plays a central role in the initiation and propagation of sporadic and TSC-related AML cells [28]. The microarray gene expression analysis revealed strong activation of PPAR $\gamma$  in an AML xenograft model, generated by an injection of  $10^6$  UMB cells (cells derived by TSC-related AML) into NOD/SCID mice and in primary human AML cells. Consequently, Pleniceanu et al., show that the inhibition of this molecule, induced by one of its antagonists (GW9662), significantly and specifically halts the in vitro growth of cells and strongly limited their tumor-initiation capacity in the in vivo model.

Another *in vivo* study, conducted on a murine model of TSC, analyzed the mTOR and YAP (Hippo–Yes-associated protein 1) pathways that is involved in tumorigenesis. YAP is up-regulated by mTOR in mouse and human PEComas and its inhibition blunts abnormal proliferation and induces apoptosis of TSC1-2 deficient cells both *in vivo* (PEComas of mosaic Tsc1 mutant mice) and *in vitro* models (HEK293 and MEFs, mouse embryonic fibroblasts, cell lines) [29].

Fibronectin is involved in cell adhesion, cell motility, host defense and metastasis [26]. Evans and colleagues suggested that the aberrant proliferation of LAM cells might be associated with overexpression of fibronectin [30], a glycoprotein present in a soluble and dimeric form in the plasma, and a dimeric or multimeric form on the cell surface and in extracellular matrix (ECM). Altered fibronectin levels have been demonstrated in various diseases such as interstitial lung diseases as well as LAM. Concordant with these findings, they proposed that the deposition of fibronectin might result in tissue remodeling and perhaps fibronectin might be involved in LAM pathogenesis [30]. Other factors that are involved in the metastatic and tumor mechanisms are the matrix metalloproteinases (MMPs).

Physiologically matrix metalloproteinases are a group of enzymes able to degrade components of the ECM; they are secreted as inactive proenzymes which become active when cleaved [31]. MMPs play a major role in cell proliferation, migration (adhesion/dispersion), differentiation, angiogenesis, apoptosis, and host defense [32]. The gelatinases, MMP-2 and MMP-9 can degrade native type IV collagen, denatured type I collagen (gelatin) and elastic fibers [33].

Immunohistochemical studies have found that MMP-2 and MMP-9 are predominantly expressed, in comparison to other MMPs, in LAM cells, suggesting their involvement in the destructive cystic formation and in the pathogenesis of LAM [33,34,35].

MMP-2 is a zinc-dependent enzyme capable of remodeling the vasculature, involved in angiogenesis, tissue repair, tumor invasion and inflammation. MMP-2 is predominantly expressed by mesenchymal cells, smooth muscle cells and fibroblasts [33]. An increased level of MMP-2 was found in AML cells derived from a LAM patient and in serum of patients with pulmonary LAM [31,32,35].

MMP-9 gene encodes for the enzyme matrix metalloproteinase 9; it is significantly up-regulated in many human diseases (arthritis, diabetes and cancer), and this aberrant activity is thought to contribute to pathological processes such as tissue remodeling, invasion and cell migration [36]. The levels of metalloproteinase 9 in circulating blood are elevated in various pathological states such as asthma, pulmonary emphysema, lung cancer and ischemic heart disease [33].

Cell metastasis to specific organs may depend on cytokines and from the interaction between soluble factors produced by the microenvironment with metastatic cell receptors. In this regard, it has been hypothesized that ligands and receptors of the chemokines can participate in the migration of AML cells to other organs [37]. Stromal cell-derived factor-1 $\alpha$  (SDF-1 $\alpha$  or CXCL12) and its unique receptor CXC chemokine receptor-4 (CXCR4) have prominent roles in invasion and metastasis of a diverse number of cancers [37,38,39,40].

The interaction between SDF-1 $\alpha$  and CXCR4 has been shown to guide tumor cells to organ sites with high levels of SDF-1 $\alpha$  expression, which suggests a key role in chemotaxis and homing of metastatic cells [27]. Therefore, the CXCL12-CXCR4 axis is essential for the regulation of cell migration [37].

### **1.3 Lymphangiomyomatosis**

Another disease associated with TSC is lymphangiomyomatosis (LAM), which can, nevertheless, occur also in a sporadic form [41].

LAM is an age and gender related disease primarily affecting young women and which, in the TSC form, develops with different degrees of severity and disability [42]. It is characterized, histologically, by smooth muscle infiltration of the lung alveolar walls, leading to cystic degeneration.

Lung function abnormalities consist of decreased expiratory flow expressed as a decreased lung diffusion capacity, leading to a reduction in breathing capacity and hypoxemia during exercise or at rest [43]. LAM presents with dyspnea, recurrent pneumothoraxes, pleural effusions, ascites, and extrapulmonary features that include bleeding renal angiomyolipomas and lymphangiomyomas [8].

In some cases, lung disease progresses slowly; in others, typically in younger women, LAM tends to run a more rapid evolution. In both cases, it occurs a decline in lung function leading to respiratory failure. In cases of severe functional respiratory or rapid evolution of the disease, the treatment of election is the pulmonary transplantation [44].

The median transplant free survival time is of approximately 29 years from the onset of symptoms. There are no efficacious drugs for the treatment of LAM; based on current evidence, it is recommended that LAM patients in whom lung function is declining rapidly or having symptomatic lymphangioliomyomas, pleural effusions or ascites are treated with sirolimus or everolimus [45, 46]. Trials with sirolimus suggest its efficacy in slowing the evolution of the pulmonary disease [45].

## **1.4 Tuberos sclerosis**

TSC is a rare autosomal dominant multisystem disorder that can cause circumscribed, benign, non-invasive lesions in multiple organs including brain, skin, liver, lung, kidney, heart and eyes [47]. The birth incidence of TSC is estimated to be approximately 1 in 6,000 to 1 in 11,000 [48,49,50]. Renal lesions, collectively occurring in 50–80% of patients with TSC, include angiomyolipomas, renal cysts, renal cell carcinoma, and oncocytomas [50].

TSC arises from inactivating heterozygous or mosaic mutations in either TSC1 (~21%) or TSC2 (~79%) with subsequent deregulation of the Rheb/mTOR/p70S6K pathway. The TSC1 gene is located on chromosome 9q34, and consists of 21 exons encoding the 1164 amino acid protein hamartin. The TSC2 gene on chromosome 16p13 contains 41 exons and encodes the 1807 amino acid protein tuberin [14]. Hamartin and tuberin are likely tumor suppressors regulating cellular proliferation [51,52].

There are different types of gene mutations in TSC1 and TSC2 genes, with an equal distribution in family cases while in the sporadic cases mutation occur more frequently in the TSC2 gene [51]. Mutations in TSC1 are often small insertion or deletions that result in truncated protein and patients



with these mutations have generally a mild clinical phenotype [51]; whereas TSC2 mutations include large deletions, nonsense, and missense mutations [53]. These mutations in these genes are believed to prevent the formation of the complex between TSC1 and TSC2, culminating in loss of inhibition of the mTOR pathway [53]. Mutations in TSC2 gene often result in more severe clinical profiles, including higher frequency and severity of renal angiomyolipomas.

The different nature of hamartomas observed in patients with TSC suggests that these cancers develop according to "second hit" theory (Knudson, 1971). In hereditary cases, a first genetic alteration ("first hit") is inherited in the germ line by a parent affection, while the second mutation occurs in a cell that already has the first mutation. The second mutation can cause the complete inactivation of either of the two genes of TSC1 or TSC2 and, of consequence, loss of heterozygosity (LOH) [22].

LOH in the TSC1 or TSC2 region occurs in most angiomyolipomas, rhabdomyomas, and astrocytomas from TSC patients. TSC2 LOH in renal lesions occurs in 10% of sporadic angiomyolipomas and in 60% of TSC-associated angiomyolipomas [25, 54].

## **1.5 mTOR pathway**

The TSC1/TSC2 complex is the principal cellular regulator of mTOR (mammalian target of rapamycin), a serine/threonine protein kinase in the PI3K-related kinase family that controls different important biological processes such as cellular growth, proliferation, transduction, transcription, autophagy and metabolism [55]. A few of the metabolically active tissues in which mTOR plays an important role include the heart, pancreas [56] and kidney [57].

mTOR is a component of two functional complexes: TORC1 and TORC2; TORC1 is the rapamycin-sensitive mTOR complex responsible for the regulation of protein translation initiation and efficiency, and is activated by the presence of growth factors, amino acids and energy status [58]. TORC2 responds to growth factors and is not directly inhibited by rapamycin and induces cell cycle exit and differentiation [58].

The role of the proteins encoded by TSC1 and TSC2 (hamartin and tuberin respectively) in this pathway is to form a heterodimer that activates a GTPase enzyme called Rho, which by reducing Rheb activity, indirectly inhibits mTOR. The production of tuberin and hamartin is also physiologically regulated by different factors such as PI3K (phosphoinositide 3-kinase) and PDK1 (phosphoinositide-dependent kinase-1), which induce the phosphorylation of Akt. Activated Akt, as well as extracellular signal-regulated kinase (ERK), phosphorylates TSC2 resulting in inhibition of its activity as a GTP-ase [14].

In tuberous sclerosis, mutations in one of the TSC genes result in the abnormal formation of the hamartin/tuberin complex and so the subsequent inhibition of Rheb is lost and this induces an increase of cell proliferation [14].

Therefore, deficiency of hamartin or tuberin due to mutations of TSC1 or TSC2 in patients with TSC gives rise to hyperactivation of the mTOR pathway, resulting in a downstream kinase signaling cascade that can consequently lead to abnormalities in numerous cell processes, including cell cycle progression, transcription, translation, and metabolic control [46].

### **1.5.1 The PI3K/Akt and MAPK pathways**

mTOR can be activated either through the PI3K/Akt or MAPK (mitogen-activated protein kinase) ERK1/2 axes [59]. The PI3K/Akt and MAPK pathways play important roles in modulating cellular function in response to extracellular signals, including growth factors and hormones. These pathways are activated in certain kinds of malignancies for example bone and soft tissue tumors and certain sarcomas, and in renal angiomyolipoma [60,61,62].

Akt is a serine/threonine kinase activated by phosphoinositide 3-kinase (PI3K), regulates many cellular processes (proliferation, survival and cell growth) and when deregulated can contribute to the progression of cancer [63].

Akt has also been shown to contribute to tumor invasion and metastasis by promoting the secretion of MMP-9 [64] and the induction of epithelial–mesenchymal transition [65]. The higher secretion of MMP-9, associated with an overexpression of AKT, facilitates the movement and thus invasion of tumor cells [63,66]. The PI3K/AKT/mTOR pathway is regulated by a wide-range of upstream signaling proteins and it regulates many downstream effectors by collaborating with various compensatory signaling pathways, primarily with RAF/MEK/ERK pathway [67].

The Ras/Raf/MEK/extracellular signal regulated kinase (ERK) pathway, also known as the MAPK pathway, also regulates a variety of cell functions such as proliferation, growth, and survival. The two forms of ERK, ERK1 and ERK 2, belong to the family of MAP kinases, are ubiquitously expressed and are involved in the regulation of meiosis, mitosis, post-mitotic functions in differentiated cells and in cell proliferation and survival [68,69].

The activation of the ERK1/2 cascade mainly depends on the membrane receptors, such as G protein–coupled receptors (GPCRs), ion channels, and others; ERK1/2 were demonstrated to regulate several members in the subgroup of nuclear receptors, including estrogen receptor and in different type of cells, the rapid activation of ERK1/2 pathway can be induced by estradiol [69].

## **1.6 mTOR inhibitor: Everolimus**

Since the TSC gene products form a tumor suppressor complex that inhibits mTORC1 activity, this latter complex can be targeted for therapy in patients with TSC renal, lung and subependymal giant cell astrocytoma disease. Sirolimus and everolimus are administrated as mTOR inhibitors; sirolimus is a macrolide compound that is used to prevent organ transplant rejection and to treat a rare lung disease (LAM). Everolimus is an orally bioavailable, structurally similar derivative of sirolimus that exhibits antiproliferative and immunosuppressive effects.

Everolimus was designed to improve the pharmacokinetics of the sirolimus; in fact, it has greater stability, solubility, rapid and consistent absorption and lower nephrotoxicity, and reaches its peak concentration after 1.3–1.8 hours [70].

Everolimus forms a complex with the intracellular binding protein FKBP12 which directly interacts with mTORC1; this complex which block the constitutively upregulated downstream PI3K/Akt/mTOR signaling by reducing the phosphorylation of downstream mTOR effectors and the downstream signaling events responsible for the many manifestations of TSC [13,71].

At now the pharmacological treatment of AML and LAM associated with TSC is limited to mTOR inhibitors. Everolimus is administrated to reduce the tumor progression but, unfortunately, not all patients respond adequately; moreover, it has very important side effects such as ulcers, fatigue, rash, mucositis, anorexia, diarrhea, nausea, arthralgia, thrombocytopenia, and effects on lipid metabolism [72]. The recent literature suggests that everolimus is efficacious and safe in controlling AML tumor burden in patients with TSC, while preserving the renal parenchyma. However, tumor responses after treatment with only everolimus are usually only partial, and regrowth occurs after drug withdrawal [73]. For example, Yang and colleagues tested the antitumor efficacy of everolimus in combination with sorafenib, a kinase inhibitor, on renal lesions in patients with TSC. They suggested that this combination might improve therapeutic efficacy, compared to everolimus alone, for TSC-associated solid tumors [73].

Questions regarding the durability of responses, period of treatment and impact of toxicity from chronic therapy remain, and the role of mTOR inhibitors in the treatment of patients with non-TSC associated AMLs is still to be determined [9, 74].

## **1.7 The role of estrogen in AML**

The higher frequency of LAM and AML in women, suggests the hypothesis that the growth and migration of TSC2-deficient cells can be influence by estrogens [24].

The majority of female patients with these diseases are at child-bearing age at the time of diagnosis; pregnancy and use of oral contraception, in LAM, are associated with a higher frequency of exacerbations and a more aggressive disease course [75]. Boorjian and colleges observed a positivity of both estrogen receptors on smooth muscle cells of sporadic and TSC-associated renal AML.

Moreover, the carboxy terminal of TSC2 interacts with the estrogen receptor alpha functioning as transcriptional corepressor of estrogen receptor. Sex steroids might play a role in the pathogenesis of renal AMLs, hormone receptors could be potential therapeutic targets [76].

17- $\beta$ -estradiol (estrogen or E2) is a typically gender hormone; through the estrogen receptors (ER) it acts a variety of biological processes including reproduction, differentiation, cell proliferation [77].

This hormone exerts its activity in different tissues through three major receptors: the soluble nuclear receptors, ER $\alpha$  and ER $\beta$ , and GPR30.

The two nuclear receptors, ER $\alpha$  and ER $\beta$ , are highly homologous in their DNA- and ligand-binding domains [78]. Although ER $\alpha$  and ER $\beta$  are coexpressed in certain target tissues, they also exhibit different tissue/cell expression patterns and are functionally distinct. ER $\alpha$  is a more potent transcriptional activator than ER $\beta$ , and in tissues where both ERs are expressed, ER $\beta$  has been suggested to have a role as an attenuator of ER $\alpha$  [79].

GPR30 is a seven-transmembrane spanning G protein-coupled receptor [80] that binds 17- $\beta$ -estradiol with high affinity and lead to rapid and transient activation of numerous intracellular signaling pathways, for example calcium mobilization, cAMP production, PI3K activation and ERK1/2 activation in a G-protein dependent manner [81].

These receptors can mediate gene transcription events, either directly (genomic), as in the case of ER $\alpha$  and ER $\beta$  [Edwards D.P. et al., 2005; Marino M. et al., 2006], or indirectly (non-genomic), as in the case of GPR30 in which the MAPK, PI3K, Scr kinase and related pathways are activated [78,83,84].

The most known antagonist of the 17- $\beta$ -estradiol is tamoxifen (TAM); TAM is a non-steroidal anti-estrogen, extensively used in the treatment of hormone responsive breast cancer [85].

The principal mechanism of action of TAM is the inhibition of estrogen receptor, inducing a conformational change in the receptor with a consecutive modification in the expression of estrogen dependent genes [86]. Tamoxifen acts as an anti-estrogen (inhibiting agent) in the mammary tissue, but as an estrogen (stimulating agent) in cholesterol metabolism, bone density, and cell proliferation

in the endometrium [85]. Tamoxifen is a partial agonist of ER $\alpha$ , a selective agonist for GPR30 and a pure antagonist for ER $\beta$  [86]. The different effects, agonism or antagonism, mediated by TAM in various tissues may depend on the different expression of alpha and beta estrogen receptors and on the type of receptor-ligand interaction [86,87].

Recent experimental studies have revealed, other than estrogen receptors, new tamoxifen targets, such as protein kinase C, phospholipase C and antiangiogenic agents, which are key mediators of signaling pathways activating additional non-ER-mechanisms [88].

Tamoxifen has been used, besides the breast and endometrial carcinomas [89], in the treatment of malignancies such as renal carcinoma [86]. In this ER-negative cancer, the therapeutic efficacy of TAM has been obtained at doses at 4 to 8 folds above those used in ER-positive tumors [86]. The anti-tumor effect of tamoxifen is believed to be due to a combination of ER and non-ER-mediated mechanisms [86].

Since sex steroids might play a role in the pathogenesis of renal AMLs, a possible strategy for the treatment of AML and LAM might correspond to the inhibition of the effect of the estrogen [68].

## **1.8 Other approaches in AML treatment**

Despite publication of several observational papers [1,90], little is known about efficient pharmacological treatments on AML mass. Aside from mTOR inhibitors, no other drugs are known for the therapy of this disease; therefore, an effort has to be done to identify molecules able to slow down its development. Since very few recent in vitro studies on AML cells are published in the literature, we based our literature researches on other cell models with a similar origin and behavior of AML.

Several in vitro experiments conducted on renal cancer cells and other cancer cell models suggest that drugs such as simvastatin and zoledronic acid (ZOL) might be used also for their anti-proliferative effect [91,92,93].

### 1.8.1 Zoledronic acid

Bisphosphonates (BPs) are simple chemical compounds and are similar to endogenous pyrophosphates [94].

Some in vitro cell culture experiments have shown that BPs induce apoptosis and inhibit cancer cell invasion and angiogenesis in several human tumor cell lines such as breast, prostate, lung and kidney; [92,94]. Data from the literature report that caspase-dependent apoptosis appears to be the major mechanism responsible for BP-induced tumor cell apoptosis, and caspase-3 is certainly the major player in the antitumor activity [92,95].

BPs exert anticancer activity by stimulating the expansion of  $\gamma\delta$  T-cells (a subset of human T-cells that have antitumor activity) [96] by mimicking phosphoantigens and/or rising circulating phosphoantigen levels, and increasing sensitivity of cancer cells to the cytotoxic effects of  $\gamma\delta$  T-cells [97].

Zoledronic acid (ZA) belongs to the third generation of BPs; it inhibits the activity of farnesyl pyrophosphate synthase (FPPS) in the mevalonate pathway. The inhibition of FPPS reduces the activity of some small GTPases, such as Rho and Ras, which are among the key signal pathways that promote cell proliferation, vesicular traffic, cell adhesion and induction of phosphorylation of mTOR [98].

The possible mechanism of action through which zoledronic acid induces a decrease in tumor growth includes the inhibition of angiogenic factors such as VEGF, and modification of the tumor microenvironment (i.e. reduction of vascularization and macrophage infiltration) [99,100].

ZA inhibits the activity of some metalloproteinases (such as MMP-2 and MMP-9) essential for cell migration and adhesion [101,102], and modulates the expression of adhesion molecules (such as cadherin and integrin) which regulate the cellular invasion [103]. Therefore, in vitro studies on prostate and breast carcinoma cells hypothesized the use of zoledronic acid as a growth and cell migration inhibitor.

### **1.7.2 Simvastatin**

Statins are inhibitors of the first committed enzyme of mevalonate pathway, 3-hydroxy-methylglutaryl (HMG) CoA reductase. In general, statins decrease LDL levels, and are effective in preventing cardiovascular diseases [104].

At now, several in vitro experiments have demonstrated that lipophilic statins, such as simvastatin and atorvastatin, exert antiproliferative effects on different cells such as renal cancer [91] and prostate cancer [105]. Antiproliferative effects of statin include growth inhibition caused by cell cycle arrest, induction of apoptosis, and reduction of metastatic potential. These effects are regulated by Akt/mTOR axis through a Rho dependent mechanism [104,106,107].

Fang and colleagues found that the treatment of human renal carcinoma cell lines with simvastatin, significantly suppresses the phosphorylation/activation of Akt and inhibits the phosphorylation of mTOR. This suggests that simvastatin may exert its anti-cancer effects by inhibiting the Akt/mTOR axis [91].

Moreover, Atochina-Vasserman et al. compared the effect of simvastatin and atorvastatin on in vitro and in vivo mouse model of LAM, and showed that simvastatin, through AKT/PKB axis, inhibits the growth of these cells better than atorvastatin. Additionally, simvastatin, but not atorvastatin, also induces concentration-dependent inhibition of phosphorylation of ERK1/2 and mTORC1 [108].



## **2. Aim of the study**

The overall objective of this study is the improvement of the knowledge of AML cells biology and, in particular, the ascertainment of their migratory properties. Despite being classified as a benign tumor, hypothesis, never confirmed, have been put forward concerning their metastatic potential.

Our study will try to clarify if and how AML cells can migrate to lung or other organs, and if their behavior is influenced by hormonal milieu.

Moreover, our study may clarify the high diversity between the incidence of AML in female and male patients and the possible link between LAM and AML diseases.

In conclusion, we want to identify molecules capable to modify AML cell proliferation, migration which might be an outstanding information for considering new treatment protocols in AML patients, in order to replace as much as possible surgical removal of AML.

### **3. Material and methods**

### **3.1 Angiomyolipoma cells, tissue and ethical approvals**

Human primary AML cells have been obtained from patients that underwent surgical nephron-sparing AML ablation for therapeutic purposes at the Urology Unit of the San Luigi Gonzaga Hospital. The study was approved by the Ethical Committee of the San Luigi Gonzaga Hospital, (Protocol 0006771, approved on April 18, 2016). All patients provided written informed consent in accordance with the Declaration of Helsinki.

AML3 derives from a male patient, AML4 from a female patient. None of the patients had any clinical signs or symptoms or a family history of tuberous sclerosis.

Primary cells were isolated from excess material not required for diagnostic use, which was divided into small fragments and treated with type II collagenase. Resulting cell suspensions were plated into T25 tissue culture flasks in AML medium (adapted from Lesma et al.), composed of phenol red DMEM medium, ferrous sulphate 1.6  $\mu$ M, 20% fetal bovine serum (FBS) and 10  $\mu$ g/mL epidermal growth factor.

### **3.2 Stabilized cell culture**

Human 621-101 cells derived from renal angiomyolipoma of LAM female patients, kindly provided by Prof. Henske, (Harvard Medical School, USA) and human 4004 cells derived from renal angiomyolipoma cells derived from TSC male patients were purchased from ATCC (Rockville, MD, USA). 621-103 cell lines, also kindly provided by Prof. Henske, derive from the 621-101 cell line by restoration of the TSC2 gene.

621-101 cells carry biallelic mutations in exon 16 of the TSC2 gene (G1832A) [18], 4004 cells carry mutations in exon 33 of TSC2 gene (4083-4087 del AGTCG) [109].

Cells were maintained at 37°C in a humidified 5% CO<sub>2</sub> atmosphere in phenol red DMEM medium containing 1% penicillin and streptomycin solution and 10% Fetal Bovine Serum (FBS).

### 3.3 Immunofluorescence

Primary cells were grown on round sterilized coverslips under standard conditions for 2 days, and then washed with PBS followed by fixation in 4% paraformaldehyde (PAF) for 15 minutes.

After washing in PBS, cells were treated with PBS containing 1% normal goat serum (NGS), 0.1% Triton X-100 at room temperature (RT) for 1 hour. After incubation time cells were incubated overnight at 4°C with the following primary antibodies (diluted in PBS) against: S-100 (rabbit, 1: 800; Dako, Glostrup, Denmark),  $\alpha$ -Smooth-Muscle Actin (mouse, 1: 100; NeoMarkers, Fremont, CA), HMB45 (mouse, 1:100, Dako, Glostrup, Denmark), Keratin 8/18 (mouse, 1:100 Menarini, Florence, Italy) Vimentin (mouse, 1 : 70; Novocastra Lab, Newcastle, UK) and Melan-a (mouse; 1:100; NeoMarkers, Fremont, CA). After washing, cells were incubated for 1 hour at RT with the appropriate secondary antibodies: goat anti-mouse IgG Alexa-Fluor-488-conjugated (1: 200, Molecular Probes, Eugene, Oregon) and CY3-conjugated anti-rabbit IgG (dilution 1 :400, Dako, Milan, Italy). Finally, washed slides 3 times in PBS, added DAPI solution (dilution 1:1000) and after the last washing mounted with antifade mounting media [110]. The immunostained coverslips were analyzed on a Zeiss fluorescence microscope and images were captured with an Axiovision Imaging System.

### 3.4 Proliferation assay

Angiomiolipoma cells, primary or stabilized, were seeded into flat-bottomed 96-well microplates (1,000/100  $\mu$ L culture medium/well) and allowed to attach overnight in complete medium before drugs addition.

Drugs were added to culture medium testing various concentrations from 24 to 72 hours:

- From 0.1 to 100 nM and 17- $\beta$ -estradiol [18] and from 0.2 to 20  $\mu$ M tamoxifen [18] on primary and stabilized cells.
- From 0.001 to 100  $\mu$ M zoledronic acid [111] and everolimus [111], and from 1 to 100  $\mu$ M simvastatin [91] for stabilized cells.

The MTT ((3-(4,5-Dimethylthiazol-2-yl)-2,5-diphenyltetrazolium bromide assay was performed according to routine protocols. Briefly, 10  $\mu$ l of MTT prepared at a concentration of 5 mg/ml in PBS, was added to each well. Cell culture was placed in the incubator for another 3 hours at 37°C; after discarding supernatant, 100  $\mu$ l of DMSO were then added to each well and the absorbance was measured using a microculture plate reader (Microplate 450, Bio-Rad, Hercules, CA, USA) with a wavelength of 595 nm. Data (mean  $\pm$  standard errors) were the average values of 8 replicates. Each experiment was repeated thrice. Cell viability was expressed as percentage of living cells with respect to controls.

### **3.5 Two-dimensional migration assay-wound healing**

Primary AML cells were seeded in a 12-well plate at 300,000 cells/well. When they were confluent, a cross “wound” was made in each well with a p200 tip, then wells were washed thrice with PBS, and cultured in AML medium supplemented either with SDF-1 $\alpha$  (Peprotech, London, UK) 13 nM, plerixafor 100 nM, 17- $\beta$ -estradiol 1 nM, or tamoxifen 2  $\mu$ M. We photographed “wounds” on time-laps every hour to highlight migration, until a maximum of 8 hours. Experiments were repeated three times, and every time five different spots for each experimental condition were considered. Images were analysed using ImageJ software (Wayne Rasband, NIH, USA): the healing percentage was quantified comparing the wound area at t = 0 to the following time-points for each treatment.

### **3.6 Three-dimensional migration assay**

To measure the three-dimensional (3D) movements of primary and stabilized cells in response to different drugs, migration assays were performed through transwell (BD Falcon cell culture inserts incorporating polyethylene terephthalate membrane with 8.0  $\mu$ M pores,  $6\pm 2\times 10^4$  pores/cm<sup>2</sup>). DMEM was placed on the bottom of a 24-well microplates, and the transwell was inserted within the same: the multiwell plate was placed in the incubator for 30 minutes for medium equilibration. In the meanwhile the angiomyolipoma cells were suspended in 200 $\mu$ L; cell suspension was carefully placed

in the transwell and multiwell was placed in incubator. At the end of migration time, each transwell was taken off from its well and gently washed twice with PBS  $\text{Ca}^{2+}/\text{Mg}^{2+}$  to prevent the detachment of cells from the membrane of the transwell and then with use of cotton swabs the cells located in the internal part of the transwell taken off. The transwell was immersed in a solution of glutaraldehyde 2% for 20 minutes to fix cells and then washed five times in deionized water and allowed to dry. Each transwell was immersed in crystal violet 0.1% for 20 minutes to stain cells and then washed again five times in deionized water and allowed to dry. Wells were photographed using a BRESSER MikroCam 3 Mpx camera, with an optical microscope (Leica DC 100) at 100x. Five pictures were randomly chosen per well, and used to count the migrated cells with ImageJ software using cell-counter plug-in. Results from different experiments (performed at least three times in duplicate) were expressed as mean  $\pm$  standard error.

The experimental scheme for the different performed tests was schematically described in the following tables (Table 1-3).

The concentration of drugs used in transwell assay represent non-toxic concentration at 24 hours as per the described viability assay.

<b>Experimental time</b>	<b>Upper chamber (200 <math>\mu\text{L}</math>)</b>	<b>Lower chamber (800 <math>\mu\text{L}</math>)</b>
4 and 8 hours	Primary cells ( $5 \times 10^4$ )	Fresh culture medium (CTRL)
		17- $\beta$ -estradiol (1 nM)
4 hours	Stabilized cells ( $8 \times 10^4$ )	Fresh culture medium (CTRL)
		17- $\beta$ -estradiol (1 nM)
		tamoxifen (2 $\mu\text{M}$ )
	Stabilized cells ( $8 \times 10^4$ ) + tamoxifen (2 $\mu\text{M}$ )	17- $\beta$ -estradiol (1 nM)

Table 1: Three-dimensional migration assay with estrogen incubation

<b>Experimental time</b>	<b>Upper chamber (200 <math>\mu\text{L}</math>)</b>	<b>Lower chamber (800 <math>\mu\text{L}</math>)</b>
4 hours	Stabilized cells ( $8 \times 10^4$ )	Fresh culture medium (CTRL)
	Stabilized cells ( $8 \times 10^4$ ) + simvastatin (10 $\mu\text{M}$ )	Fresh culture medium
	Stabilized cells ( $8 \times 10^4$ ) + zoledronic acid (10 $\mu\text{M}$ )	
	Stabilized cells ( $8 \times 10^4$ ) + everolimus (10 nM)	
	Stabilized cells ( $8 \times 10^4$ ) + zoledronic acid (10 $\mu\text{M}$ ) + everolimus (10 nM)	

Table 2: Three-dimensional migration assay with drug incubation

Experimental time	Upper chamber (200 $\mu$ L)	Lower chamber (800 $\mu$ L)
4 and 8 hours	Primary cells ( $5 \times 10^4$ )	Fresh culture medium (CTRL)
		SDF-1 $\alpha$ (13 nM)
		plerixafor (100 nM)
	Primary cells ( $5 \times 10^4$ ) + plerixafor* (100 nM)	SDF-1 $\alpha$ (13 nM)

Table 3: Three-dimensional migration assay in presence of SDF-1 $\alpha$  and plerixafor.

\* For this test, primary cells were pre-incubated for 30 min at 37°C with plerixafor.

### 3.7 Western blot

Cells were seeded in 10 cm-diameter Petri dishes, cultured until sub-confluence and treated with drugs (17- $\beta$ -estradiol 1nM, tamoxifen 2  $\mu$ M, simvastatin 10 $\mu$ M, zoledronic acid 10 $\mu$ M and everolimus 10nM). Following incubation period (5 min -1 hours for estradiol and 4 hours for others treatment), the medium was removed and the cell monolayer was first washed with PBS, then covered with ice-cold PBS and incubated for 5 minutes to facilitate detachment. Subsequently, adherent cells were gently scraped, collected and centrifuged at 1000 rpm for 5 minutes. Then the pellet was resuspended in 50  $\mu$ l of RIPA buffer, placed in ice for one hour and gently shuffled every 20 minutes to facilitate the membrane breakup. The mixture was then centrifuged at 13200 rpm for 30 minutes at 4°C, the supernatant collected and protein content quantified with the Bradford assay (1  $\mu$ l RIPA suspension/999  $\mu$ l Bradford solution 1:5) (Bio-Rad): sample were read with a spectrophotometer (Beckman DU® 640 Spectrophotometer – U.S.A.) at 595 nm wavelength.

Thirty  $\mu$ g of proteins were resolved in the Biorad system by SDS-PAGE gels, denaturing conditions, and then transferred onto nitrocellulose membranes (GE Healthcare), and immunoblotted with the following antibodies (Table 4) according to Racca et al 2012 [112].



Primary antibody	Protein molecular weight	Dilution	Antibody manufacturer
Anti-vinculin (mouse)	116 kDa	1: 2000	Sigma Aldrich
Anti-estrogen receptor $\alpha$ (rabbit)	67 kDa	1:600	
Anti-estrogen receptor $\beta$ (rabbit)	59 kDa	1:600	
Anti-GPR30 (rabbit)	42 kDa	1:600	
Anti-p42/44 Erk 1/2 (mouse)	42/44 kDa	1: 2000	Cell Signaling Technology
Anti-phospho p42/44 Erk 1/2 (mouse)	42/44 kDa	1: 2000	
Anti-Akt (rabbit)	60 kDa	1: 1000	
Anti-phospho Akt (rabbt)	60 kDa	1: 1000	

Table 4: Antibodies used for performing western blot.

The anti-vinculin, anti-estrogen alpha and beta were diluted in PBS Tween 0.1%; the other antibodies were suspended in 5% w/v nonfat dry milk + PBS tween 0.1%.

HRP-conjugated anti-mouse and anti-rabbit (Amersham-GE Healthcare, Buckinghamshire, UK) were diluted 1:6000 in PBS Tween 0.1%. Bands were quantified using the ImageJ software.

Phosphorylation levels of ERK<sub>1/2</sub> and Akt were expressed as ratio pERK<sub>1/2</sub>/ERK<sub>1/2</sub> and pAkt/Akt respectively. Each experiment was repeated thrice and all data were expressed as percentage modification relative to control conditions.

### 3.8 Gelatin zymography

MMP-2 and MMP-9 activities in medium samples were assayed by gel zymography. Proteins (100  $\mu$ g) were separated by electrophoresis in 8% SDS-PAGE gel containing gelatin (0.8 mg/mL) under non-reducing conditions. The gel was washed with Tris buffer (2.5% Triton X-100 in 50 mM Tris-HCl, pH 7.5, final solution) for 1 hour, then incubated overnight at 37°C in a proteolysis buffer (40 mM Tris-HCl, 200 mM NaCl, 10 mM CaCl<sub>2</sub>, 0.02% NaN<sub>3</sub>, pH 7.5, final solution). The gel was stained for 3 hours with Coomassie Blue solution (0.05% Coomassie Brilliant Blue R-250, 50% methanol, 10% acetic acid, final solution) and finally destained with 5% methanol and 7% acetic acid (final solution). Reagents and chemicals were obtained from VWR International (Milan, Italy). MMPs activity was detected as a clear band on a blue background and estimated by densitometric analysis using ImageJ Software. The results were expressed as percentages of control values.

### 3.9 Quantitative real-time PCR (qRT-PCR)

In order to perform quantitative real-time PCR (qRT-PCR), total RNA was extracted from treated cells by using Trizol (Invitrogen Life Technologies Italy). After its purification and treatment with DNase I (Fermentas, St. Leon-Rot, Germany), 1 µg was retrotranscribed in cDNA with the RevertAid™ H Minus First Strand cDNA Synthesis Kit (Fermentas) using oligo (dT) primers. Gene assays were performed in triplicate for each treatment in a 20 µL reaction volume containing 1 µL of RT products, 10 µL Sso-Fast EVA Green SMX (Bio-Rad), 500 nM each forward and reverse primers. Gene expression was normalized on the housekeeping gene ribosomal 18S rRNA. Table 5 resumes the primer sequences that were adopted. Automated CFX96 real-time thermocycler (Bio-Rad) was used and the reaction conditions were 95°C for 1 minute, followed by 45 cycles 98°C for 5 seconds and anneal–extend step for 5 seconds at 60°C, with data collection. At the end of these cycles, a melting curve (65°C to 95°C, with plate read every 0.5°C) was performed in order to assess the specificity of the amplification product by single peak melting temperature verification. Results were analysed with Bio-Rad CFX Manager. Calculations and statistical analyses were performed using GraphPad Prism version 5.00 for Windows (GraphPad Software, San Diego California USA).

GENE	SEQUENCE	AMPL. SIZE	NCBI REF. SEQ.
ER $\alpha$	Fw: 5'-TGGAGTCTGGTCCTGTGAGG-3'	172 bp	NT_025741.16
	Rev: 5'-CCCACCTTTCATCATTCCTCACT-3'		
Er $\beta$	Fw: 5'-GAGCAAAGATGAGCTTGCCG-3'	142 bp	NM_001437.2
	Rev: 5'-AGCTGGGCCAAGAAGATTCC-3'		
GPR30	Fw: 5'-AGTCGGATGTGAGGTTTCAG-3'	240 bp	NM_001505.2
	Rev: 5'-TCTGTGTGAGGAGTGCAAG-3'		
CXCR4	Fw: 5'-TGACGGACAAGTACAGGCTGC-3'	406 bp	NM_001348056.1
	Rev: 5'-CCAGAAGGGAAGCGTGATGA-3'		
MMP-2	Fw: 5'-GGCCCTGTCCTCCTGAGAT-3'	474 bp	NM_001302510.1
	Rev: 5'-GGCATCCAGGTTATCGGGGA-3'		
MMP-9	Fw: 5'-CAACATCACCTATTGGATCC-3'	480 bp	NM_004994.2
	Rev: 5'-CGGGTGTAGAGTCTCTCGCT-3'		
FN1	Fw: 5'-AGACCCAGGCACCTATCAC-3'	263 bp	NM_017003695.1
	Rev: 5'-TCGGTCACTTCCACAACTG-3'		
SDF-1 $\alpha$	Fw: 5'-GGTGGAGCTGGAGAAGACAGA-3'	73 bp	NM_000609.6
	Rev: 5'-CAGCCGGGCTACAATCTGAA-3'		
18S rRNA	Fw: 5'-GTGGAGCGATTTGTCTGGTT-3'	201 bp	X03205.1
	Rev: 5'-ACGCTGAGCCAGTCAGTGTA-3'		

Table 5: Primers sequences, size of the amplification product and NCBI Reference Sequence. Fw=forward, Rev= reverse

### **3.10 Statistical analysis**

All the data in this study were shown as mean  $\pm$  standard error (SE). Two group means were compared using the unpaired t-test, and more than two group means were analyzed by one-way analysis of variance (ANOVA), where  $P < 0.05$  was considered statistically significant. For gene expression level comparison One-way ANOVA with Dunnett's post tests were performed using GraphPad Prism version 5.00 for Windows (GraphPad Software, San Diego California USA).

Coefficient of Drug Interaction (CDI) was used to define the type of interactions between the employed drugs. CDI was calculated by means of the equation:  $CDI = AB / (A \times B)$ , where AB is the relative cell migration of the combination; A or B, relative cell migration of the single agent.  $CDI < 1$  indicates a synergistic effect;  $CDI = 1$  indicates an additive effect;  $CDI > 1$  indicates an antagonistic effect.

## **4. Results**

## **Part I: Primary cells**

### **4.1 Immunohistochemistry to confirm the AML diagnoses**

AML diagnoses were confirmed by standard histological examination including specific immunostaining for alpha-smooth muscle Actin, HMB-45 and Pancytokeratin antigens conduct by the Patholgy Unit of San Luigi Gonzaga Hospital.

### **4.2 Cells characterization by immunofluorence**

To better characterize isolated AML primary cells, immunofluorescence was performed with several antibodies. Overall, both cell lines showed similar immunophenotype and partly elongated, partly rounded shapes. Both primary culture cells were strongly and totally positive for smooth muscle actin antibody (in both elongated and rounded cells), with a diffused stain throughout the cytoplasm (Figure 1a and 1a'). Furthermore, in both cell lines there were single rounded element positive for keratin 8/18 and elongated cells strongly positive for vimentin (Figure 1d, 1e, 1d', and 1e') together with single negative ones for both the antigens. Finally, a strong nuclear and cytoplasmic positivity was found for S100 in both cells (Figure 1f and 1f'). Overall this phenotype confirmed the mixed (either muscle, epithelioid, lipomatous and mesenchimal) nature of the cultures, according to the heterogeneous nature of AML. As a matter of fact, even if scattered, some AML3 cells were focally positive for intracytoplasmic HMB45 (Figure 1b and 1b'), and AML4 cells were focally positive for Melan-A antigen (Figure 1c and 1c'), both of which being consistent with the AML phenotype.

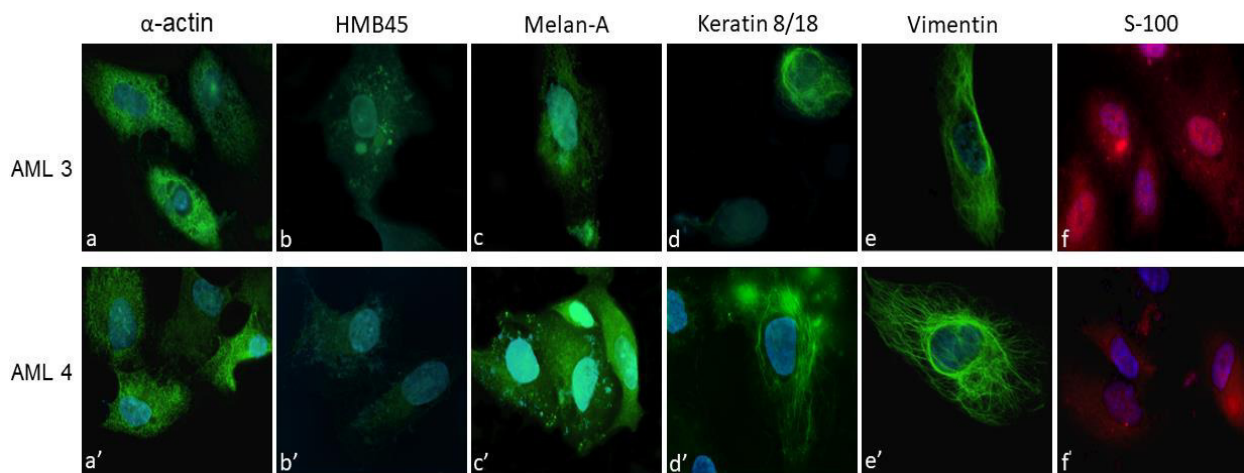


**Figure 1: Primary angiomyolipoma cells characterization by immunofluorescence.**

*Cells isolated from the two AML were stained with different antibodies to detect their immunophenotype. Fields were chosen to clearly show both the morphological aspect and the specific marker expression.*

### 4.3 Estrogen and SDF-1 $\alpha$ receptor gene expression

Early passages AML cells underwent qRT-PCR for CXCR4, GPR30, ER $\alpha$  and ER $\beta$  mRNA expression analysis, which demonstrated a significant presence of mRNA for CXCR4 (SDF-1 $\alpha$  receptor), GPR30, ER $\alpha$ , but not for ER $\beta$  (Figure 2). The level of each gene was similar in the two cultures, with no significant difference.

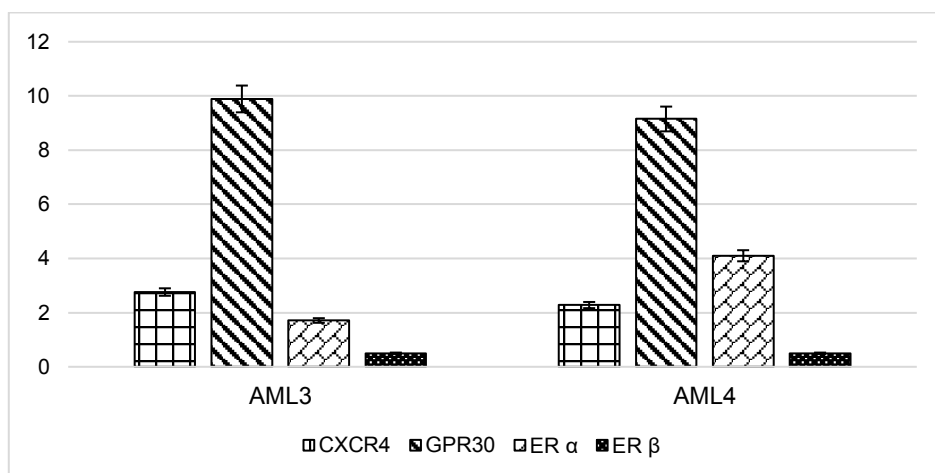


**Figure 2: Receptors gene expression.**

*Early passages AML cells underwent qRT-PCR for CXCR4, GPR30, ER $\alpha$  and ER $\beta$  mRNA expression analysis. Data are shown as the absolute mRNA expression normalized by the housekeeping 18S rRNA.*

#### 4.4 Influence of estrogen on cell proliferation

Treatment of primary cells for 24-72 hours with 17- $\beta$ -estradiol from 0.1 nM to 100 nM (Figure 3A) or with tamoxifen from 0.2 to 20  $\mu$ M (Figure 3B) did not modify AML cells proliferation, nor did the combination of 17- $\beta$ -estradiol (1 nM) and tamoxifen (2  $\mu$ M) (Figure 4).

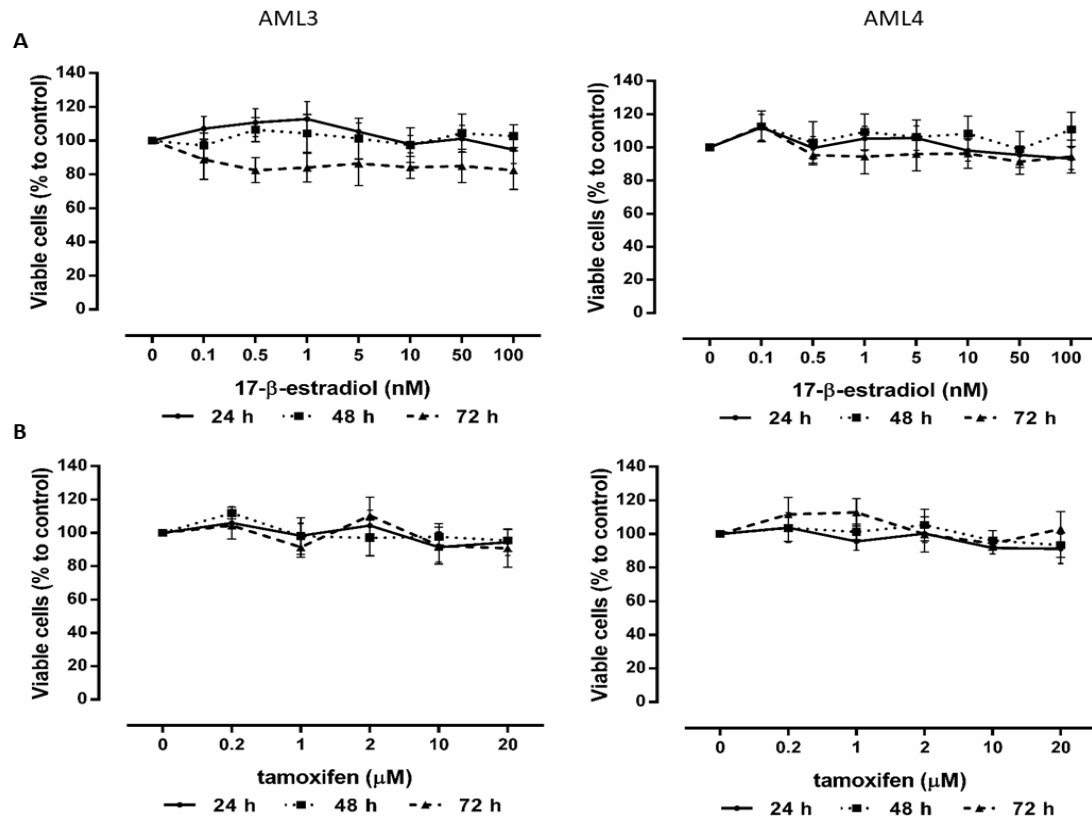


**Figure 3: Proliferation assay**

*Effect of increasing concentration of 17- $\beta$ -estradiol (A) or tamoxifen (B) after 24, 48 and 72 hours culture.*

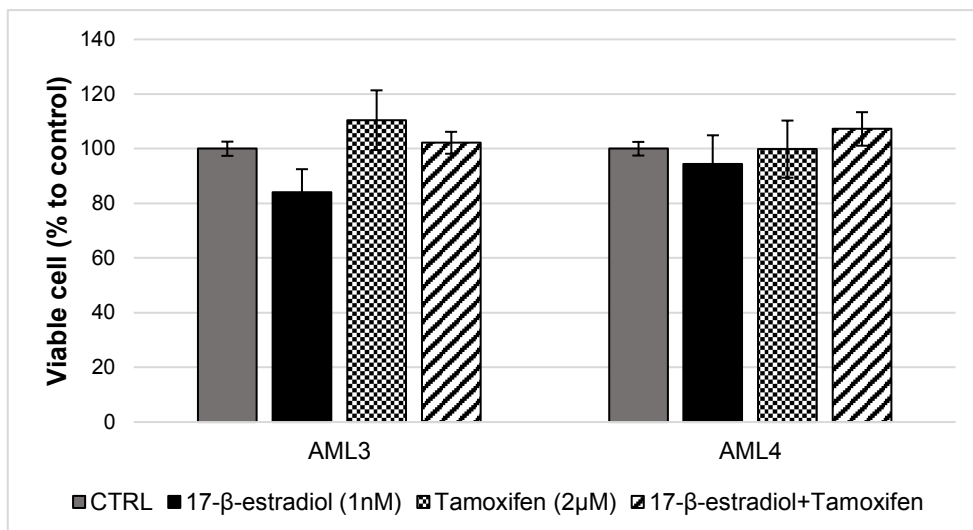


**Figure 4: Effect of 17-β-estradiol alone and of its combination with tamoxifen on AML cells growth**

*Proliferation assay after 72 hours culture in presence of 17-β-estradiol (1 nM), tamoxifen (2 μM) or the combination of both.*

#### **4.5 Influence of estrogen on two- dimensional migration (wound healing)**

The in vitro wound healing assay was performed on male and female cells to observe whether estrogen modifies the motility of AML cells. Figure 5A shows a scratch wound generated after cell confluence; figure 5B shows the same wounded area after 8 hours of assay. Wound healing was quantified, and data are displayed graphically as healing percentage (Figure 5 D-E). Panel C compares basal migration of AML3 and AML4: the early migration rate of AML3 was higher, a significant difference being demonstrated at 4 hours. This difference was promptly quenched since after 8 hours the movement rate of the two AMLs was similar. Two-dimensional migration was significantly modulated by 17-β-estradiol (1 nM), although with some differences between the two AMLs. In fact, AML3 (D) of male origin, showed a significant motility increase in the first 4 hours of incubation with 17-β-estradiol, and a prevalent logarithmic pattern. On the other hand, migration of AML4 cells, of female origin (E), significantly increased, following an exponential pattern, at any of the time points considered. The treatments with the ER-antagonist tamoxifen alone (2 μM)



had no influence on two-dimensional motility of any cell type, while it was able to abolish the effects of estradiol.

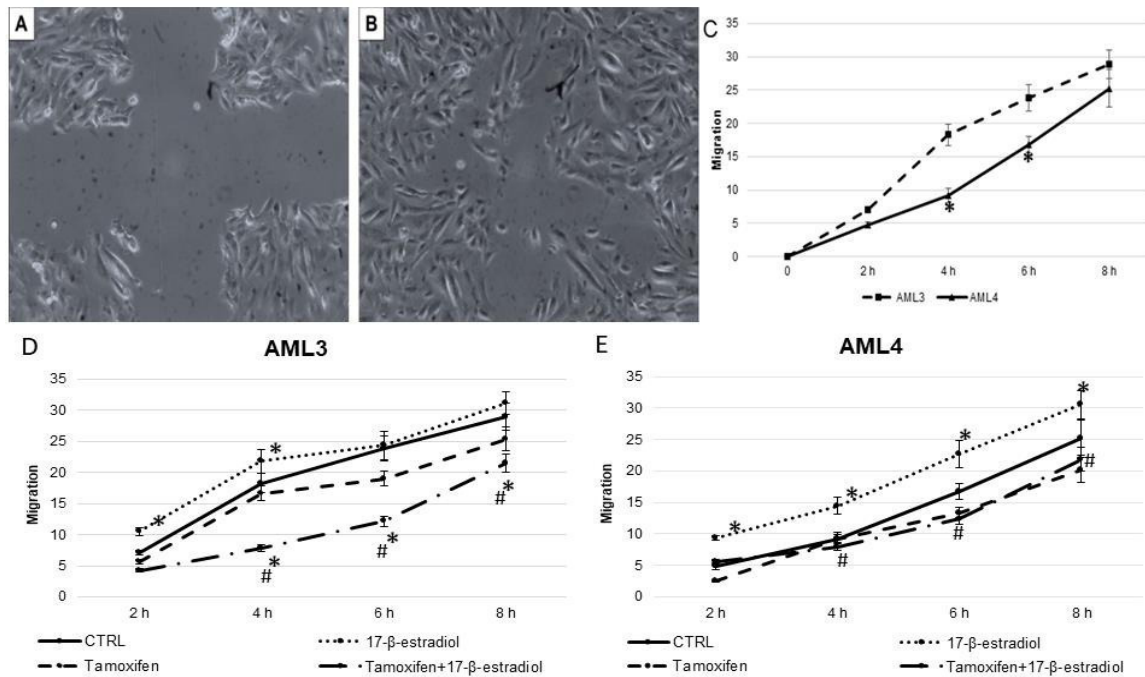


**Figure 5: Analyses of primary AML cells migration by *in vitro* wound healing assay.**

Scratch wound healing assay in a representative experiment before (A) and after (B) the incubation period. Panel C shows bi-dimensional migration of the two AMLs in basal conditions. Migration in presence of 17-β-estradiol (1 nM) or its antagonist tamoxifen (2 μM), or a combination of both, is shown in panel D (AML3) and E (AML4). Migration is expressed in arbitrary units. Data are expressed as the percentage of migration vs  $t = 0$  h. \*= $P < 0.05$  vs control; #= $P < 0.05$  vs 17-β-estradiol.

#### 4.6 Influence of estrogen on three-dimensional migration

The transwell migration experiments performed in presence of 17-β-estradiol demonstrated a different behavior between cells originating from the two AMLs. Migration of AML3 cells of male origin was not modified all along the stimulation period (Figure 6A). AML4 cells (Figure 6B) responded to the stimulation by increasing the migration rate already at 4 hours while after 8 hours the stimulating effect was lost.

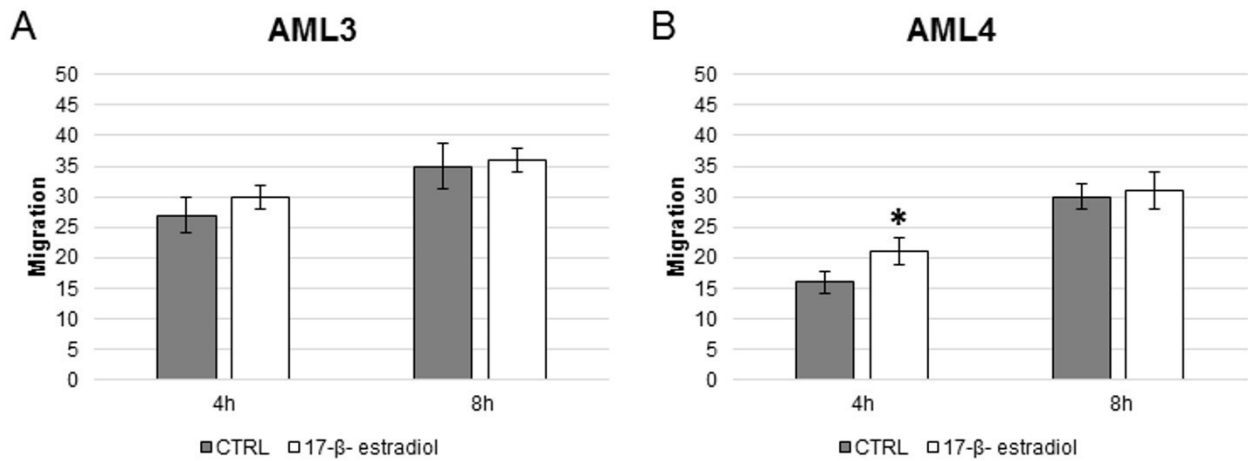


**Figure 6. Three-dimensional migration.**

Cells were incubated with 17-β-estradiol (1 nM) for 4 and 8 hours. Migration is expressed in arbitrary units.

\*= $P < 0.05$  vs control.

#### 4.7 ERK phosphorylation

Treatment of AML3 cells with 17-β-estradiol increased ERK phosphorylation at 4 hours, while pERK was significantly augmented in AML4 cells already at 5 minutes and was stable until 4 hours (Figure 7).

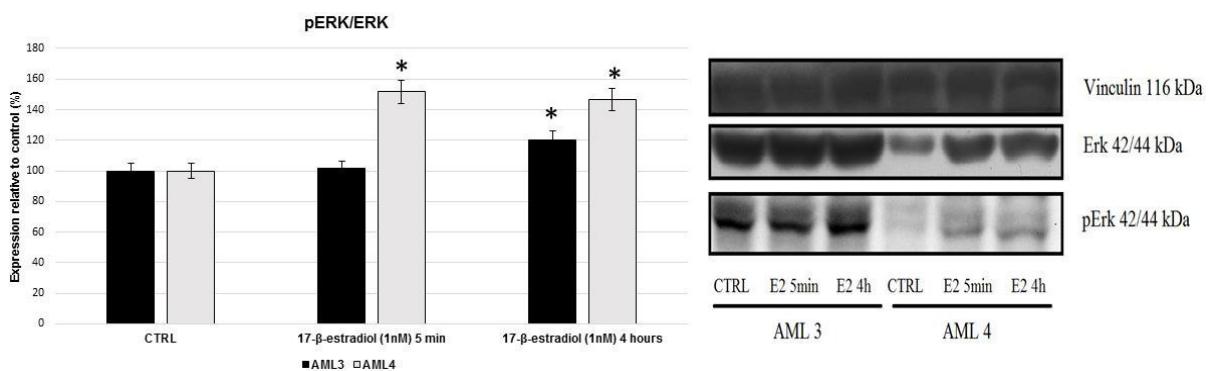


**Figure 7: ERK phosphorylation**

Effect of 17-β-estradiol (1 nM) on pERK/ERK in AML3 and AML4 cells after 5 minutes and 4 hours of incubation. Vinculin as internal control. \*= $P < 0.05$  vs control.

#### 4.8 Influence of SDF-1 $\alpha$ on two and three-dimensional migration

SDF-1 $\alpha$  treatment, in wound healing assay, induced statistically significant motility increase already after 2 hours treatment in cells from both AMLs (Figure 8 A-B) and the difference persisted all along the experimental period (up until 8 hours). The results, for the transwell assay, show that the number of migrating cells significantly increased in response to SDF-1 $\alpha$  both after 4 and 8 hours incubation (Figure 8 C-D). In both assays, the effects induced by SDF-1 $\alpha$  were abolished by the SDF-1 $\alpha$ -receptor antagonist plerixafor, while no significant effects were induced by plerixafor alone.

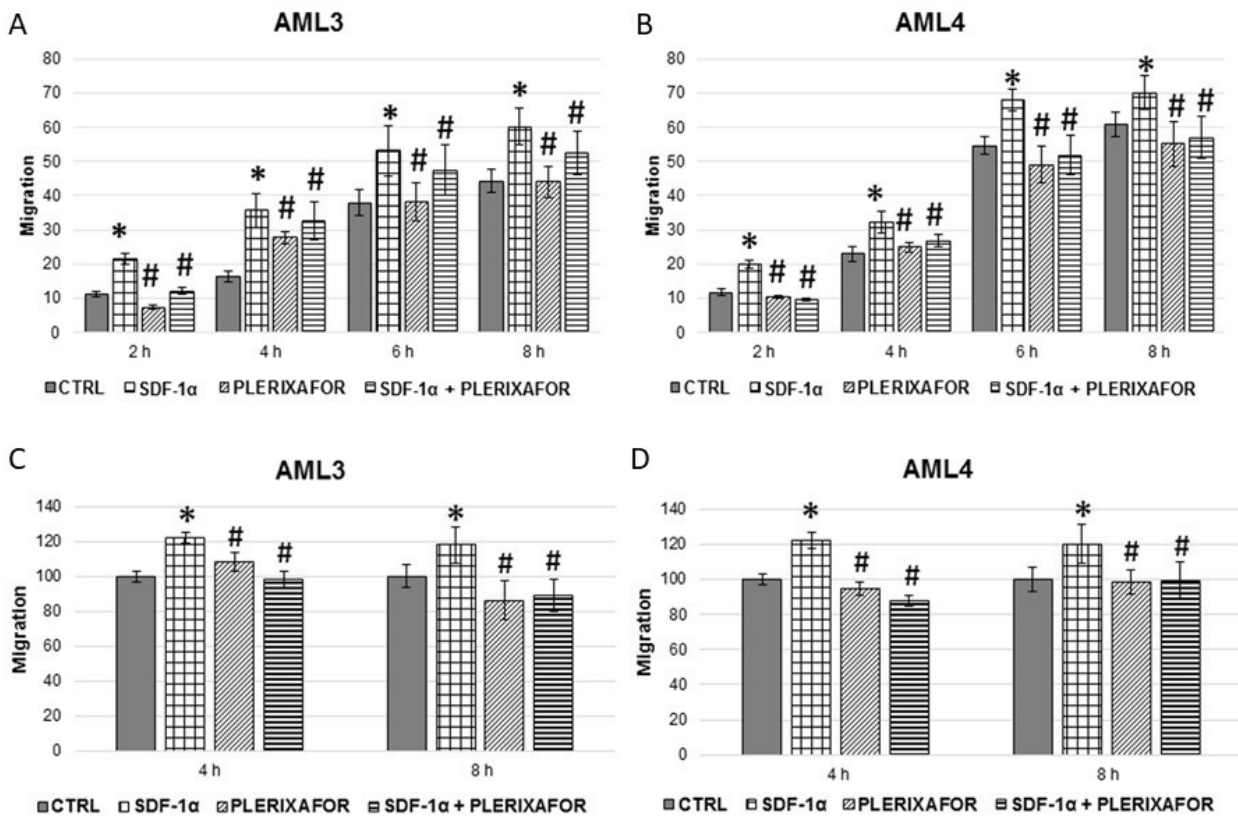


**Figure 8: Two and three-dimensional migration (SDF-1 $\alpha$ )**

*Bi-dimensional migration in presence of SDF-1 $\alpha$  13 nM or its receptor antagonist plerixafor 100 nM, or a combination of both (A-B). Three-dimensional migration with SDF-1 $\alpha$  (13 nM) and its receptor blocker plerixafor (100 nM) or a combination of both (C-D). \*= $P < 0.05$  vs control; #= $P < 0.05$  vs SDF-1 $\alpha$ .*

#### 4.9 Metalloproteases activity in supernatant derived from 3D-migration test

The activity of two metalloproteases involved in malignant phenotype acquisition, MMP-2 and MMP-9, was measured by zymography in the supernatant collected at the end of the 3D-migration test performed in presence of SDF-1 $\alpha$ , plerixafor and 17- $\beta$ -estradiol (4 hours) (Figure 9). While the diverse treatments induced no significant difference in MMP-2 activity, SDF-1 $\alpha$  enhanced MMP-9 enzymatic activity. Coherently, plerixafor inhibited MMP-9 activity increase provoked by SDF-1 $\alpha$ . No difference was induced by incubation with 17- $\beta$ -estradiol.

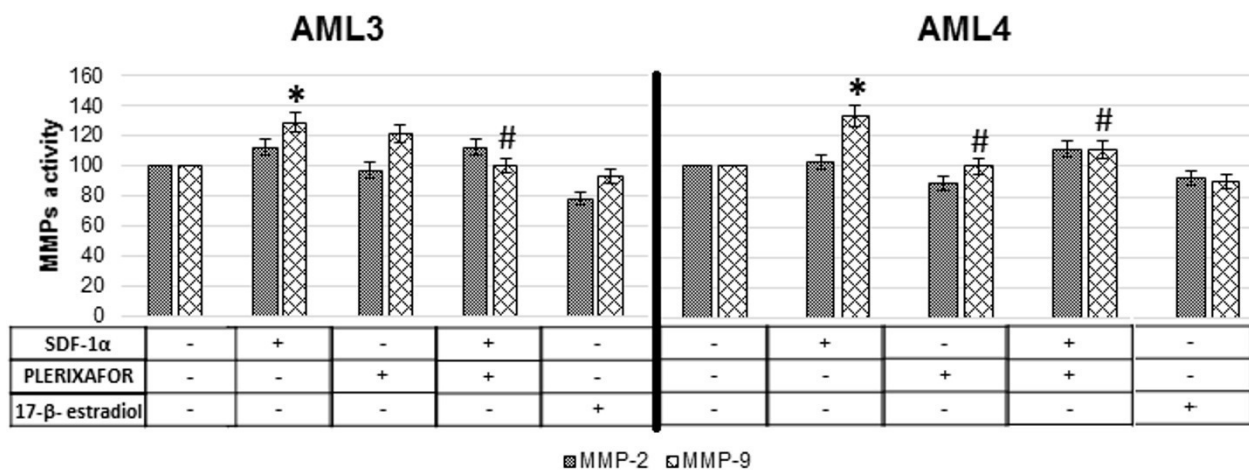


**Figure 9: Metalloproteases activity**

MMP-2 and MMP-9 activity in presence of SDF-1 $\alpha$ , plerixafor and 17- $\beta$ -estradiol. Data are expressed as the relative activity calculated by densitometric analyses. \*= $P < 0.05$  vs control; #= $P < 0.05$  vs SDF-1 $\alpha$ .

## Part II: Stabilized cell lines

### 4.10 Estrogen receptor expression

The qRT-PCR analysis for estrogen gene receptor demonstrated a significant presence of mRNA for GPR30, ER $\alpha$  and ER $\beta$  for 4004 and 621-103; the level of GPR30 expression appeared to be lower in 621-101 cells than the other cells (Figure 10A). Instead, by western blot we detected the protein expression for all the estrogen receptor considered. In this case, high levels of expression for ER $\beta$  were observed in 4004 and 621-103 cells (Figure 10B). We observed a significant expression of ER $\alpha$  only in female 621-101 cell lines by immunofluorescence, The receptor was localized in the cell cytoplasm (Figure 10C). Unfortunately, due to technical problems, the expression for ER $\beta$  and GPR30 were not available by immunofluorescence.

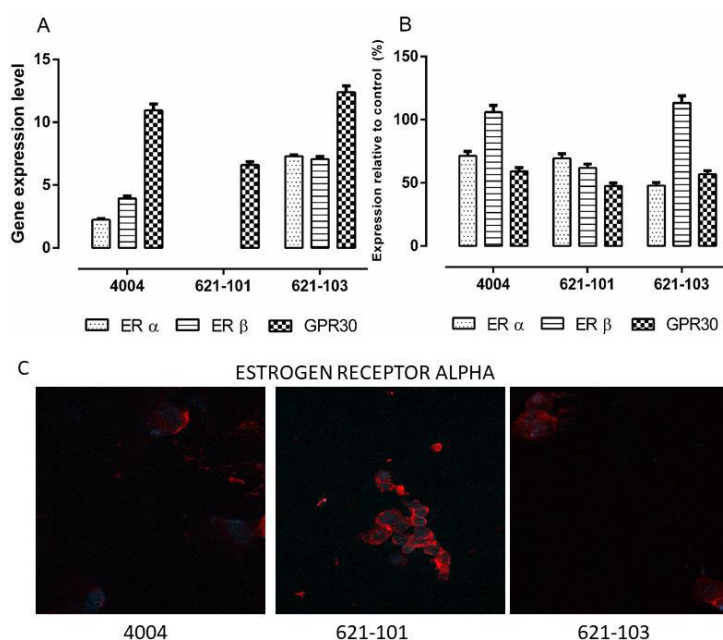


**Figure 10: Receptors gene expression**

(A) 4004, 621-101 and 61-103 cells underwent qRT-PCR for ER $\alpha$ , ER $\beta$  and GPR30 mRNA expression analysis. Data are shown as the absolute mRNA expression normalized by the housekeeping 18S rRNA. (B) Expression of ER $\alpha$ , ER $\beta$  and GPR30 protein underwent western blot. (C) Expression of ER $\alpha$  in cell lines by immunofluorescence. Figures show representative fields of 4004, 621-101 and 621-103 cells immune-stained with anti-ER $\alpha$  antibody.

#### 4.11 Influence of 17- $\beta$ -estradiol, tamoxifen and combination of both on cell proliferation

Treatment for up to 72 hours with increasing concentration of 17- $\beta$ -estradiol (0.1-100 nM) did not modify 4004, 621-101 and 621-103 cell proliferation *in vitro* (Figure 11A).

Unexpectedly, the growth of all angiomyolipoma cell lines was strongly inhibited by 10  $\mu$ M tamoxifen already after 24 hours of treatment (Figure 11B).

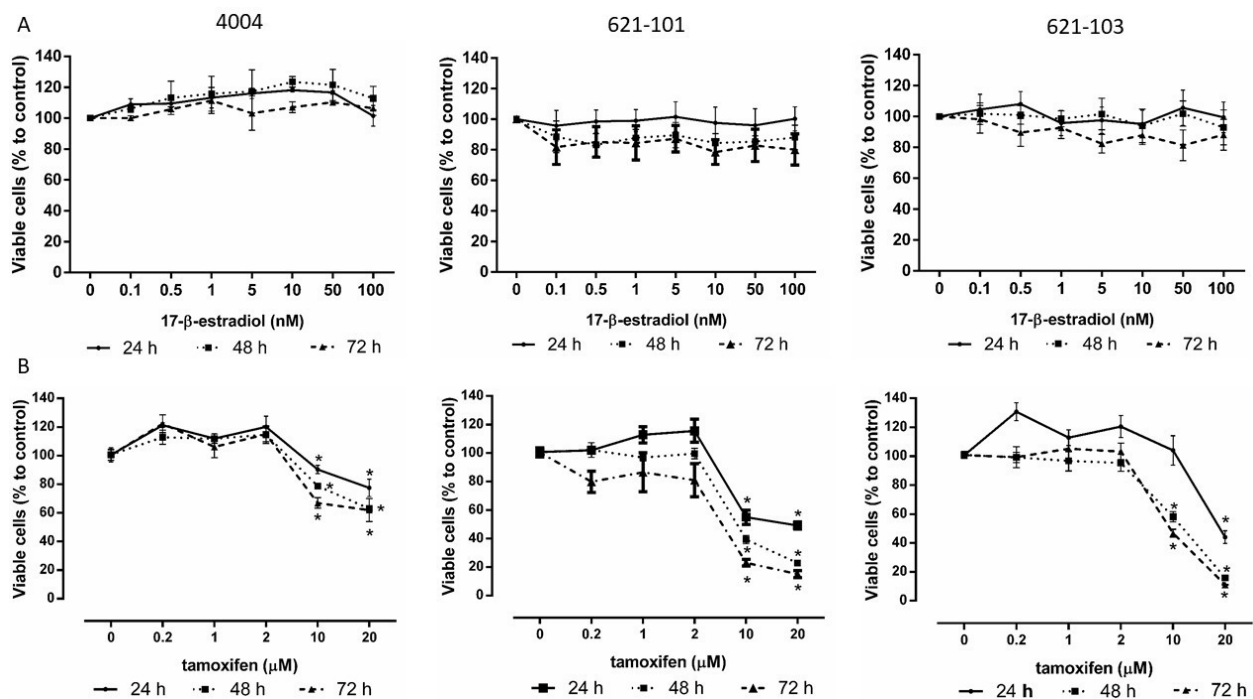


**Figure 11: Influence of 17- $\beta$ -estradiol and tamoxifen on cell proliferation**

*Effect of 17- $\beta$ -estradiol (A) or tamoxifen (B) on 4004, 621-101 and 621-103 cell growth. \*= $P < 0.05$  vs control.*

The treatment of all cell lines with 17- $\beta$ -estradiol (10  $\mu$ M) did not modify the cell proliferation. Treatment for 24 and 48 hours demonstrated that only in female 621-101 cells the combination of tamoxifen (10  $\mu$ M) and 17- $\beta$ -estradiol (10  $\mu$ M) provoked an unusual increase of cell proliferation (Figure 12 B). In the male 4004 and female 621-103 cells the combination of these drugs did not modify the proliferation (Figure 12 A, C).

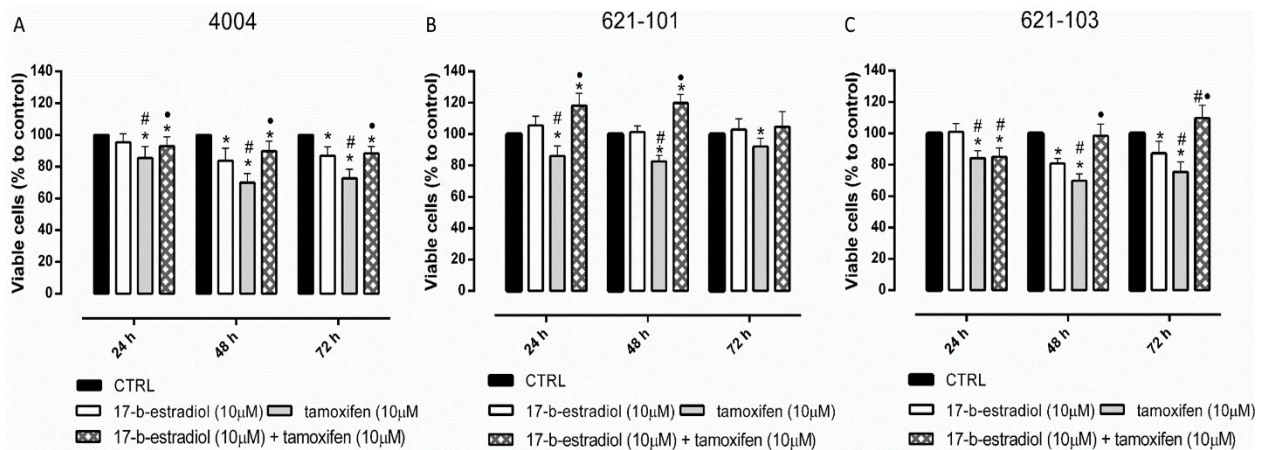


**Figure 12: Influence of 17-β-estradiol and tamoxifen and combination of both on cell proliferation**

*Effect of 17- β-estradiol (10 μM) and tamoxifen (10 μM) on 4004 (A), 621-101 (B) and 621-103 (C) cells.*

*\*=P<0.05 vs control; #=P<0.05 vs 17-β-estradiol; •= P<0.05 vs tamoxifen.*

#### 4.12 Influence of 17-β-estradiol and tamoxifen on three-dimensional migration

The migration of all cell lines was evaluated after 4 hours of incubation time in basal conditions, or in response to 17-β-estradiol (1 nM), tamoxifen (2 μM) and the combination of both. None of the tested molecules modified the migration of male 4004 cells. On the other hand, 17-β-estradiol (1 nM) significantly increased the rate of female 621-101 and 621-103 cell migration (50% and 37%, respectively). The treatment with tamoxifen (2 μM) and its combination with 17-β-estradiol also increased the number of migrating female cells (P<0.05) (Figure 13).

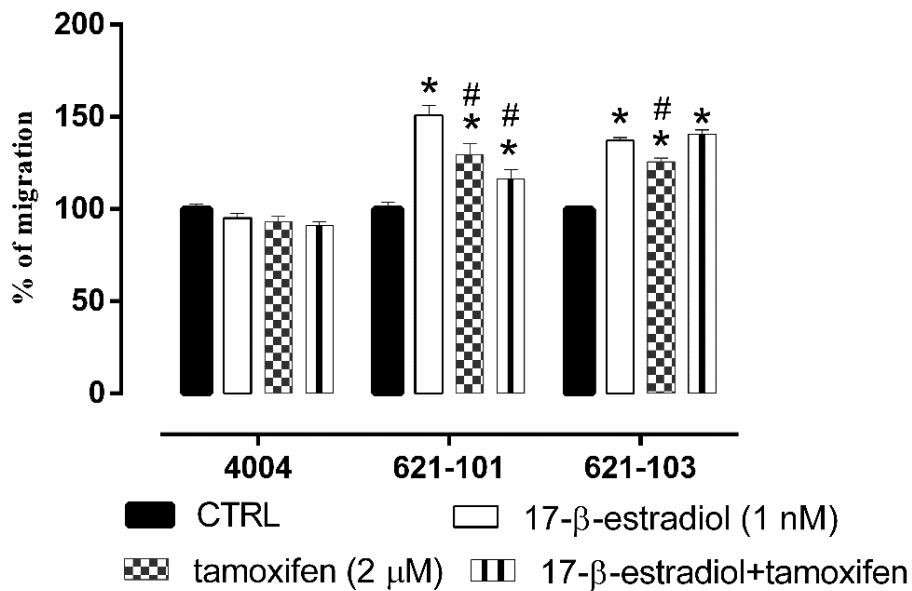


**Figure 13: Three-dimensional migration assay**

Cells were incubated with 17-β-estradiol (1 nM), tamoxifen (2 μM) or a combination of both for 4 hours. Data are expressed as the percentage of migration vs control. \*= $P < 0.05$  vs control; #= $P < 0.05$  vs 17-β-estradiol.

#### 4.13 ERK and AKT phosphorylation

No significant modification in phosphorylation rate of ERK was induced on 4004 and 621-103 cells by 17-β-estradiol or tamoxifen incubation. Furthermore, for the female 621-101 cells the treatment with estradiol and tamoxifen for 4 hours induced a lower increase in pERK (Figure 14).

Neither of the two tested drugs induced a significant change in pAKT/AKT ratio in all cell lines (Figure 15).



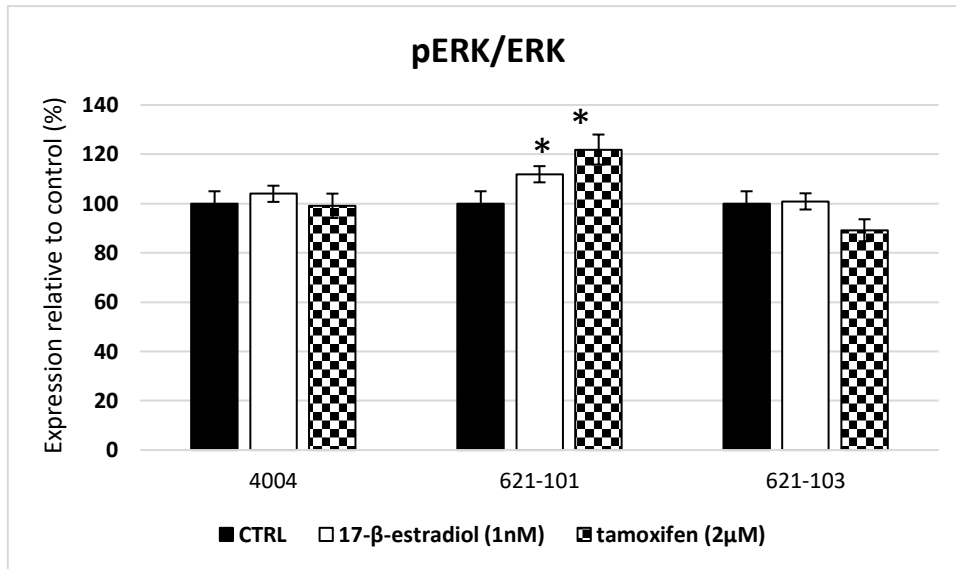


**Figure 14: ERK phosphorylation**

*Effect of 17-β-estradiol (1 nM) and tamoxifen (2 μM) on pERK/ERK after 4 hours of incubation on all cell lines. \*=P<0.05 vs control.*

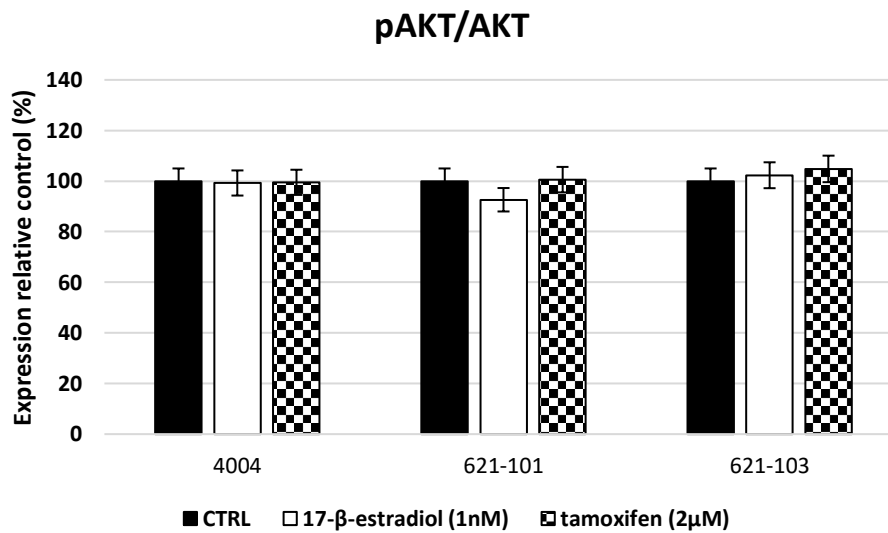


**Figure 15: AKT phosphorylation**

*Effect of 17-β-estradiol (1 nM) and tamoxifen (2 μM) on pAKT/AKT after 4 hours of incubation on all cell lines.*

#### 4.14 Effect of 17- $\beta$ -estradiol and tamoxifen on adhesion/invasiveness gene expression

Cell lines were treated with 17- $\beta$ -estradiol (1 nM) and tamoxifen (2  $\mu$ M) for 4 hours.

In 4004 cells (Figure 16) treatment with estradiol provokes a low decrease of the expression of FN1, GPER30 and MMP-2 genes; with tamoxifen treatment the diminution of the expression of these genes were more evident for MMP-2 especially. Both the treatments induced an increase, without evident differences, of the expression of SDF-1 $\alpha$ .

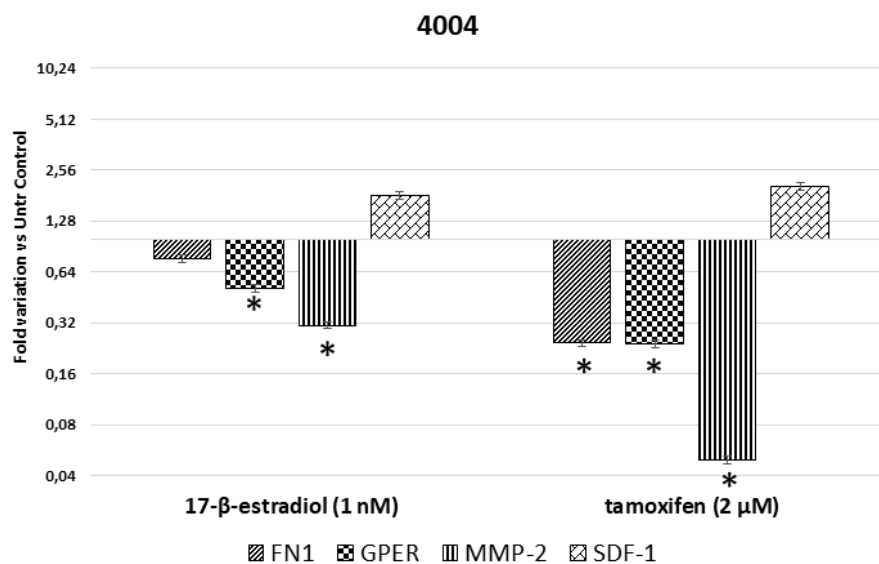


**Figure 16: Effects of 17- $\beta$ -estradiol (1 nM) and tamoxifen (2  $\mu$ M) on gene expression.**

Data from qRT-PCR are expressed as fold variation of gene expression in 4004 cells. Data are expressed as mean  $\pm$  SD of at least three experiments. \*= $P < 0,05$  vs control.

In 621-101 cells, the treatment with estradiol induce a diminution in the MMP-2 gene expression, whereas tamoxifen treatment provoked a significant reduction of FN-1 gene expression. For the other analyzed genes, the treatment did not induce noteworthy variation in their expression (Figure 17).

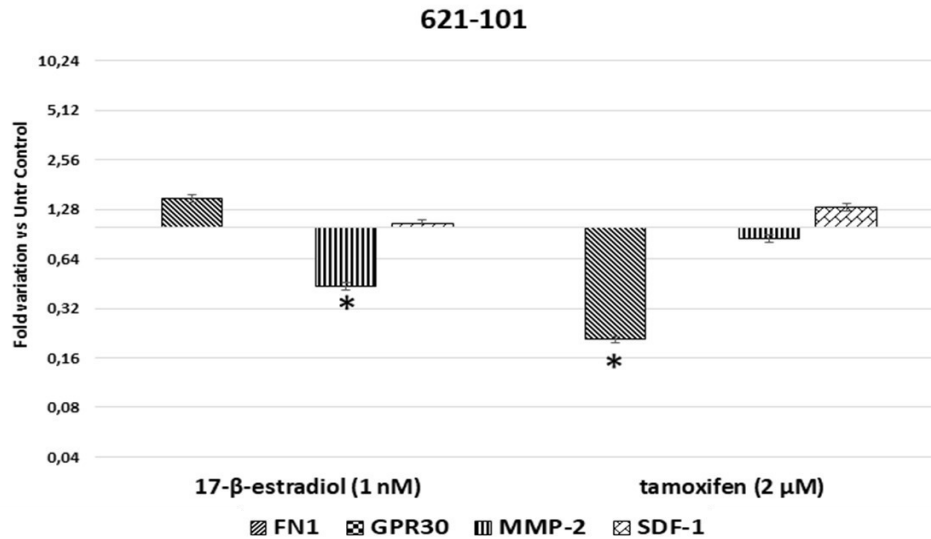


**Figure 17: Effects of 17-β-estradiol (1 nM) and tamoxifen (2 μM) on gene expression.**

Data from qRT-PCR are expressed as fold variation of gene expression in 621-101 cells. Data are expressed as mean ± SD of at least three experiments. \*=P<0.05 vs control.

Finally, the treatment with estradiol on 621-103 female cells (Figure 18) induced an increase in the expression of GPR30 gene, and after treatment with tamoxifen, the expression of MMP-2 gene was strongly decreased as observed in 4004 male cells.

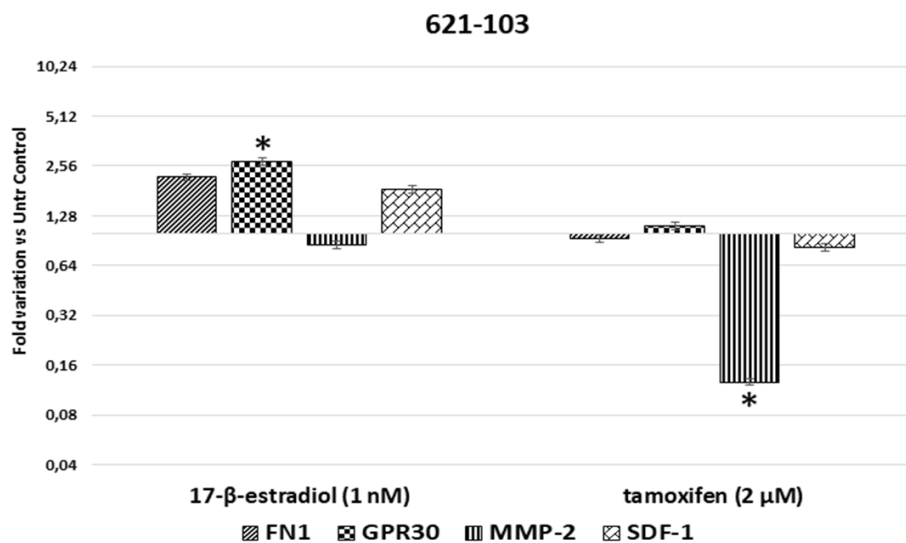


**Figure 18: Effects of 17-β-estradiol (1 nM) and tamoxifen (2 μM) on gene expression.**

Data from qRT-PCR are expressed as fold variation of gene expression in 621-103 cells. Data are expressed as mean ± SD of at least three experiments. \*=P<0.05 vs control.

#### 4.15 Influence of simvastatin, zoledronic acid and everolimus on cell proliferation

To evaluate the effect of different drugs on the proliferation of AML cells; 4004, 621-101 and 621-103 cells were exposed to different concentrations of simvastatin, zoledronic acid and everolimus for 24, 48 and 72 hours. Simvastatin showed its inhibitory effect on cell growth at 10  $\mu\text{M}$  after 48 hours incubation (Figure 19).

The 621-101 cells were more sensitive to simvastatin at 72 hours respect to 4004 and 621-103 cells; the inhibition growth of 621-101 cells, at 1  $\mu\text{M}$ , was 10% more than the other cells.

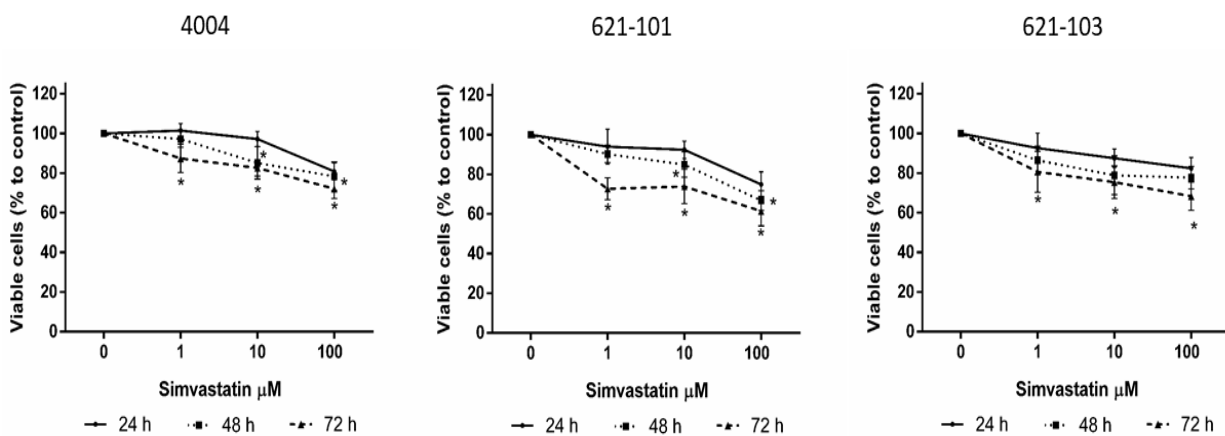


**Figure 19: Influence of simvastatin on cell proliferation**

*Effect of increasing concentration of simvastatin on 4004, 621-101 and 621-103 cell growth.  $*=P < 0.05$  vs control.*

Zoledronic acid (0.001-100  $\mu\text{M}$ ) strongly inhibited cell proliferation; 4004 cells growth was inhibited by concentrations as low as 1  $\mu\text{M}$  after 48 hours and even more strikingly after 72 hours culture (Figure 20A). Growth inhibition on 621-103 cells was less striking at 48 hours but comparable at 72 hours (Figure 20B, C).

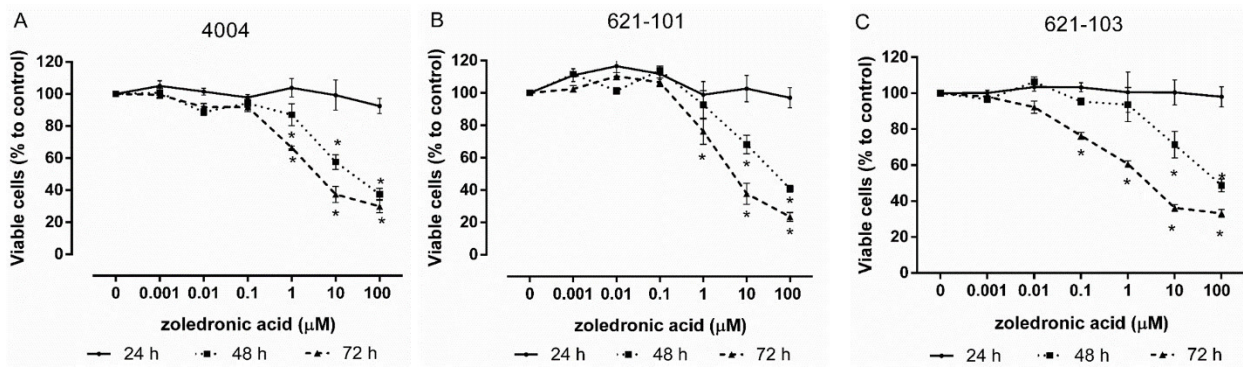


**Figure 20: Influence of zoledronic acid on cell proliferation**

*Effect of increasing concentration of zoledronic acid on 4004 (A), 621-101 (B) and 621-103 (C) cell growth after 24, 48 and 72 hours of incubation. \*=P<0.05 vs control.*

Everolimus inhibited cell proliferation at 1 μM for 4004, 10 μM for 621-101 and 100 μM for 621-103 after 24 hours of treatment (Figure 21A, B, C). After 48 hours of treatment 4004 and 621-101 cell growth were inhibited after already at 0.001 μM.

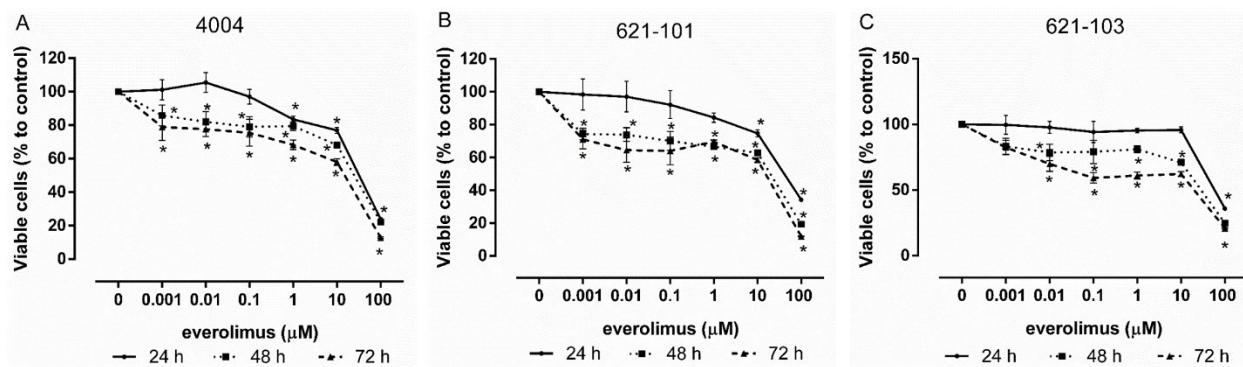


**Figure 21: Influence of everolimus on cell proliferation**

*Effect of increasing concentration of everolimus on 4004 (A), 621-101 (B) and 621-103 (C) cell growth. \*=P<0.05 vs control.*

To evaluate if everolimus and zoledronic acid have a synergic effect we also tested the combination of these two drugs on all cell lines. We observed that the simultaneous presence of these drugs influenced proliferation less than zoledronic acid alone. At 48 hours the combination of these drugs, caused a 40% (in 4004 and 621-101 cells) or a 20% (in 621-103 cells) growth inhibition, a

significantly greater effect on cell growth compared with the treatment with everolimus alone (Figure 22). The table 6 reports the coefficient of drug interaction (CDI) after 24 hours of treatment.

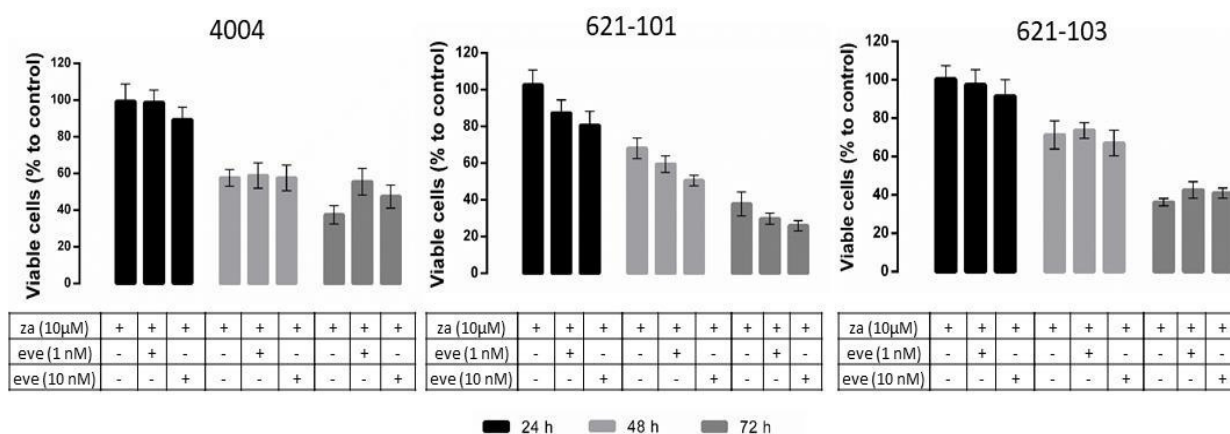


**Figure 22: Effect of everolimus, zoledronic acid and combination of both on cell proliferation**

*Effect of everolimus (EVE) and zoledronic acid (ZA) on 4004, 621-101 and 621-103 cell lines after 24-72 hours of incubation.*

**Table 6: Drug interactions after 24 hours of treatment**

	AB	A	B	CDI
4004	zoledronic acid + everolimus (24 hours)	zoledronic acid (10µM)	everolimus (1 nM)	0,98
			everolimu (10 nM)	0,86
621-101	zoledronic acid + everolimus (24 hours)	zoledronic acid (10µM)	everolimus (1 nM)	0,87
			everolimu (10 nM)	0,81
621-103	zoledronic acid + everolimus (24 hours)	zoledronic acid (10µM)	everolimus (1 nM)	0,95
			everolimu (10 nM)	0,91

*CDI < 1 indicates a synergistic effect; CD=1 indicates an additive effect*

#### 4.16 Three dimensional migration assay in presence of zoledronic acid, everolimus and

##### simvastatin

Treatment with zoledronic acid, everolimus and the combination of both significantly decreased the migration rate of all cell lines if compared to the control conditions (Figure 23). In this test, the simultaneous presence of zoledronic acid and everolimus influenced migration less than each single drug.

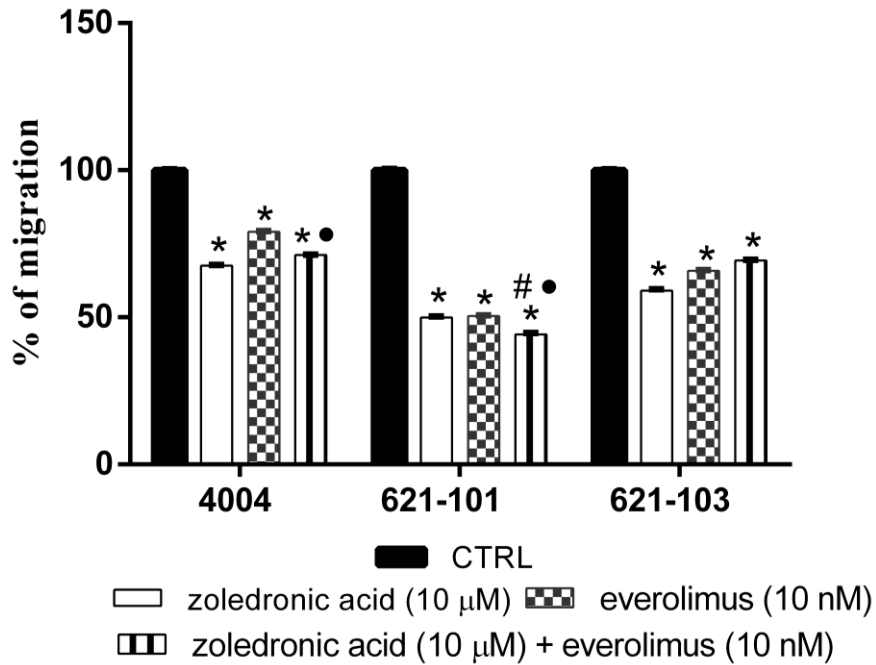


**Figure 23: Effect of zoledronic acid, averolimus and combination of both on three-dimensional migration**

*Effect of 4 hours treatment with zoledronic acid (10 μM), everolimus (10 nM) or a combination of both on 3D migration. Data are expressed as the percentage of migration vs control. \*=P<0.05 vs control; #=P<0.05 vs zoledronic acid; •=P<0.05 vs everolimus.*

Simvastatin decreased migration of all cell lines. Likewise the proliferation test, we observed in 3D migration assay a significant difference between cells: 621-101 cells were much more inhibited than 4004 and 621-103 (50% vs 34 and 30%, respectively) (Figure 24).

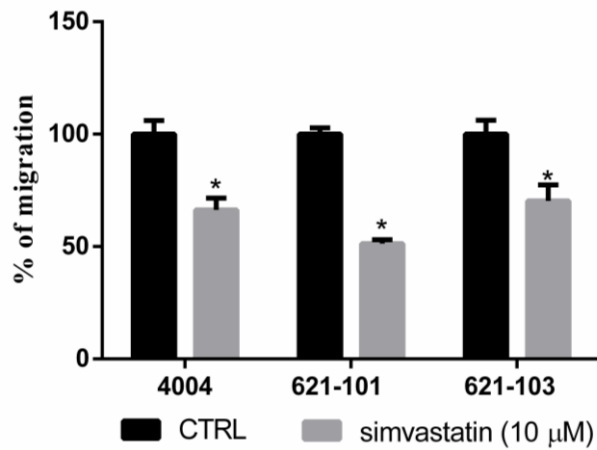


**Figure 24: Effect of simvastatin on three-dimensional migration**

*Effect of 4 hours treatment with simvastatin (10 μM). Data are expressed as percentage of migration vs control. \*=P<0.05 vs control.*

#### 4.17 ERK and AKT phosphorylation

Treatment with zoledronic acid (10 μM) and everolimus (10 nM) for 4 hours did not modify significantly the pERK/ERK ratio for any cell line. pERK/ERK ratio was similarly decreased by simvastatin (10 μM) in 4004 and 621-101 cells; in 621-103 cells the treatment did not change the ratio of ERK (Figure 25).

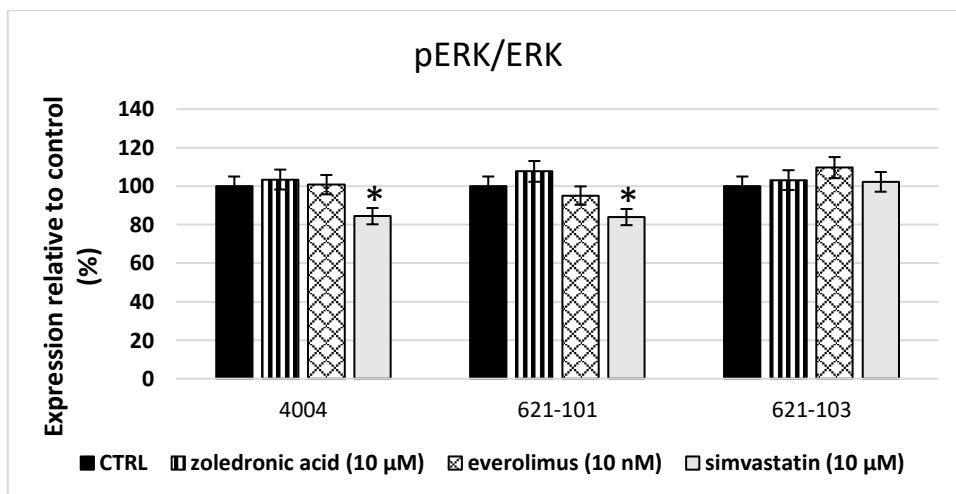


**Figure 25: ERK phosphorylation**

*Effect of zoledronic acid (10 μM), everolimus (10 nM) and simvastatin (2 μM) on pERK/ERK after 4 hours of incubation on all cell lines. \*=P<0.05 vs control.*



Exposure of 4004 and 621-103 cells to everolimus and simvastatin for 4 hours significantly decreased pAKT/AKT, while zoledronic acid after 4 hours had no effect compared to the untreated control. On the other hand, in 621-101 cells the treatments with zoledronic acid and everolimus induced a significant inhibition of pAKT/AKT, in this case the treatment with simvastatin did not significantly change this ratio (Figure 26).

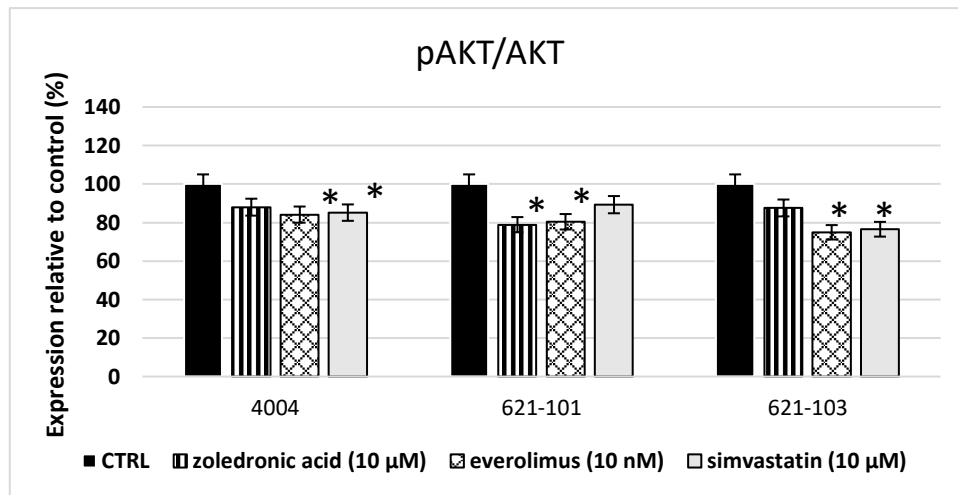


**Figure 26: AKT phosphorylation**

*Effect of zoledronic acid (10 μM), everolimus (10 nM) and simvastatin (2 μM) on pAKT/AKT after 4 hours of incubation on all cell lines. \*=P<0.05 vs control*

#### **4.18 Effect of zoledronic acid, everolimus and simvastatin on adhesion/invasiveness gene expression**

The treatment with zoledronic acid, simvastatin and everolimus on 4004 cells induced change in the level gene expression. Zoledronic acid induced only a reduction in MMP-2 level gene, simvastatin induced a significant increase in FN-1 and SDF-1α expression and a significant decrease in GPR30 and MMP-2 gene expression (Figure 27).

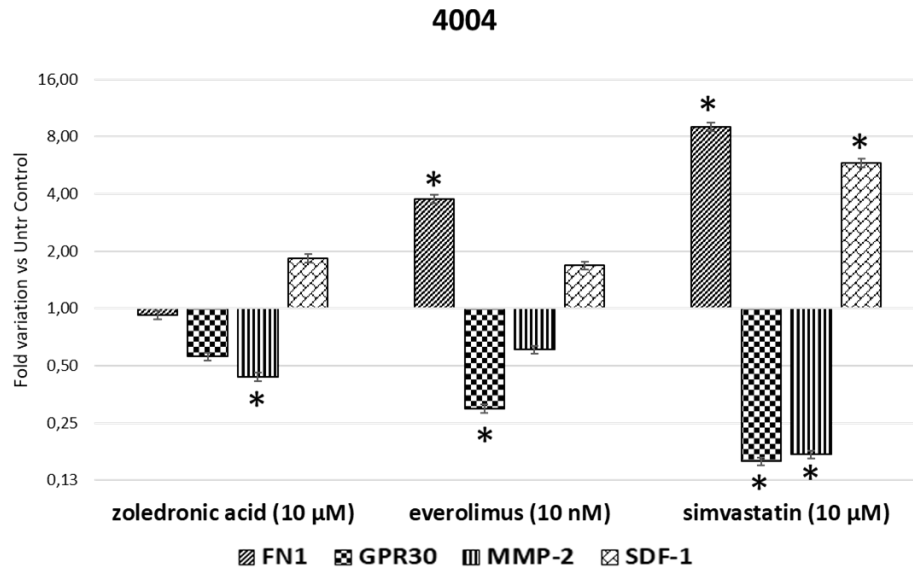


**Figure 27: Effects of zoledronic acid (10 µM), everolimus (10 nM) and simvastatin (10 µM) on gene expression.**

*Data from qRT-PCR are expressed as fold variation of gene expression in 4004 cells. Data are expressed as mean ± SD of at least three experiments. \*= $P < 0.05$  vs control.*

Treatment of 621-101 cells with zoledronic acid and simvastatin induced a significant increase in the expression level of MMP-2 gene, while the treatment with everolimus induced a decrease in the expression of FN-1 and SDF-1 $\alpha$  genes.

The treatments did not induce any noteworthy variation in the expression of the other genes analyzed (Figure 28).

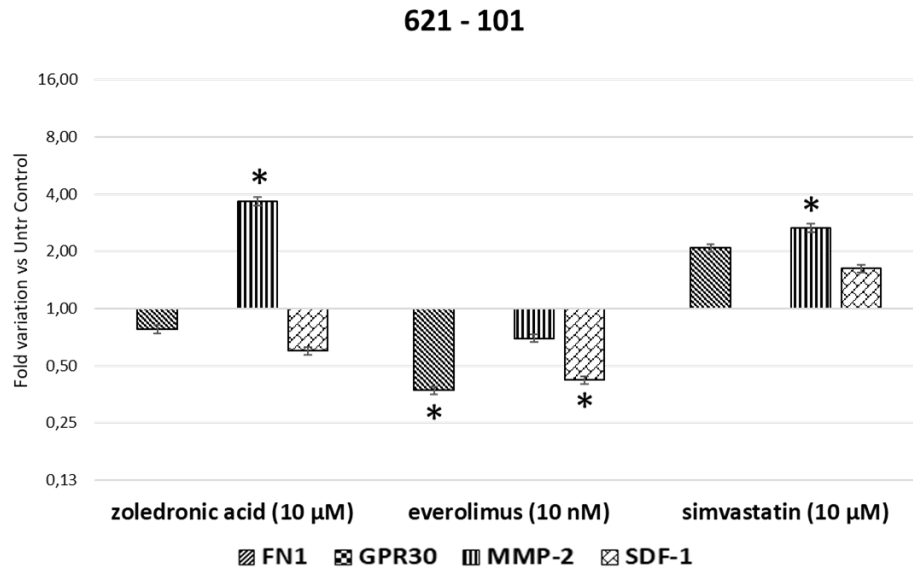


**Figure 28: Effects of zoledronic acid (10 µM), everolimus (10 nM) and simvastatin (10 µM) on gene expression.**

*Data from qRT-PCR are expressed as fold variation of gene expression in 621-101 cells. Data are expressed as mean ± SD of at least three experiments. \* = P < 0.05 vs control.*

Finally, in 621-103 cells zoledronic acid and simvastatin induced a strong increase of SDF-1α expression, furthermore only the zoledronic acid provoked a reduction in MMP-2 gene expression. Everolimus did not induce any significant modification in the expression of the genes analyzed (Figure 29).

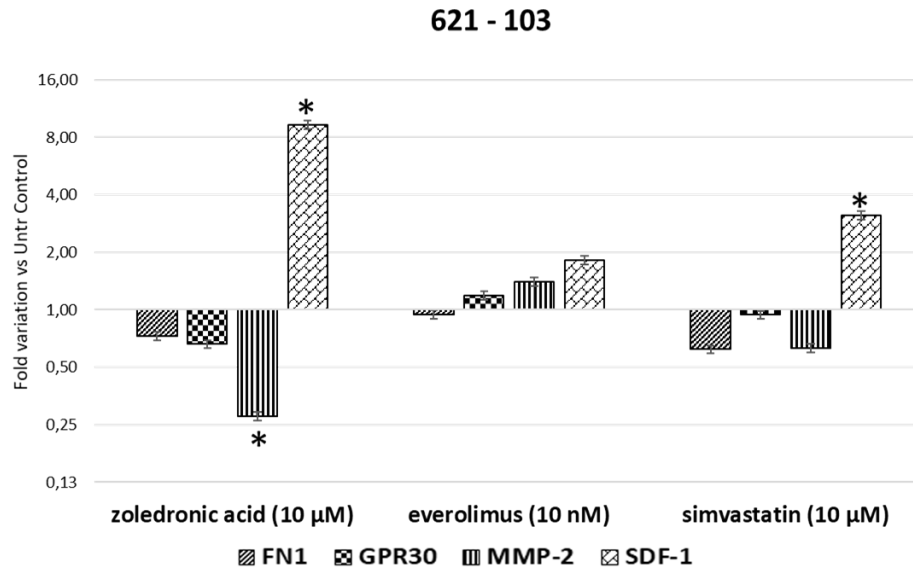


**Figure 29: Effects of zoledronic acid (10 µM), everolimus (10 nM) and simvastatin (10 µM) on gene expression.**

*Data from qRT-PCR are expressed as fold variation of gene expression in 621-103 cells. Data are expressed as mean ± SD of at least three experiments. \*= $P < 0.05$  vs control.*

## **5. Discussion**

Renal angiomyolipoma is a rare disease that can occur sporadically or in association with TSC.

Despite different observational studies, at now AML cell biology is still poorly defined and the underlying mechanisms of this disease are not yet known.

The heterogeneous nature of this benign mass adds more complexity in understanding the behavior and the possible therapeutic approaches.

In the first part of this study, for the first time, we describe the behavior of primary AML cells, originating from male and female patients, in terms of proliferation and migration in vitro, both in basal condition and in response to environmental stimuli.

Our findings clearly demonstrated that primary AML cells were able to migrate in vitro. We isolated a great number of cells by male (AML3) and female (AML4) angiomyolipoma, without a clinical history of TSC, on which we made different in vitro experiments.

First, we characterized the isolated cells: the two cultures were similar to each other regarding a mixed cell composition, according to the heterogeneous nature of AML. None of the cell types (smooth muscle, epithelioid, lipomatous and mesenchimal) in the cultures seemed to be predominant and this characteristic is an advantage in a pharmacology study, since the complexity of the tumor should be taken into account.

Independently from their TSC mutational status, we decided to ascertain whether these cells were able to migrate and if this process could be modulated pharmacologically.

In particular, taking advantage from the fact that our cells originated from male and female patients, we focused our attention on estrogen to investigate the high difference between the incidences of AML in patients with opposite gender. Moreover, we evaluated if the hypothesis that renal AML cells might migrate to the lung or other organs is true.

Despite the presence of the estrogen receptors, we have observed that there was no estrogenic influence on proliferation of both AMLs.

Although some common properties between the two AMLs have been described, we reported that other aspects seemed to differentiate the cells originating from male and female patients. We showed that the basal unstimulated migration of male AML3 had more rapid onset, respect to female AML4. This difference in spreading was already striking 4 hours after seeding, and also evident in the ability to invade, as demonstrated by three-dimensional assays. Together with this observation, we also reported that the higher basal migration of AML3 is less influenced by estrogen, while spreading of AML4 cells is significantly increased already after 2 hours incubation with 17- $\beta$ -estradiol (1 nM). In order to explain the response to estrogen, we investigated the expression of estrogen receptor: ER $\alpha$ , ER $\beta$ , and GPR30.

In our primary cells, we detected an abundant mRNA expression of GPR30, as described by Marino et al., respect to the nuclear receptor; this is coherent with the rapid non-genomic response to 17- $\beta$ -estradiol that we observed. The existence of a rapid, non-genomic response has also been confirmed by the ability of estradiol to quickly increase ERK1/2 phosphorylation in female AML4 (after 5 minutes of treatment with 17- $\beta$ -estradiol 1 nM) [113, 82].

Moreover, to verify whether the SDF-1 $\alpha$  is indispensable for migration also in our cells, we analyzed how they cells responded to it in this process. Our results are in accordance with the well-known role of SDF-1 $\alpha$  in cell migration; in fact, we have shown its significant effect in increasing the bi- and three-dimensional migration of these cells. The specificity of this observation was confirmed by the effect of the treatment with the selective SDF-1 $\alpha$  receptor antagonist plerixafor, which completely abolished SDF-1 $\alpha$  stimulation.

Analysis of the culture media collected from three-dimensional migration experiments revealed that the stimulation of migration induced by SDF-1 $\alpha$  was accompanied by an augmented release of MMPs, in particular of MMP-2. Also in this case, these effects were consistently reverted by the selective receptor antagonist plerixafor. Strikingly, such an increase in MMPs production was not observed in estradiol-stimulated conditions, despite a significant increase in cell migration. We therefore speculated that, while SDF-1 $\alpha$ -induced migration occurred through metalloproteases

production, the migratory response to estrogen most likely did not involve MMPs activity. Our results therefore might support the hypothesis that the host microenvironment tissue *stimuli* could exert a specific chemotactic signal to promote homing of AML cells as already seen in other study [37].

The primary culture approach, has inherent strengths and unfortunately, some limitations.

The restrictions are clear: since AML is a rare disease, it is difficult to obtain fresh AML tissues, indeed we could analyze two samples only. Moreover, the use of primary cultures restricted the number of studies that we could perform before losing them. For these reasons, we decided to strengthen our results by studying three immortalized AML cell lines: 4004 from male and 621-101, 621-103 from female patients with TSC.

In the second part of the study, to improve the results obtained on the primary cells, the same experiments were repeated on stabilized cells; then, we evaluated the effects of some drugs, belonging to different therapeutic classes, on the proliferation and migration of AML cells and on the expression of some genes crucial for these mechanisms.

At first, we decided to evaluate the effect of estrogen on the proliferation and migration of male and female cells. Renal AML masses are known to express estrogen receptor [76]; the analysis by means of western blot allowed us to affirm that even in all our cells great protein level of these receptors were expressed. However, through a qRT-PCR we observed an abundant mRNA expression of transmembrane estrogen receptor (GPR30) in 621-103 and 4004 cells with no significant differences between them. The discrepancy between the absence of signal in qRT-PCR and protein expression that we observed in 621-101 cells is astonishing, and hence we supposed that the most realistic way to explain it is to ascribe to a technical problem occurred during cell processing.

Although the presence of estrogen receptor, we reported also for these stabilized cells, that treatment with an increasing concentration of 17- $\beta$ -estradiol did not modify their proliferation.

The treatment of our cells with estrogen antagonist, tamoxifen, emphasized its dual action; already after 24 hours, low concentrations of tamoxifen provoked an increase of growth (statistically not significant), while over 10  $\mu$ M it induced a strong inhibition of proliferation in all cell lines. This



behavior confirmed the hypothesis of Prossnitz and colleagues according to tamoxifen promotes or inhibits cell proliferation based on the estrogen receptor it binds to [78].

Tamoxifen is able to bind ER $\alpha$  and ER $\beta$  and to inhibit proliferative stimulation, but it can also bind the transmembrane estrogenic receptors on which it acts like an agonist stimulating the proliferation [78]. Increased cell growth at low tamoxifen concentrations may indicate a greater affinity of the drug to transmembrane receptors rather than to nuclear estrogenic receptors.

About migration, we observed that also these stabilized cells were able to migrate in vitro in basal conditions. After 4 hours, the female cells were more responsive to the estrogen *stimuli* respect to the male cells.

Tamoxifen induced an increase in migration only for the female cells; this rapid increase might be associated to the agonist effect of tamoxifen on GPR30 receptor [82]. Moreover, in female 621-101 cells, this rapid increase in migration, induced both by 17- $\beta$ -estradiol and tamoxifen, can be associated with the phosphorylation of p42/44 MAPK that we observed through western blot analysis; an analogous situation has been described by Liu et al. in non-small cell lung cancer [114].

In 4004 and 621-103 cells the treatment with these molecules did not induce any modification in phosphorylation of ERK1/2; the ratio of pAkt/Akt was not modified in any cell line after these treatments. Therefore, we can suggest that the phosphorylation of Akt did not correlate with the migration under hormonal *stimuli*. Analogous results were previously observed by Clements and colleagues in a xenograft AML in which phosphorylation of Akt and p42/44 MAPK were not affected by oestrogen treatment [20].

The effect on the MMP-2 gene expression on human renal angiomyolipoma cell lines treated with 17- $\beta$ -estradiol and tamoxifen for 4 hours underlined that TSC status was involved. The decrease of MMP-2 gene was similar in 4004 and 621-101 (TSC2<sup>-/-</sup>) cells under the effect of 17- $\beta$ -estradiol; on the contrary, after the treatment with tamoxifen, the inhibition on MMP-2 was similar in the 4004 and in 621-103 (TSC2<sup>+/+</sup>).

Although the molecular events responsible for angiomyolipomas development are not fully understood, mutations in TSC1 or TSC2 result in a hyper-activation of the mammalian target of rapamycin (mTOR) signaling pathway [115,116].

Rapamycin and its derivatives, such as everolimus, have been suggested as therapeutic approaches for AML, since they block mTOR pathway, and some clinical trials demonstrated that these drugs reduce AML size. [46; 117].

The first study demonstrating an anti-proliferative effect of mTOR inhibitors in angiomyolipoma, was published in 2008 [118], since then, clinical data suggest that alternative or adjuvant drugs are still needed because of the side effects of the mTOR inhibitor.

The treatment with everolimus reduced the growth already after 24 hours of treatment at different drug concentrations for our cell lines. For TSC2<sup>-/-</sup> cells the inhibition occurred at 1 and 10  $\mu$ M (for 4004 and 621-101 cells respectively); while for 621-103 the inhibition occurred after at 100  $\mu$ M. This different sensitivity to everolimus could be caused by mutation in TSC2: when TSC2 is missing mTOR is active, when TSC2 is present (as in 621-103) mTOR is inactive. We may suppose that everolimus exert a greater cytotoxic effect in cells in which mTOR is hyperactive; such as on 4004 and 621-101 cells.

The treatment of AML with bisphosphonates such as like zoledronic acid provoked a decrease in cell proliferation probably by inhibiting angiogenetic factors or inducing microenvironment changes that decreased tumor growth [97, 99,119,100]. In all cell lines, the association of these drugs caused a inhibition of cell growth at any incubation time.

Moreover, the simultaneous incubation of zoledronic acid and everolimus potentiate their inhibitory migration properties; however the combination of these drugs had major effect on female 621-101 cells compared to the male ones. The association of everolimus and zoledronic acid led to a double action on the mTOR pathway: everolimus acted directly on mTOR, zoledronic acid acted further upstream, inhibiting the action of GTPase Rho and leading to a consequent inactivation of mTOR.

Our encouraging results on AML cells allow us to affirm that combination of these drugs may be used to limit the side effects of high everolimus doses. Additionally, we have studied drugs with different mechanism of action, such as simvastatin, that have been proposed to inhibit AML cell growth and migration through the signal transduction Akt-mTOR axis. In our study, the treatment with simvastatin inhibited both proliferation and three dimensional migration of our cells, so it may be a potential therapeutic agent for the treatment of AML.

Mevalonate is not only a precursor of cholesterol synthesis but also a precursor of nonsteroidal isoprenoid compounds. In a precedent study, Martin and colleagues described that statins inhibit the activity of PPAR $\gamma$  [120]. PPAR $\gamma$  has been classically regarded as a master regulator of adipogenesis [121], but more recent studies have demonstrated its involvement in various cellular processes, including proliferation, apoptosis, angiogenesis, and cancer [28]. On these bases, we can speculate that the action of statin observed on our cells might depend on PPAR $\gamma$ , as recently observed on in vivo xenograft AML model by Pleniceanu and colleagues. Therefore, also in our cells PPAR $\gamma$  might be a new potential therapeutic target for AML.

To clarify the signaling pathways underlying everolimus, zoledronic acid and simvastatin mediated responses in AML cells we further examined the effect of these drugs on the activation of the AKT and ERK pathways. We found that the treatment for 4 hours with zoledronic acid and everolimus significantly suppressed the phosphorylation of Akt in 621-101 cells; in the other cell lines the reduction of this phosphorylation was observed after treatment with everolimus or simvastatin. Treatment with simvastatin induced a reduction in ERK phosphorylation only in 621-101 and 4004 cells only.

A striking difference was observed between cell lines in terms of Akt and Erk phosphorylation and the modulation of the expression of genes involved in adhesion/invasiveness despite the similar response to drugs in terms of cell migration.

It is important to underline that all drugs exerted important effects in regulation of MMP-2 and FN-1 genes, both implicated in neoplastic aggressiveness, in 621-101 female cells compared to 4004 cells

and also, in 4004 and 621-103 cells. The differences observed in the expression of these important genes involved in migration, suggest that it is necessary a different therapeutic approach in female and male patients with TSC-associated or sporadic AML.

In conclusion, the results obtained from primary and stabilized cells, for what concerns the estradiol treatment, confirmed the different behavior of female and male cells with or without mutations in TSC2 gene. In either models, estrogen did not modify the proliferation of AML cells, but increased the migration only for the female cells. Moreover, analyzing the different experiments performed on stabilized cells, we can conclude that, in most of our tests, the male 4004 TSC2<sup>-/-</sup> cells and the female 621-103 TSC<sup>+/+</sup> cells had a similar behavior, such as that the restoration of the mutation was responsible for masculinization of the cellular phenotype.

These studies have provided valuable results to support the hypotheses seen in the literature of the involvement of estrogens in the migration of AML toward other sites such as lung and potential development of LAM. This might be of great importance under a diagnostic and prognostic point of view, since patients with AML might be monitored more closely to identify LAM as soon as possible. Furthermore, our results could lead to the definition of an effective drug therapy that almost completely replaces, or delays, AML mass removal surgery or nephrectomy in order to offer a higher quality of life to the patient.

## **6. Bibliography**

1. Barnard M. and Lajoie G. Angiomyolipoma: Immunohistochemical and Ultrastructural Study of 14 Cases. *Ultrastructural Pathology* 2001, 25:21-29.
2. Esheba G.E.S. and Esheba N.E.S. Angiomyolipoma of the kidney: Clinicopathological and immunohistochemical study. *Journal of the Egyptian National Cancer Institute* 2013, 25, 125–134.
3. Martignoni G., Pea M., Reghellin D., Zamboni G., Bonetti F. PEComas: the past, the present and the future. *Virchows Arch* 2008, 452:119–132.
4. Ashfaq R., Weinberg A.G., Albores-Saavedra J. Renal angiomyolipomas and HMB-45 reactivity. *Cancer* 1993, 71,;3091-7.
5. Pea M., Bonetti F., Zamboni G., Martignoni G., Riva M., et al. Melanocyte-marker-HMB-45 is regularly expressed in angiomyolipoma of the kidney. *Pathology* 1991, 23:185-8.
6. de Silva S., Copping R., Malouf D., Hutton A., Maclean F., Aslan P. Frequency of Angiomyolipomas Among Echogenic Nonshadowing Renal Masses (> 4 mm) Found at Ultrasound and the Utility of MRI for Diagnosis. *AJR* 2017, 209, 1-7.
7. Hohensee S.E., La Rosa F.G., Homer P., Suby-Long T., Wilson S., et al. Renal epithelioid angiomyolipoma with a negative premelanosome marker immunoprofile: a case report and review of the literature. *Journal of Medical Case Report* 2013, 7:118.
8. Taveria-DaSilva A.M., Stegall W.K., Moss J. Lymphangioliomyomatosis. *Cancer Control* 2006, 13:276-85.
9. Flum A.S., Hamoui N., Said M.A., Yang X.J., Casalino D.D., et al. Update on the Diagnosis and Management of Renal Angiomyolipoma. *J Urol.* 2017, 195:834-46.
10. Rabenou R.A. and Charles H.W. Differentiation of Sporadic Versus Tuberous Sclerosis Complex-Associated Angiomyolipoma. *AJR Am J Roentgenol.* 2015, 205:292-301.
11. Oesterling J.E., Fishman E.K., Goldman S.M., Marshall F.F. The management of renal angiomyolipoma. *J Urol.* 1986, 135:1121-4.

12. Bissler J.J., Franz D.N., Frost M.D., Belousova E., Bebin E.M., et al. The effect of everolimus on renal angiomyolipoma in pediatric patients with tuberous sclerosis being treated for subependymal giant cell astrocytoma. *Pediatr Nephrol.* 2018, 33:101-109.
13. Coombs E.J. Role of mTOR inhibition in the treatment of patients with renal angiomyolipomas. *J Am Assoc Nurse Pract.* 2013, 25:588-96.
14. Grzegorek I., Drozd K., Podhorska-Oklow M., Szuba A., Dziegiel P. LAM cells biology and lymphangioliomyomatosis. *Folia Histochem Cytobiol.* 2013, 51:1-10.
15. Kobayashi T., Hirayama Y., Kobayashi E., Kubo Y., Hino O. A germline insertion in the tuberous sclerosis (Tsc2) gene gives rise to the Eker rat model of dominantly inherited cancer. *Nat Genet* 1995, 9:70-74
16. Kobayashi T., Urakami S., Cheadle J.P., Aspinwall R., Harris P., et al. Identification of a leader exon and a core promoter for the rat tuberous sclerosis 2 (Tsc2) gene and structural comparison with the human homolog. *Mamm Genome* 1997, 8: 554-8.
17. Onda H, Lueck A, Marks PW, Warren HB, Kwiatkowski DJ. TSC2<sup>+/-</sup> mice develop tumors in multiple sites which express gelsolin and are influenced by genetic background. *J Clin Invest* 1999, 104: 687-95.
18. Yu J., Astrinidis A., Howard S., Henske E.P. Estradiol and tamoxifen stimulate LAM-associated angiomyolipoma cell growth and activate both genomic and nongenomic signaling pathways. *Am J Physiol Lung Cell Mol Physiol.* 2004, 286:L694-700.
19. Lesma E., Grande V., Carelli S., Brancaccio D., Canevini M.P., et al. Isolation and growth of smooth muscle-like cells derived from tuberous sclerosis complex-2 human renal angiomyolipoma: epidermal growth factor is the required growth factor. *Am J Pathol.* 2005, 167:1093-103.
20. Clements D., Asprey S.L., McCulloch T.A., Morris T.A., Watson S.A., Johnson S.R. Analysis of the oestrogen response in an angiomyolipoma derived xenograft model. *Endocr Relat Cancer* 2009, 16:59–72

21. Henske E.P. Metastasis of benign tumor cells in tuberous sclerosis complex. *Genes Chromosomes Cancer*. 2003,38:376-81.
22. Curatolo P., Bombardieri R., Jozwiak S. Tuberous sclerosis. *Lancet*. 2008, 372:657-68.
23. Carsillo T., Astrinidis A., Henske E.P. Mutations in the tuberous sclerosis complex gene TSC2 are a cause of sporadic pulmonary lymphangiomyomatosis. *Proc Natl Acad Sci U S A*. 2000, 23, 97:6085-90.
24. Crino P.B., Nathanson K.L., Henske E.P. The tuberous sclerosis complex. *N Engl J Med*. 2006, 28, 355:1345-56.
25. Karbowniczek M., Yu J., Henske E.P. Renal angiomyolipomas from patients with sporadic lymphangiomyomatosis contain both neoplastic and non-neoplastic vascular structures. *Am J Pathol*. 2003,162:491-500.
26. Kay R.A., Ellis I.R., Jones S.J., Perrier S., Florence M.M., et al. The expression of migration stimulating factor, a potent oncofetal cytokine, is uniquely controlled by 3'-untranslated region-dependent nuclear sequestration of its precursor messenger RNA. *Cancer Res*. 2005, 1, 65:10742-9.
27. Pacheco-Rodriguez G., Kumaki F., Steagall W.K., Zhang Y., Ikeda Y., et al. Chemokine-enhanced chemotaxis of lymphangiomyomatosis cells with mutations in the tumor suppressor TSC2 gene. *J Immunol*. 2009, 182:1270-7.
28. Pleniceanu O., Shukrun R., Omer D., Vax E., Kanter I., et al. PPAR $\gamma$  is central to the initiation and propagation of human angiomyolipoma, suggesting its potential as a therapeutic target. *EMBO Mol Med*. 2017, 9:508-530.
29. Liang N., Zhang C., Dill P., Panasyuk G., Pion D., et al. Regulation of YAP by mTOR and autophagy reveals a therapeutic target of tuberous sclerosis complex. *J Exp Med*. 2014, 211:2249-63.



30. Evans S.E., Colby T.V., Ryu J.H., Limper A.H. Transforming growth factor-beta 1 and extracellular matrix-associated fibronectin expression in pulmonary lymphangioleiomyomatosis. *Chest*. 2004, 125:1063-70.
31. Moir L.M., Ng H.Y., Poniris M.H., Santa T., Burgess J.K., et al. Doxycycline inhibits matrix metalloproteinase-2 secretion from TSC2-null mouse embryonic fibroblasts and lymphangioleiomyomatosis cells. *Br J Pharmacol*. 2011, 164:83-92.
32. Lee P.S., Tsang S.W., Moses M.A., Traves-Gibson Z., Hsiao L.L., et al. Rapamycin-insensitive up-regulation of MMP2 and other genes in tuberous sclerosis complex 2-deficient lymphangioleiomyomatosis-like cells. *Am J Respir Cell Mol Biol*. 2010, 42:227-34.
33. Odajima N., Betsuyaku T., Nasuhara Y., Inoue H., Seyama K., Nishimura M. Matrix metalloproteinases in blood from patients with LAM. *Respir Med*. 2009, 103:124-9.
34. Matsui K., Takeda K., Yu Z.X., Travis W.D., Moss J., Ferrans V.J. Role for activation of matrix metalloproteinases in the pathogenesis of pulmonary lymphangioleiomyomatosis. *Arch Pathol Lab Med*. 2000, 124:267-75.
35. Hayashi T., Fleming M.V., Stetler-Stevenson W.G., Liotta L.A., Moss J., et al. Immunohistochemical study of matrix metalloproteinases (MMPs) and their tissue inhibitors (TIMPs) in pulmonary lymphangioleiomyomatosis (LAM). *Hum Pathol*. 1997, 28:1071-8.
36. Scannevin R.H., Alexander R., Haarlander T.M., Burke S.L., Singer M., et al. Discovery of a highly selective chemical inhibitor of matrix metalloproteinase-9 (MMP-9) that allosterically inhibits zymogen activation. *J Biol Chem*. 2017, 292:17963-17974.
37. Clements D., Markwick L.J., Puri N., Johnson S.R. Role of the CXCR4/CXCL12 axis in lymphangioleiomyomatosis and angiomyolipoma. *J Immunol*. 2010, 185:1812-21.
38. Tanaka T., Bai Z., Srinoulprasert Y., Yang B., Hayasaka H., Miyasaka M. Chemokines in tumor progression and metastasis. *Cancer Sci*. 2005, 96:317-22.

39. Li J.K., Yu L., Shen Y., Zhou L.S., Wang Y.C., Zhang J.H. Inhibition of CXCR4 activity with AMD3100 decreases invasion of human colorectal cancer cells in vitro. *World J Gastroenterol.* 2008, 21, 14:2308-13.
40. Baggiolini M., Dewald B., Moser B. Human chemokines: an update. *Annu Rev Immunol.* 1997, 15:675-705.
41. Ryu J.H., Moss J., Beck G.J., Lee J.C., Brown K.K., et al. The NHLBI lymphangioleiomyomatosis registry: characteristics of 230 patients at enrollment. *Am J Respir Crit Care Med.* 2006, 173:105-11.
42. Cohen M.M., Pollock-BarZiv S., Johnson S.R. Emerging clinical picture of lymphangioleiomyomatosis. *Thorax.* 2005, 60:875-9.
43. Johnson S.R. Lymphangioleiomyomatosis. *Eur Respir J.* 2006, 27:1056-65.
44. Taveira-DaSilva A.M. and Moss J. Management of lymphangioleiomyomatosis. *F1000Prime Rep.* 2014, 6:116.
45. McCormack F.X., Inoue Y., Moss J., Singer L.G., Strange C., et al. Efficacy and safety of sirolimus in lymphangioleiomyomatosis. *N Engl J Med.* 2011, 364:1595-606.
46. Taveira-DaSilva A.M., Hathaway O., Stylianou M., Moss J. Changes in lung function and chyloous effusions in patients with lymphangioleiomyomatosis treated with sirolimus. *Ann Intern Med.* 2011, 21, 154:797-805, W-292-3.
47. Inoki K. and Guan K.L. Tuberous sclerosis complex, implication from a rare genetic disease to common cancer treatment. *Hum Mol Genet.* 2009, 18:R94-100.
48. O'Callaghan F.J., Shieff A.W., Osborne J.P., Martyn C.N. Prevalence of tuberous sclerosis estimated by capture-recapture analysis. *Lancet* 1998, 351(9114):1490.
49. Henske E.P. Tuberous sclerosis and the kidney: from mesenchyme to epithelium, and beyond. *Pediatr Nephrol* 2005, 20:854–857.
50. Orlova K.A. and Crino P.B. The tuberous sclerosis complex. *Ann N Y Acad Sci.* 2010, 1184: 87–105.

51. Rakowski S.K., Winterkorn E.B., Paul E., Steele D.J., Halpern E.F., Thiele E.A. Renal manifestations of tuberous sclerosis complex: Incidence, prognosis, and predictive factors. *Kidney Int.* 2006, 70:1777-82.
52. Giannikou K., Malinowska I.A., Pugh T.J., Yan R., Tseng Y.Y., et al. Whole Exome Sequencing Identifies TSC1/TSC2 Biallelic Loss as the Primary and Sufficient Driver Event for Renal Angiomyolipoma Development. *PLoS Genet.* 2016, 12:e1006242.
53. Caban C., Khan N., Hasbani D.M., Crino P.B. Genetics of tuberous sclerosis complex: implications for clinical practice. *Appl Clin Genet.* 2016,10:1-8.
54. Smolarek T.A., Wessner L.L., McCormack F.X., Mylet J.C., Menon A.G., Henske E.P. Evidence that lymphangiomyomatosis is caused by TSC2 mutations: chromosome 16p13 loss of heterozygosity in angiomyolipomas and lymph nodes from women with lymphangiomyomatosis. *Am J Hum Genet.* 1998, 62:810-5.
55. Wullschleger S., Loewith R., Hall M.N. TOR Signaling in Growth and Metabolism. *Cell.* 2006, 10,124:471-84.
56. Kennedy B. and Pennypacker J.K. Mammalian Target of Rapamycin: A Target for (Lung) Diseases and Aging. *Ann Am Thorac Soc.* 2016,13:S398-S401.
57. Grahammer F., Wanner N., Huber T.B. mTOR controls kidney epithelia in health and disease. *Nephrol Dial Transplant* 2014, 29: 9–18.
58. Laboucarié T., Detilleux D., Rodriguez-Mias R.A., Faux C., Romeo Y., et al. TORC1 and TORC2 converge to regulate the SAGA co-activator in response to nutrient availability. *EMBO reports* 2017,
59. Planelles M., Macías L., Peiró G., Bulimbasič S., Hes O., et al. Rheb/mTOR/p70s6k Cascade and TFE3 Expression in Conventional and Sclerosing PEComas of the Urinary Tract. *Appl Immunohistochem Mol Morphol.* 2016, 24:514-20.

60. Dobashi Y., Suzuki S., Sato E., Hamada Y., Yanagawa T., Ooi A. EGFR-dependent and independent activation of Akt/mTOR cascade in bone and soft tissue tumors. *Mod Pathol.* 2009,22:1328-40.
61. Ishii T., Kohashi K., Iura K., Maekawa A., Bekki H., et al. Activation of the Akt-mTOR and MAPK pathways in dedifferentiated liposarcomas. *Tumor Biol.* 2016, 37:4767–4776.
62. Chuang C-K., Lin A.C.A., Tasi H-Y., Lee K-H., Kap Y., et al. Clinical presentations and molecular studies of invasive renal epithelioid angiomyolipoma. *Int Urol Nephrol* 2017, 49:1527–1536.
63. Altomare D.A. and Testa J.R. Perturbations of the AKT signaling pathway in human cancer. *Oncogene* 2005, 24, 7455–7464.
64. Thant A.A., Nawa A., Kikkawa F., Ichigotani Y., Zhang Y., et al. Fibronectin activates matrix metalloproteinase-9 secretion via the MEK1-MAPK and the PI3K-Akt pathways in ovarian cancer cells. *Clin Exp Metastasis.* 2000,18:423-8.
65. Larue L. and Bellacosa A. Epithelial–mesenchymal transition in development and cancer: role of phosphatidylinositol 30 kinase/AKT pathways. *Oncogene* 2005, 24, 7443–7454.
66. Sen T., Dutta A., Maity G., Chatterjee A. Fibronectin induces matrix metalloproteinase-9 (MMP-9) in human laryngeal carcinoma cells by involving multiple signaling pathways. *Biochimie* 2010, 92, 1422-1434.
67. Ersahin T., Tuncbag N., Cetin-Atalay R. The PI3K/AKT/mTOR interactive pathway. *Mol. BioSyst.* 2015, 11, 1946-1954.
68. Johnson S.R. and Tattersfield A.E. Lymphangiomyomatosis. *Seminars in respiratory and critical care medicine* 2002, 23, 2.
69. Wortzel I. and Seger R. The ERK Cascade: Distinct Functions within Various Subcellular Organelles. *Genes & Cancer* 2011, 2:195–209.
70. Kirchner G.I., Meier-Wiedenbach I., Manns M.P. Clinical pharmacokinetics of everolimus. *Clin Pharmacokinet.* 2004,43:83-95.

71. Hartford C.M. and Ratain M.J. Rapamycin: something old, something new, sometimes borrowed and now renewed. *Clin Pharmacol Ther.* 2007,82:381-8.
72. Moavero R., Pinci M., Bombardieri R., Curatolo P. The management of subependymal giant cell tumors in tuberous sclerosis: a clinician's perspective. *Childs Nerv Syst.* 2011,27:1203-10.
73. Yang J., Samsel P.A., Narov K., Jones A., Gallacher D., et al. Combination of Everolimus with Sorafenib for Solid Renal Tumors in Tsc2<sup>+/-</sup> Mice Is Superior to Everolimus Alone. *Neoplasia.* 2017,19:112-120.
74. Samuels J.A. Treatment of Renal Angiomyolipoma and Other Hamartomas in Patients with Tuberous Sclerosis Complex. *Clin J Am Soc Nephrol.* 2017, 12:1196-1202.
75. Glassberg M.K., Elliot S., Fritz J., Catanuto P., Potier M., et al. Activation of the estrogen receptor contributes to the progression of pulmonary lymphangiomyomatosis via matrix metalloproteinase-induced cell invasiveness. *J Clin Endocrinol Metab.* 2008,93:1625-33.
76. Boorjian S.A., Sheinin Y., Crispen P.L., Lohse C.M., Kwon E.D., Leibovich B.C. Hormone receptor expression in renal angiomyolipoma: clinicopathologic correlation. *Urology* 2008, 72:927-32.
77. Bernstein L. and Ross R.K. Endogenous hormones and breast cancer risk. *Epidemiologic Review* 1993, 15: 48-65.
78. Prossnitz E.R., Arterburn J.B., Smith H.O., Opera T.I. Sklar L.A., Hathaway H.J. Estrogen Signaling through the Transmembrane G Protein–Coupled Receptor GPR30. *Annu. Rev. Physiol.* 2008, 70:165–90.
79. Edwards D.P. Regulation of signal transduction pathways by estrogen and progesterone. *Annu. Rev. Physiol.* 2005, 67:335–76.
80. Dennis M.K., Field A.S., Burai R., Ramesh C., Petrie W.K., et al. Identification of a GPER/GPR30 antagonist with improved estrogen receptor counterselectivity. *J Steroid Biochem Mol Biol.* 2011, 127:358-66.

81. Jala V.R., Radde B.N., Haribabu B., Klinge C.M. Enhanced expression of G-protein coupled estrogen receptor (GPER/GPR30) in lung cancer. *BMC Cancer*. 2012,12:624.
82. Marino M., Galluzzo P., Ascenzi P. Estrogen signaling multiple pathways to impact gene transcription. *Curr Genomics*. 2006, 7:497-508.
83. Lange C.A. Integration of progesterone receptor action with rapid signaling events in breast cancer models. *J Steroid Biochem Mol Biol*. 2008, 108:203-12.
84. Pandey D.P., Lappano R., Albanito L., Madeo A., Maggiolini M., Picard D. Estrogenic GPR30 signalling induces proliferation and migration of breast cancer cells through CTGF. *EMBO J*. 2009, 28:523-32.
85. McGuire W.L. Current status of estrogen receptors in human breast cancer. *Cancer* 1975, 36: 638-644.
86. Mandlekar S. and Kong A.N. Mechanisms of tamoxifen-induced apoptosis. *Apoptosis*. 2001, 6:469-77.
87. Katzenellenbogen B.S. and Katzenellenbogen J.A. Estrogen receptor transcription and transactivation: Estrogen receptor alpha and estrogen receptor beta: regulation by selective estrogen receptor modulators and importance in breast cancer. *Breast Cancer Res*. 2000, 2:335-44.
88. Bogush T., Dudko E., Bogush E., Polotsky B., Tjulandin S., Davydov M. Tamoxifen non-estrogen receptor mediated molecular targets. *Oncol Rev*. 2012, 6:e15.
89. Rondón-Lagos M., Rangel N., Di Cantogno L.V., Annaratone L., Castellano I., et al. Effect of low doses of estradiol and tamoxifen on breast cancer cell karyotypes. *Endocr Relat Cancer* 2016, 23:635-50.
90. Siroky B.J., Yin H., Bissler J.J. Clinical and molecular insights into tuberous sclerosis complex renal disease. *Pediatr Nephrol*. 2011, 26:839-52.

91. Fang Z., Tang Y., Fang J., Zhou Z., Xing Z., et al. Simvastatin inhibits renal cancer cell growth and metastasis via AKT/mTOR, ERK and JAK2/STAT3 pathway. *PLoS One*. 2013, 8:e62823.
92. Ory B., Heymann M.F., Kamijo A., Gouin F., Heymann D., Redini F. Zoledronic acid suppresses lung metastases and prolongs overall survival of osteosarcoma-bearing mice. *Cancer* 2005,104:2522-9.
93. Yamasaki M., Yuasa T., Uehara S., Fujii Y., Yamamoto S., et al. Improvement of renal function by changing the bone-modifying agent from zoledronic acid to denosumab. *Int J Clin Oncol*. 2016, 21:1191-1195.
94. Heymann D., Ory B., Gouin F., Green J.R., Rédini F. Bisphosphonates: new therapeutic agents for the treatment of bone tumors. *Trends Mol Med*. 2004,10:337-43.
95. Benford H.L., McGowan N.W., Helfrich M.H., Nuttall M.E., Rogers M.J. Visualization of bisphosphonate-induced caspase-3 activity in apoptotic osteoclasts in vitro. *Bone* 2001, 28:465–473.
96. Fiore F., Castella B., Nuschak B., Bertieri R., Mariani S., et al. Enhanced ability of dendritic cells to stimulate innate and adaptive immunity upon short-term incubation with zoledronic acid. *Blood* 2007, 110:921-927.
97. Cimini E., Piacentini P., Sacchi A., Gioia C., Leone S., et al. Zoledronic acid enhances V $\delta$ 2 T-lymphocyte antitumor response to human glioma cell lines. *Int J Immunopathol Pharmacol*. 2011,24:139-48.
98. Denoyelle C., Hong L., Vannier J.P., Soria J., Soria C. New insights into the actions of bisphosphonate zoledronic acid in breast cancer cells by dual RhoA-dependent and -independent effects. *Br J Cancer* 2003, 88:1631-40.
99. Santini D., Vincenzi B., Galluzzo S., Battistoni F., Rocci L., Venditti O., et al. Repeated intermittent low-dose therapy with zoledronic acid induces an early, sustained, and long-

- lasting decrease of peripheral vascular endothelial growth factor levels in cancer patients. *Clin Cancer Res.* 2007, 13:4482-6.
100. Holen I. and Coleman R.E. Anti-tumour activity of bisphosphonates in preclinical models of breast cancer. *Breast Cancer Res.* 2010, 12:214.
101. Mognetti B., La Montagna G., Perrelli M.G., Marino S., Pagliaro P., et al. Zoledronic Acid and Leuprorelin Acetate, Alone or in Combination, Similarly Reduce Proliferation and Migration of Prostate Cancer Cells In Vitro. *International Journal of Medical Biology.* 2014, 1:1–7.
102. Boissier S., Ferreras M., Peyruchaud O., Magonetto S., Ebetino F.H., et al. Bisphosphonates inhibit breast and prostate carcinoma cell invasion, an early event in the formation of bone metastases. *Cancer Res.* 2000, 60:2949-54.
103. Pécheur I., Peyruchaud O., Serre C.M., Guglielmi J., Volland C., et al. Integrin alpha(v)beta3 expression confers on tumor cells a greater propensity to metastasize to bone. *FASEB J.* 2002, 16:1266-8.
104. Osmak M. Statins and cancer: Current and future prospects. *Cancer Lett.* 2012, 324:1-12.
105. Sekine Y., Furuya Y., Nishii M., Koike H., Matsui H., Suzuki K. Simvastatin inhibits the proliferation of human prostate cancer PC-3 cells via down-regulation of the insulin-like growth factor 1 receptor. *Biochem Biophys Res Commun.* 2008, 372:356-61.
106. Goncharova E.A., Goncharov D.A., Li H., Pimtong W, Lu S., et al. mTORC2 is required for proliferation and survival of TSC2-null cells. *Mol Cell Biol.* 2011, 31:2484-98.
107. Rattan R., Giri S., Singh A.K., Singh I. Rho/ROCK pathway as a target of tumor therapy. *J Neurosci Res.* 2006, 83:243-55.
108. Atochina-Vasserman E.N., Goncharov D.A., Volgina A.V., Milavec M., James M.L., Krymskaya V.P. Statins in lymphangiomyomatosis. Simvastatin and atorvastatin induce



- differential effects on tuberous sclerosis complex 2-null cell growth and signaling. *Am J Respir Cell Mol Biol.* 2013, 49:704-9.
109. Lim S.D., Stallcup W., Lefkove B., Govindarajan B., Au K.S. et al. Expression of the Neural Stem Cell Markers NG2 and L1 in Human Angiomyolipoma: Are Angiomyolipomas Neoplasms of Stem Cells? *Mol Med.* 2007, 13, 160-165.
110. Pascal D., Giovannelli A., Gnani S., Hoyng S.A., de Winter F., et al. Characterization of glial cell models and in vitro manipulation of the neuregulin1/ErbB system. *Biomed Res Int.* 2014, 2014:310215.
111. Moriceau G., Ory B., Mitrofan L., Riganti C., Blanchard F., et al. Zoledronic Acid Potentiates mTOR Inhibition and Abolishes the Resistance of Osteosarcoma Cells to RAD001 (Everolimus): Pivotal Role of the Prenylation Process. *AACR.* 2010, 70, 10329-39.
112. Racca S., Piccione F., Spaccamiglio A., Carriero V. M.A., De Francia S., et al. Effects of sub-chronic nandrolone administration on hormonal adaptive response to acute stress in rats. *Psychoneuroendocrinology* 2012, 37, 1234-1247.
113. Henske E.P. The genetic basis of kidney cancer: why is tuberous sclerosis complex often overlooked? *Curr Mol Med.* 2004, 4:825-31.
114. Liu C., Liao Y., Fan S., Tang H., Jiang Z., et al. G protein-coupled estrogen receptor (GPER) mediates NSCLC progression induced by 17 $\beta$ -estradiol (E2) and selective agonist G1. *Med Oncol.* 2015,32:104.
115. Curatolo P. and Moavero R. mTOR Inhibitors in Tuberous Sclerosis Complex. *Curr Neuropharmacol.* 2012, 10:404-15.
116. Kapoor A., Girard L., Lattouf J.B., Pei Y., Rendon R., Card P., So A. Evolving Strategies in the Treatment of Tuberous Sclerosis Complex-Associated Angiomyolipomas (TSC-AML). *Urology.* 2016, 89:19-26.

117. Hatano T., Atsuta M., Inaba H., Endo K., Egawa S. Effect of everolimus treatment for renal angiomyolipoma associated with tuberous sclerosis complex: an evaluation based on tumor density. *Int J Clin Oncol.* 2017, 18.
118. Bissler J.J., McCormack F.X., Young L.R., Elwing J.M., Chuck G., et al. Sirolimus for angiomyolipoma in tuberous sclerosis complex or lymphangiomyomatosis. *N Engl J Med.* 2008, 358:140-51.
119. Lacerna L. and Hohneker J. Zoledronic acid for the treatment of bone metastases in patients with breast cancer and other solid tumors. *SeminOncol.* 2003, 30:150-60. 6.
120. Martin G., Duez H., Blanquart C., Berezowski V., Poulain P., et al. Statin-induced inhibition of the Rho-signaling pathway activates PPARalpha and induces HDL apoA-I. *J Clin Invest.* 2001, 107:1423-32.
121. Lehrke M. and Lazar M.A. The many faces of PPARgamma. *Cell* 2005, 123: 993 – 999.

## 7. PUBLICATIONS

1. Francesca Bertolini, Giulia Casarotti, Luisella Righi, Enrico Bollito, Carlo Albera, Silvia Anna Racca, Donato Colangelo, Barbara Moggetti. Human renal angiomyolipoma cells of male and female origin can migrate and are influenced by microenvironmental factors. Submitted for publication to Plos One.
2. Giuseppe La Montagna, Francesca Bertolini, Barbara Moggetti. Zoledronic acid and leuprorelide acetate affect DU-145 migration towards stem cell conditioned medium. Submitted for publication to The Prostate.

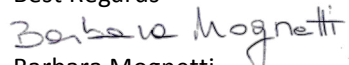
Orbassano, October 16<sup>th</sup>, 2017

Dear Editor, dear Reviewers

We are grateful for the determination of the Academic Editor.

We hope we fulfilled your request, we thank you for having positively reconsidered our manuscript for publication and we are waiting for a your final communication on PLOS ONE decision. Please do not hesitate to contact us for any further information you might need.

Best Regards

  
Barbara Mognetti

1  
2 **Human renal angiomyolipoma cells of male and female origin can migrate and are influenced by**  
3 **microenvironmental factors**

4  
5 Running title: In vitro migration of cells derived from human renal angiomyolipoma

6  
7 **Authors:**

8 Francesca Bertolini<sup>1</sup>, Giulia Casarotti<sup>2</sup>, Luisella Righi<sup>3</sup>, Enrico Bollito<sup>4</sup>, Carlo Albera<sup>1</sup>, Silvia Anna Racca<sup>1</sup>,  
9 Donato Colangelo<sup>2</sup>, Barbara Mognetti<sup>1\*</sup>.

10  
11 <sup>1</sup> Department of Clinical and Biological Science, University of Turin, Regione Gonzole 10, 10043, Orbassano,  
12 Italy

13 <sup>2</sup> Department of Health Sciences, Università del Piemonte Orientale, Via Solaroli 17, 28100 Novara, Italy

14 <sup>3</sup> Pathology Unit, Department of Oncology, University of Turin, Regione Gonzole 10, 10043, Orbassano, Italy

15 <sup>4</sup> Pathology Unit, San Luigi Gonzaga Hospital, Regione Gonzole 10, 10043, Orbassano, Torino, Italy

16  
17 \*[barbara.mognetti@unito.it](mailto:barbara.mognetti@unito.it) (BM)

18  
19  
20 **Keywords:**

21 Angiomyolipoma; Lymphangioliomyomatosis; Cell Migration; Estrogen Effect; In Vitro Techniques

## Abstract

Improving the knowledge of angiomyolipoma physiopathology might help in understanding the link with pulmonary lymphangioleiomyomatosis lesions. We investigated if angiomyolipoma cells have migratory properties, how their growth and motility can be influenced by the hormonal milieu, and if this can be related to a specific gender. Primary cells were isolated from angiomyolipomas surgically resected for therapeutical reasons in a female and in a male patient. Bi- (wound healing) and three-dimensional (transwell assay) migration were analyzed in vitro in basal conditions and under the influence of 17- $\beta$ -estradiol and SDF-1 $\alpha$ . Treatment up to 72 hours with 17- $\beta$ -estradiol (0.1-100 nM), tamoxifen (0.2-20  $\mu$ M) or with both, does not modify angiomyolipoma cells proliferation. On the other hand, SDF-1 $\alpha$  and 17- $\beta$ -estradiol treatment induce a significant motility increase (both bi- and three-dimensional) which becomes evident already after 2 hours of incubation. Angiomyolipoma cells express mRNA coding for SDF-1 $\alpha$  and 17- $\beta$ -estradiol receptors and secrete both the metalloproteases principally involved in malignant phenotype acquisition, i.e. MMP-2 and MMP-9. Angiomyolipoma cells behave similarly, despite their different source. Primary angiomyolipoma cells migrate in response to hormonal milieu and soluble factors, and produce active metalloproteases, both aspects being consistent with the theory claiming they can migrate to the lungs (and/or other organs) and colonizing them. No main feature, among the aspects we analyzed, seems to be referable to the gender of origin.

## 41 **Introduction**

42 Widespread use of cross-sectional imaging of kidneys has resulted in a significant increase in incidentally  
43 diagnosed small masses. The prognosis is usually favourable since they rarely progress to metastases [1].

44 Angiomyolipomas (AMLs) most commonly occur in the kidneys as small masses and, although often  
45 asymptomatic, may enlarge and bleed leading to haemorrhage and renal impairment [2]. These mesenchymal  
46 lesions are characterized by proliferation of spindle cells, epithelioid cells and adipocytic cells in concert with  
47 many thick-walled blood vessels [3]. A normal tissue counterpart has not been identified and genetic analyses  
48 indicate that all three tissue components derive from a common progenitor cell [4,5]. In case of intractable  
49 pain, large mass size (>4 cm) and risk of bleeding, surgical intervention is needed [6]. The preferred treatment  
50 for AML is nephron-sparing surgery or selective renal artery embolization, since both methods preserve  
51 residual renal function in comparison to radical nephrectomy [7]. On the other hand, asymptomatic patients  
52 are managed conservatively with long-term surveillance (mainly by imaging).

53 Although most AMLs are clinically insignificant benign tumors, an uncommon subtype, the epithelioid AML,  
54 can behave more aggressively and develop distant metastases [8,9,10].

55 AMLs are twice as common in females, and can occur sporadically or in association with other disorders, such  
56 the autosomal dominant condition Tuberous Sclerosis Complex (TSC) and sporadic  
57 lymphangiomyomatosis (LAM). In particular, LAM is a progressive disease of the lung histologically  
58 characterized by a diffuse proliferation of atypical smooth muscle cells (LAM cells) in the alveoli and cystic  
59 degeneration of the normal lung parenchyma [11].

60 AML and LAM share the same origin from mesenchymal perivascular epithelioid cell (PEC) and therefore  
61 both are considered as belonging to the PEComas lesion family [12]. The smooth muscle-like LAM cells that  
62 diffusely infiltrate the lungs and the lymphatic vessels have a low proliferation index and little or no evidence  
63 of cellular atypia. In the handful of patients who have had multiple tissues available for sequencing, identical  
64 inactivating mutations of TSC1 or TSC2, with subsequent deregulation of the Rheb/mTOR/p70S6K pathway,

65 were demonstrated in AML, in lymph nodes, and in pulmonary LAM cells, but not in normal lung of the same  
66 patient [13].

67 It has been also shown that both AML and LAM cells share immune-expression of HMB-45 antigen [14,15].

68 Furthermore, both LAM and AML cells express estrogen receptor  $\alpha$  [16], and estrogen is thought to cause  
69 clinical worsening in women with LAM [17]. Even more strikingly than AML, LAM preferentially affects  
70 women, especially at childbearing age, more often than AML. To date the underlying reasons for this  
71 behaviour are not known.

72 These, and other data [18,19], support a model in which both LAM and AML pathogenesis share some genetic  
73 and biological mechanisms, and are consistent with the hypothesis that pulmonary LAM might result from the  
74 metastatic spread of AML smooth muscle cells [20], possibly influenced by the hormonal milieu.

75 Therefore, considering the diffuse approach of delaying AML ablation in asymptomatic patients to preserve  
76 renal function, and that there is no reliable imaging technique able to differentiate a benign AML from one  
77 undergoing malignant change, we deem of paramount importance the study of migratory properties of AML  
78 cells. A clear demonstration that AML cells migration is involved in pathogenesis of lesions in several  
79 different organs might suggest important hints on new preventive drug therapies.

80 For this reason, we undertook a study on the proliferative and migratory properties of primary cells isolated  
81 from two different surgically removed AMLs, respectively from a male and a female patient. We evaluated if  
82 17- $\beta$ -estradiol could modulate their growth and their two- and three-dimensional migration. Furthermore, we  
83 compared the hormone-dependent effects to those induced by the stromal cell-derived factor 1  $\alpha$  (SDF-1 $\alpha$ ), a  
84 soluble factor known to induce cellular migration [21]. We also investigated metalloproteases 2 and 9 (MMP-  
85 2 and MMP-9) activities of AML cells, both in basic and stimulated conditions, since these MMPs play a  
86 pivotal role in the pathogenesis of cystic lung destruction in LAM [22,23].

87 MMPs modification of the extracellular matrix usually contributes to cell migration as well as to tissue  
88 invasion and metastasis. Similar modifications may facilitate AML cell migration and pulmonary colonization  
89 [20]. In fact, MMPs imbalance, together with other factors like a strong expression of cathepsin K, bcl-2 and  
90 HMB-45, characterize this pathology [19].



91 We focused our attention on estrogens in order to investigate if there are some differences in AML cells  
92 behaviour according to the hormonal milieu, as suggested by the hypothesis that pulmonary LAM in women  
93 might derive from the metastatic spread of AML abnormal smooth muscle cells.

94

## 95 **Materials and Methods**

### 96 **Materials**

97 All reagents were purchased from Sigma (St. Louis, MO, USA) unless otherwise stated. Tissue culture  
98 plasticware was from Falcon (Franklin Lakes, NJ, USA).

### 00 **Angiomyolipoma cells, tissue and ethical approvals**

01 Human primary AML cells have been obtained from patients that underwent surgical nephron-sparing AML  
02 ablation for therapeutic purposes at the Urology Unit of the San Luigi Gonzaga Hospital. The study was  
03 approved by the Ethical Committee of the San Luigi Gonzaga Hospital, University of Turin, Orbassano, Turin,  
04 Italy (Protocol 0006771, approved on April 18, 2016). All patients provided written informed consent in  
05 accordance with the Declaration of Helsinki.

06 AML3 derives from a male patient, AML4 from a female patient. None of the patients had any clinical signs  
07 or symptoms or a family history of tuberous sclerosis. No genetic analysis of TSC mutation were performed.

08 AML diagnoses were confirmed by standard histological examination including specific immunostaining for  
09 alpha-smooth muscle Actin, HMB-45 and Pancytokeratin antigens.

10 Primary cells were isolated from excess material not required for diagnostic use, which was divided into small  
11 fragments and treated with type II collagenase. Resulting cell suspensions were plated into T25 tissue culture  
12 flasks in AML medium (adapted from Lesma et al. [24]), composed of phenol red DMEM medium, ferrous  
13 sulphate 1.6  $\mu$ M, 20% foetal calf serum (FCS) and 10  $\mu$ g/mL epidermal growth factor. Experiments were  
14 performed on cells at passage 3-6.

### 16 **Immunofluorescence**

17 AML cells were fixed in 4% paraformaldehyde (PAF) for 15 minutes. After washing in PBS cells were treated  
18 with PBS containing 1% normal goat serum (NGS), 0.1% Triton X-100 at room temperature (RT) for 1 hour.

19 Cells were incubated overnight at 4°C with the following primary antibodies against: S-100 (rabbit, 1: 800;  
20 Dako, Glostrup, Denmark),  $\alpha$ -Smooth-Muscle Actin (mouse, 1: 100; NeoMarkers, Fremont, CA), HMB45  
21 (mouse, 1:100, Dako, Glostrup, Denmark), Keratin 8/18 (mouse, 1:100 Menarini, Florence, Italy) Vimentin  
22 (mouse, 1 : 70; Novocastra Lab, Newcastle, UK) and Melan-a (mouse; 1:100; NeoMarkers, Fremont, CA).  
23 After washing, cells were incubated for 1 hour at RT with the appropriate secondary antibodies: goat anti-  
24 mouse IgG Alexa-Fluor-488-conjugated (1 : 200, Molecular Probes, Eugene, Oregon) and CY3-conjugated  
25 anti-rabbit IgG (dilution 1 :400, Dako, Milan, Italy) [25]. The immunostained coverslips were analyzed on a  
26 Zeiss fluorescence microscope and images were captured with an Axiovision Imaging System.

## 28 **2D migration assay-wound healing**

29 Two-dimensional migration assays were performed as described in Mognetti et al. [26]. Briefly, primary AML  
30 cells were seeded in a 12-well plate at 300,000 cells/well. When they were confluent, a cross “wound” was  
31 made in each well with a p1000 tip [27], then wells were washed thrice with PBS, and cultured in AML  
32 medium supplemented either with SDF-1 $\alpha$  (Peprotech, London, UK) 100 ng/mL, plerixafor 100 nM, 17- $\beta$ -  
33 estradiol 1 nM, or tamoxifen 2  $\mu$ M. We photographed “wounds” on time-laps every hour to highlight  
34 migration, until a maximum of 8 hours.

35 Experiments were repeated three times, and every time five different spots for each experimental condition  
36 were considered. Images were analysed using ImageJ software (Wayne Rasband, NIH, USA): the healing  
37 percentage was quantified comparing the wound area at t = 0 to the following time-points for each treatment.

## 39 **3D migration assay**

40 The transwell migration assay, performed as previously described in Mognetti et al. [28], was used to measure  
41 the three-dimensional movements of cells. Migration assays were performed in transwells (BD Falcon cell  
42 culture inserts incorporating polyethylene terephthalate membrane with 8.0  $\mu$ M pores,  $6\pm 2\times 10^4$  pores /cm<sup>2</sup>) in  
43 24-well plates.

44 When tests were performed in the presence of SDF-1 $\alpha$  blocker, cells were preincubated for 30 min at 37°C in  
45 100 nM plerixafor conditioned medium.  
46 Cells ( $5 \times 10^4$ ) were suspended in 200  $\mu$ L of culture medium and seeded in the upper chamber of a transwell.  
47 The lower chamber was filled with fresh culture medium with or without 100 ng/mL SDF-1 $\alpha$  or 17- $\beta$ -estradiol  
48 1 nM, and placed in the incubator. After 4 or 8 hours, cells were treated as detailed by Gambarotta et al. [27].  
49 Wells were photographed using a BRESSER MikroCam 3 Mpx camera, with an optical microscope (Leica DC  
50 100) at 100x. Five pictures were randomly chosen *per* well and used to count the migrated cells with ImageJ  
51 software using cell-counter plug-in. Results from different experiments (performed at least three times in  
52 duplicate) were expressed as mean  $\pm$  standard errors. In order to avoid any cytotoxic effect potentially  
53 confounding migration results, we performed a cytotoxicity test at the same time and same conditions of every  
54 migration test.

## 56 **Proliferation assay**

57 Primary AML cells were seeded into flat-bottomed 96-well microplates at a density of 1,000 cells in 100  $\mu$ L  
58 culture medium *per* well and allowed to attach overnight in complete medium. Drugs were then added to  
59 culture medium at concentrations ranging from 0.1 to 100 nM 17- $\beta$ -estradiol, and from 0.2 to 20  $\mu$ M  
60 tamoxifen [29] for 24–72 hours, according to protocols. The MTT (3-(4,5-dimethylthiazol-2-yl)-2,5-  
61 diphenyltetrazolium bromide) assay was performed as described in Mognetti et al. [28]. Data (mean  $\pm$  standard  
62 errors) were calculated as the mean values of 8 replicates. Each experiment was repeated thrice. Cell viability  
63 was expressed as the percentage of living cells *versus* the untreated controls.

## 65 **Quantitative real-time PCR (qPCR)**

66 In order to perform quantitative real-time PCR (qPCR), total RNA was extracted from treated cells by using  
67 Trizol (Invitrogen Life Technologies, Italy). After RNA purification and treatment with DNase I (Fermentas,  
68 St. Leon-Rot, Germany), 1  $\mu$ g was retrotranscribed in cDNA with the RevertAid™ H Minus First Strand

cDNA Synthesis Kit (Fermentas) using oligo(dT) primers. Gene assays were performed in triplicate for each treatment in a 20  $\mu$ L reaction volume containing 1  $\mu$ L of RT products, 10  $\mu$ L Sso-Fast EVA Green SMX (Bio-Rad, Hercules, CA, USA), 500 nM each forward and reverse primers. Gene expression was normalized on the housekeeping gene ribosomal 18S rRNA. Table 1 resumes the primer sequences that were used. Automated CFX96 real-time thermocycler (Bio-Rad) was used and the reaction conditions were 95°C for 1 minute, followed by 45 cycles 98°C for 5 seconds and anneal–extend step for 5 seconds at 60°C, with data collection. At the end of these cycles, a melting curve (65°C to 95°C, with plate read every 0.5°C) was performed in order to assess the specificity of the amplification product by single peak melting temperature verification. Results were analysed with Bio-Rad CFX Manager. Calculations and statistical analyses were performed using GraphPad Prism version 5.00 for Windows (GraphPad Software, San Diego California, USA).

**Table 1. Primers sequences, size of the amplification product and NCBI Reference Sequence**

GENE	SEQUENCE	AMPL. SIZE	NCBI REF. SEQ.
<b>Era</b>	Fw: 5'-TGGAGTCTGGTCCTGTGAGG-3' Rev: 5'-CCCACCTTTCATCATTCCCCT-3'	172 bp	NT_025741.16
<b>Er<math>\beta</math></b>	Fw: 5'-GAGCAAAGATGAGCTTGCCG-3' Rev: 5'-AGCTGGGCCAAGAAGATTCC-3'	142 bp	NM_001437.2
<b>GPR30</b>	Fw: 5'-AGTCGGATGTGAGGTTTCAG-3' Rev: 5'-TCTGTGTGAGGAGTGCAAG-3'	240 bp	NM_001505.2
<b>MMP-2</b>	Fw: 5'-GGCCCTGTCACTCCTGAGAT-3' Rev: 5'-GGCATCCAGGTTATCGGGGA-3'	474 bp	NM_001302510.1
<b>MMP-9</b>	Fw: 5'-CAACATCACCTATTGGATCC-3' Rev: 5'-CGGGTGTAGAGTCTCTCGCT-3'	480 bp	NM_004994.2
<b>18S rRNA</b>	Fw: 5'-GTGGAGCGATTTGTCTGGTT-3' Rev: 5'-ACGCTGAGCCAGTCAGTGTA-3'	201 bp	X03205.1

Fw=forward, Rev= reverse

## Western blotting

Cells were seeded in 10 cm diameter Petri dishes, cultured until sub-confluence, then 17- $\beta$ -estradiol (1 nM) was added. After 5 minutes and 4 hours incubation, cells were collected and treated as detailed by Mognetti et al. [21].

Blots were probed with primary monoclonal antibody anti-vinculin (mouse; 1: 2000 Sigma) resuspended in PBS Tween 0.1% and with anti-ERK1/2 (mouse; 1:2000), anti-pERK1/2 (mouse; 1:2000) (Cell Signaling Technology, Danvers, MA, USA) resuspended in 5% w/v nonfat dry milk + PBS tween 0.1%. Vinculin was used as an internal control. HRP-conjugated anti-mouse (Amersham-GE Healthcare, Buckinghamshire, UK) was diluted 1:6000 (ERK1/2 and pERK1/2) and 1:8000 (vinculin) in PBS Tween 0.1%. Densitometric analysis was performed by ImageJ software.

The ratio pERK1/2/ ERK1/2 was expressed as percentage optical density modification relative to control conditions. Experiments were repeated three times.

## Gelatin zymography

MMP-2 and MMP-9 activities in medium samples were assessed by gel zymography. Proteins (100  $\mu$ g) were separated by electrophoresis in 8% SDS-PAGE gel containing gelatin (0.8 mg/mL) under non-reducing conditions. The gel was washed with Tris buffer (2.5% Triton X-100 in 50 mM Tris-HCl, pH 7.5, final solution) for 1 hour, then incubated overnight at 37°C in a proteolysis buffer (40 mM Tris-HCl, 200 mM NaCl, 10 mM CaCl<sub>2</sub>, 0.02% NaN<sub>3</sub>, pH 7.5, final solution). The gel was stained for 3 hours with Coomassie Blue solution (0.05% Coomassie Brilliant Blue R-250, 50% methanol, 10% acetic acid, final solution) and finally destained with 5% methanol and 7% acetic acid (final solution). Reagents and chemicals were obtained from VWR International (Milan, Italy). MMPs activity was detected as a clear band on a blue background and estimated by densitometric analysis using ImageJ Software. The results were expressed as percentages of control values.

211 **Statistical analysis**

212 All the data in this study are shown as the mean  $\pm$  SE. Two group means were compared using the unpaired t-  
213 test, and more than two group means were analyzed by one-way analysis of variance (ANOVA), where P  
214  $<0.05$  was considered statistically significant [30].

215 For gene expression level comparison One-way ANOVA with Dunnett's post tests were performed using  
216 GraphPad Prism version 5.00 for Windows.

217

## Results

### Cell characterization by immunofluorescence

To better characterize isolated AML primary cells, immunofluorescence was performed with specific antibodies. Overall, both cell lines showed similar immunophenotype and partly elongated or rounded shapes. Both primary culture cells were strongly and totally positive for smooth muscle actin antibody (in both elongated and rounded cells), with a diffused stain throughout the cytoplasm (Fig 1a and 1a'). Furthermore, in both cell lines there were single rounded element positive for keratin 8/18 and for elongated cells strongly positive for vimentin (Fig 1d, 1e, 1d' and 1e'), together with single negative ones for both the antigens. Finally a strong nuclear and cytoplasmic positivity was found for S100 in both cells (Fig 1f and 1f'). As a matter of fact, even if scattered, some AML3 cells were focally positive for intracytoplasmic HMB45 (Figure 1b and 1b'), and AML4 cells were focally positive for Melan-A antigen (Fig 1c and 1c'), which is consistent with the AML phenotype.

#### Figure 1: Primary angiomyolipoma cells characterization by immunofluorescence.

Cells isolated from the two angiomyolipomas were challenged with specific antibodies to reveal their immunocytochemical characteristics:  $\alpha$ -actin antibody (a and a') specific for smooth muscle cells; HMB45 (b and b') and Melan-A (c and c'), both typical of AML; keratin 8/18 (d and d') labeling the epithelial-like cells; vimentin (e and e'), a marker of fibroblasts and S100 (f and f'), a marker of lipid-containing cells. Fields were chosen to show both the morphological aspect and the specific marker expression.

### Estrogen and SDF-1 $\alpha$ receptors gene expression

The analyses of gene expression of both AMLs demonstrated the presence of mRNA for CXCR4 (SDF-1 $\alpha$  receptor), GPR30, ER $\alpha$ , but not for ER $\beta$  (Fig 2). The level of each gene was similar in both primary AML cells, with no significant difference.



242  
243  
244  
245  
246  
247  
248  
249  
250  
251  
252  
253  
254  
255  
256  
257  
258  
259  
260  
261  
262  
263  
264  
265  
266

### **Fig 2. Receptors gene expression.**

Early passages AML cells underwent qRT-PCR for CXCR4, GPR30, ER $\alpha$  and ER $\beta$  mRNA expression analysis. Data are shown as the absolute mRNA expression normalized by the housekeeping 18S rRNA.

### **ERK phosphorylation**

Treatment of AML3 cells with 17- $\beta$ -estradiol increased ERK phosphorylation at 4 h, while pERK was significantly augmented in AML4 cells already at 5 minutes and was stable until 4 hours (Fig 3).

### **Fig 3. ERK phosphorylation**

Effect of 17- $\beta$ -estradiol (1 nM) on pERK/ERK in AML3 and AML4 cells after 5 minutes and 4 hours of incubation. Vinculin as internal control. \*= $P < 0.05$  vs control.

### **Influence of 17- $\beta$ -estradiol or tamoxifen on AML cell proliferation**

The treatment for up to 72 hours with concentrations of 17- $\beta$ -estradiol ranging from 0.1 nM to 100 nM with or without tamoxifen, or with tamoxifen alone (0.2-20  $\mu$ M, two representative experiments are shown in Fig 4) did not induce any modification on AML cells proliferation regardless of their gender. No significant difference was detected at any time point or culture condition (data not shown). Figure 4 reports two typical experiments as an example.

### **Fig 4. Effect of 17- $\beta$ -estradiol alone and of its combination with tamoxifen on AML cells growth.**

Proliferation assay after 72 hours culture in presence of increasing concentration of 17- $\beta$ -estradiol (A) or with 17- $\beta$ -estradiol 1 nM, tamoxifen 2  $\mu$ M, or both (B). Anova and Dunnett's post test analyses demonstrated that no significant modification in cell growth respect to untreated controls was induced by the molecules at any of the concentrations tested.

267

## 268 **Two-dimensional Motility Assay (wound healing)**

269 The two-dimensional motility was quantified, and data are displayed graphically as healing percentage (Fig 5,  
270 panels C, D and E). Panel C compares basal migration: the early migration rate of AML3 was higher, a  
271 significant difference being demonstrated at 4 hours. This difference is promptly quenched since after 8 hours  
272 the migration rate of the two AMLs was similar.

273

### 274 **Fig 5. Analyses of primary AML cells migration by *in vitro* wound healing assay.**

275 Wounded area in a representative experiment of *in vitro* wound healing assay is shown before (A) and after  
276 (B) the incubation period. Bi-dimensional migration was then quantified in basal conditions for both AMLs  
277 (C), and for AML3 (D) and AML4 (E) in presence of SDF-1 $\alpha$  100 ng/mL or its receptor antagonist plerixafor  
278 100 nM, or a combination of both. Migration is expressed in arbitrary units. \*=P<0.05 vs control; #=P<0.05 vs  
279 SDF-1 $\alpha$ .

280

281 SDF-1 $\alpha$  treatment induced a statistically significant motility increase already after 2 hours treatment in cells  
282 from both AMLs. Significant difference persisted all along the experimental period (up until 8 hours). The  
283 effects induced by SDF-1 $\alpha$  were abolished by the SDF-1 $\alpha$ -receptor antagonist plerixafor, while no significant  
284 effects were induced by plerixafor alone.

285 Two-dimensional migration was significantly modulated by 17- $\beta$ -estradiol (Fig 6), although some differences  
286 in migration patterns were evident. In fact, AML3 (A) of male origin, showed a significant motility increase in  
287 the first 4 hours of incubation with 17- $\beta$ -estradiol, and a prevalent logarithmic pattern. AML4 cells, of female  
288 origin (B), showed an exponential pattern and a significant increase in estradiol induced migration respect to  
289 the untreated control, evident at any of the time point considered. The treatments with the ER-antagonist  
290 tamoxifen had no influence on two-dimensional motility of both cell types, while it was able to abolish the  
291 effects of estradiol.

292  
293 **Fig 6. Wound healing assay in presence of 17- $\beta$ -estradiol 1 nM and/or tamoxifen 2  $\mu$ M.**

294 Data are expressed as the percentage of migration vs t = 0 h. \*=P<0.05 vs control; #=P<0.05 vs 17- $\beta$ -estradiol.  
295

296 **Three-dimensional Migration Assays**

297 Cells were seeded in the upper chamber of a transwell filter and allowed to migrate for 4 or 8 hours under  
298 either basal conditions, or in response to stimuli added in the lower chamber. Fig 7, panel A and B, shows that  
299 the number of migrating cells significantly increased in response to SDF-1 $\alpha$ .  
300

301 **Fig 7. Three-dimensional migration (SDF-1 $\alpha$ ).**

302 Cells were incubated with SDF-1 $\alpha$  (100 ng/mL) and its receptor blocker plerixafor (100 nM) or a combination  
303 of both for 4 or 8 hours. In each experimental condition cells were counted in 5 fields *per* insert. Data are  
304 expressed as the percentage of migration vs control. \*=P<0.05 vs control; #=P<0.05 vs SDF-1 $\alpha$ .  
305

306 Data were similar for cells originated from the two AMLs and were significant after 4 hours of continuous  
307 exposure. SDF-1 $\alpha$  stimulation was completely abolished by the SDF-1 $\alpha$ -receptor antagonist plerixafor, while  
308 no differences were shown for longer exposures.

309 The transwell migration experiments performed in presence of 17- $\beta$ -estradiol indicated a different behavior  
310 between cells originating from the two AML. AML3 cells of male origin needed at least 8 hours of stimulation  
311 before a significant difference in migration could be appreciated (Fig 8A). AML4 cells (Fig 8B) responded to  
312 the stimulation at 4 hours, while after 8 hours no differences respect to the control were evident.  
313

314 **Fig 8. Three-dimensional migration (17- $\beta$ -estradiol).**

315 Cells were incubated with 17- $\beta$ -estradiol (1 nM) for 4 and 8 hours. Migration is expressed in arbitrary units.  
316 \*=P<0.05 vs control.

317

## 318 **Metalloproteases activity in supernatant derived from 3D-migration test**

319 The activity of two metalloproteases involved in malignant phenotype acquisition, MMP-2 and MMP-9, was  
320 measured by zymography in the supernatant collected at the end of the 3D-migration test (4 hours) (Fig 9).

321

### 322 **Fig 9. Metalloproteases activity in supernatant collected from 3D-migration test.**

323 Data are expressed as the relative activity calculated by densitometric analyses. \*=P<0.05 vs control;

324 #=P<0.05 vs SDF-1 $\alpha$ .

325

326 While the diverse treatments induced no significant difference in MMP-2 activity, SDF-1 $\alpha$  enhanced MMP-9  
327 enzymatic activity. This data was in accordance with the increased migration induced by SDF-1 $\alpha$ . Coherently,  
328 plerixafor inhibited MMP-9 activity increase provoked by SDF-1 $\alpha$ . No difference was induced by incubation  
329 with 17- $\beta$ -estradiol.

330 Figure 10, panel A, shows absolute MMPs activity (not normalized) and demonstrates that MMP-2 activity, in  
331 basal conditions, is higher than MMP-9 activity for both AMLs. Consistently, Fig 10B, shows coherent  
332 mRNA expression for both enzymes.

333

### 334 **Fig 10. Absolute MMP-2 and MMP-9 activity (A) and their corresponding mRNA expression (B) in** 335 **basal conditions.**

336 Data are expressed as the activity calculated by densitometric analyses. The gene expression is shown as the  
337 level of expression normalized by the housekeeping 18S rRNA. The difference in MMP-2 vs MMP-9 activity  
338 or expression is always significant (P<0.001).

339

340

## 341 **Discussion**

342 In this paper we describe for the first time the behaviour of primary AML cells, originating from male and  
343 female patients, in terms of proliferation and migration *in vitro*, both in basal conditions and in response to  
344 environmental stimuli. Our findings clearly demonstrate that primary AML cells are able to migrate *in vitro*.

345 The main limit of this study was, by far, the small sample number. It is worth underlying, though, that AML is  
346 a rare disease and it is quite difficult to come across AML of male origin, and to isolate and grow primary  
347 cells, what we actually did. The cellular composition of the cultures were similar, as demonstrated by  
348 immunofluorescence and shown in Fig. 1. Overall, this phenotype confirmed the mixed (either muscle,  
349 epithelioid, lipomatous and mesenchimal) nature of the cultures, respectively, according to the heterogeneous  
350 nature of AML [24]. None of the cell type seemed to be predominant; we consider the miscellaneousness of  
351 the two cultures an advantage in a pharmacological study, since the complexity of the tumor should be taken  
352 into account.

353 The original aim of this study was to understand if AMLs, independently from their TSC mutational status,  
354 were able to migrate and if there was the possibility to modulate this process pharmacologically. In particular,  
355 we focused on estrogen because of the underlying hypothesis that in females during childbearing age AML  
356 cells might migrate to the lungs and generate LAM. We also investigated SDF-1 $\alpha$  since this factor is usually  
357 associated to migration and homing of several cell types [31,21]. We have shown that both AML3 (male  
358 origin) and AML4 (female origin) have analogous significant expression levels of estrogen and SDF-1 $\alpha$   
359 receptor mRNAs. Despite the presence of the estrogen receptors, we have observed that there was no  
360 estrogenic influence on proliferation of both AMLs. Therefore, the hormone therapy might not be optimal  
361 pharmacological choice to treat this pathology in female patients, and other options should be taken into  
362 consideration. Another aspect that we demonstrated in common for both AMLs was their migratory response  
363 to SDF-1 $\alpha$ . In fact, we have shown its significant effect in increasing the bi- and three-dimensional migration  
364 of these cells. The specificity of this observation was confirmed by the effect of the treatment with the  
365 selective SDF-1 $\alpha$  receptor antagonist plerixafor, which completely abolished SDF-1 $\alpha$  migratory stimulation.

366 Our results are in accordance with the well known role of SDF-1 $\alpha$  in cell migration, and might support the  
367 hypothesis that the host microenvironment tissue stimuli could exert a specific chemotactic signal to promote  
368 homing of AML cells [32].

369 Although some common properties between the two AMLs have been described so far, we report that other  
370 aspects seem to differentiate the cells originating from male from those deriving from female patients. We  
371 showed that the basal unstimulated migration of male AML3 had a more rapid onset, respect to female AML4.  
372 This difference in spreading was striking already 4 hours after seeding, and was particularly evident in the  
373 ability to invade, as demonstrated by three-dimensional assays. Alongside with this observation, we also report  
374 that the higher basal migration of AML3 is less influenced by estrogen, while spreading of AML4 cells is  
375 significantly increased already after 2 hours incubation with estradiol 1 nM.

376 In order to clarify the short-term effects of estrogen, we investigated the expression of ER $\alpha$ , ER $\beta$  and GPR30.  
377 It is worth to underline an abundant mRNA expression of GPR30 [33], which might likely mediate the early  
378 response to estradiol that we observed.

379 In this work we present some data on the response of AML cells to hormonal stimuli. While many Authors  
380 have thoroughly described the long term effects of these stimuli [34, 35], their influence on the colonization  
381 potential and short term effects needs further research. In particular, our attention focused on GPR30 role in  
382 these processes, and we have chosen the timing in order to better analyze the responses referred to this  
383 receptor pathway. The multiple effects of estrogens can be explained by different modulation of transcription  
384 and by rapid signaling events that are not associated with altered gene transcription [34]. GPR30 hormone  
385 stimulation is able to induce rapid MAPK activation pathway and ERK1/2 phosphorylation via MMP-EGFR  
386 and is responsible for several cell responses and signaling.

387 We have included to this paper some Western blot experiments that demonstrate that E2 stimulation is able to  
388 increase ERK1/2 phosphorylation in AML4. Noteworthy, both AML3 and AML4 constitutively express  
389 significant levels of ERK1/2 and pERK. In particular, AML3 has a basal level of pERK higher than AML4,  
390 and this might explain the reduced effects of E2 on pERK/ERK observed in AML3. These data are in  
391 accordance with the 2D and 3D migration data shown in Figure 6 and Figure 8 and justify why the early

392 response to estradiol in migration of AML4 cells is not related to a higher mRNA expression compared to  
393 AML3.

394 ERK protein is activated when tuberin function is lost [36], and estrogen-mediated non-genomic ERK  
395 signaling activated by GPER is involved in cell viability and motility of TNBC cells [37].

396 An interesting aspect of GPR30-E2 stimulation is the activation of the PI3K-Akt signaling pathway via mTOR  
397 and S6K that leads to different activity on DNA transcription and on proliferation. This pathway is activated  
398 from both E2 and tamoxifen, and it could explain, at least in part, the data shown in Figure 6.

399 Analysis of the culture media collected from three-dimensional migration experiments revealed that the  
400 stimulation of migration induced by SDF-1 $\alpha$  was accompanied by an augmented release of MMPs. These  
401 effects were consistently reverted by the selective receptor antagonist plerixafor. Strikingly, such an increase  
402 in MMPs production was not observed in estradiol-stimulated conditions, despite a significant increase in cell  
403 migration. We therefore speculate that, while SDF-1 $\alpha$  -induced migration occurs through metalloproteases  
404 production, the migratory response to estrogen most likely does not involve MMPs activity.

405 Noteworthy we have shown that tamoxifen induced unexpected effects on migration of the two cell types. The  
406 peculiar mechanism of action of this drug, which can bind both intracellular and membrane estrogen receptors,  
407 might give us some hints in the interpretation of our results. Further characterization of the cells may be of  
408 value, but it is outside of the scope of the present study. We are currently conducting more exhaustive  
409 investigations on this topic, also trying to correlate the different aspects to TSC mutational status, but since  
410 they go further the aim of the present study, the data will be reported in the next future.

411 Our work demonstrates that primary AML cells migrate and produce active metalloproteases, both aspects  
412 being consistent with the theory claiming these cells can migrate and invade other tissues, and for some yet  
413 unknown reasons colonize the lung.

**Acknowledgments:** authors thank Prof. Porpiglia for kindly providing AML, Prof. Biasi and Dr. Calfapietra for sharing their experience in MMPs quantification, Dr. Luisa Muratori for her invaluable assistance in immunofluorescence and Dr. La Montagna for help.

## References

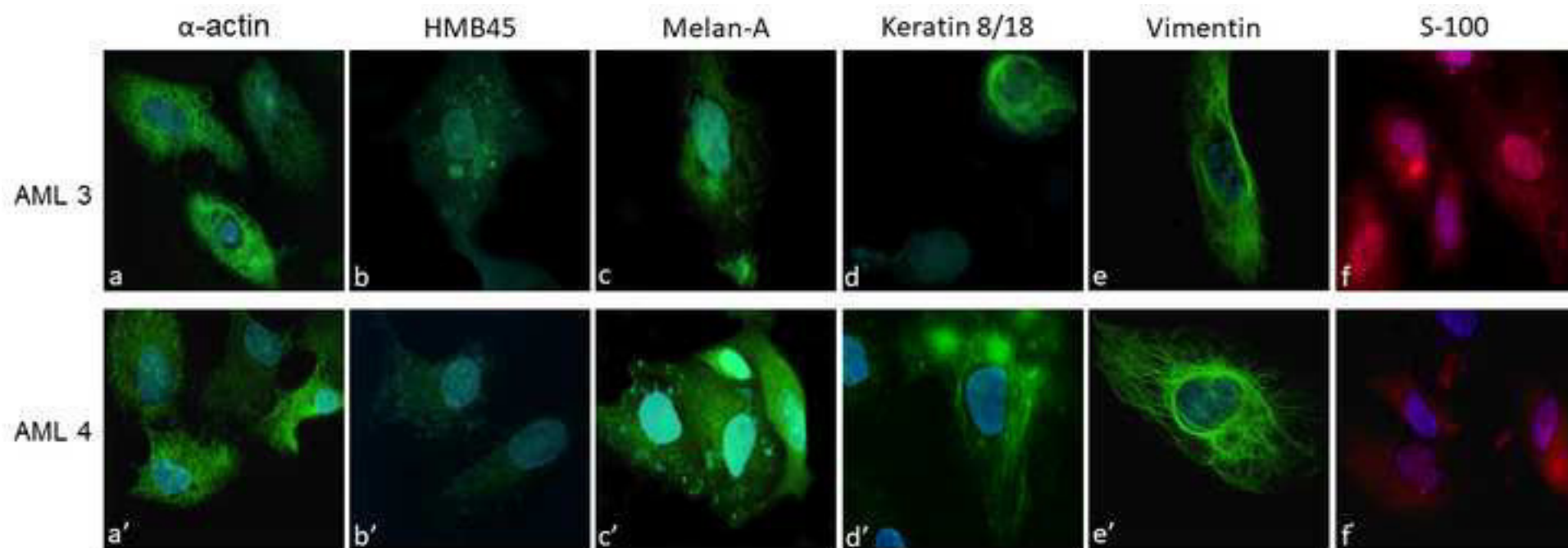
1. Yates DR, Rouprêt M. Small renal mass and low-risk prostate cancer: any more for active surveillance? *European urology*. 2011; 60:45–7.
2. Bissler JJ, Kingswood JC. Renal angiomyolipoma. *Kidney international*. 2004; 66:924–34.
3. Stone CH, Lee MW, Amin MB, Yaziji H, Gown AM, Ro JY, et al. Renal angiomyolipoma: further immunophenotypic characterization of an expanding morphologic spectrum. *Arch Pathol Lab Med*. 2001; 125:751-8.
4. Niida Y, Stemmer-Rachamimov AO, Logrip M, Tapon D, Perez R, Kwiatkowski DJ, et al. Survey of somatic mutations in tuberous sclerosis complex (TSC) hamartomas suggests different genetic mechanisms for pathogenesis of TSC lesions. *American journal of human genetics*. 2001; 69:493-503.
5. Karbowniczek M, Yu J, Henske EP. Renal angiomyolipomas from patients with sporadic lymphangiomyomatosis contain both neoplastic and non-neoplastic vascular structures. *The American journal of pathology*. 2003; 162:491–500.
6. Flum AS, Hamoui N, Said MA, Yang XJ, Casalino DD, McGuire BB, et al. An Update on the Diagnosis and Management of Renal Angiomyolipoma. *The Journal of Urology*. 2016; 195:834-46
7. Boorjian SA, Frank I, Inman B, Lohse CM, Cheville JC, Leibovich BC, Blute ML. The role of partial nephrectomy for the management of sporadic renal angiomyolipoma. *Urology*. 2007; 70:1064–8.
8. Lam ET, La Rosa FG, Suby-Long TD, Kondo KL, Wilson S, Glodé LM, Flaig TW. A Rare Case of Metastatic Renal Epithelioid Angiomyolipoma. *Oncology*. 2011; 25:832–8.
9. Cui L, Hu XY, Gong SC, Fang XM, Lerner A, Zhou ZY. A massive renal epithelioid angiomyolipoma with multiple metastatic lymph nodes. *Clinical imaging*. 2011; 35:320–3.

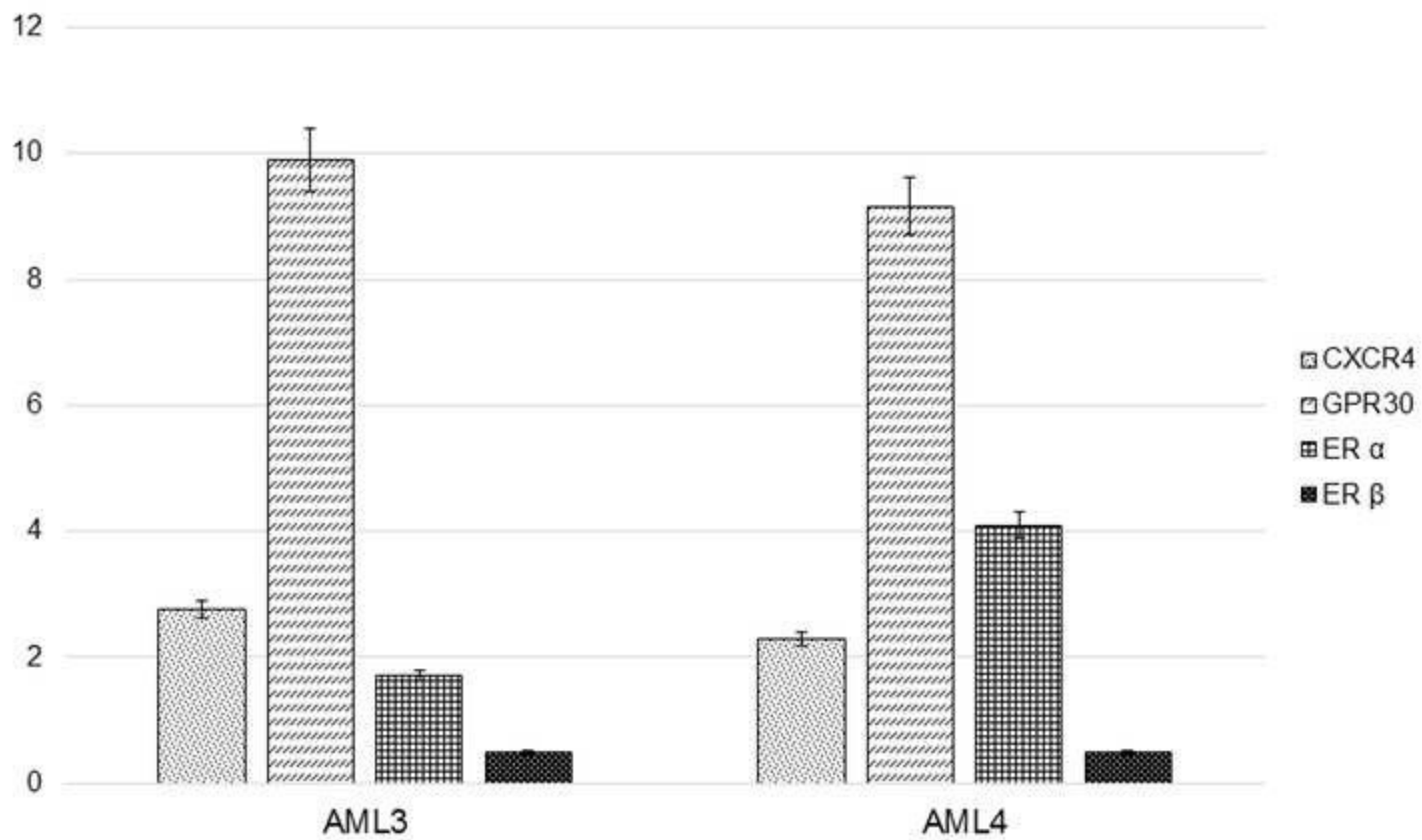


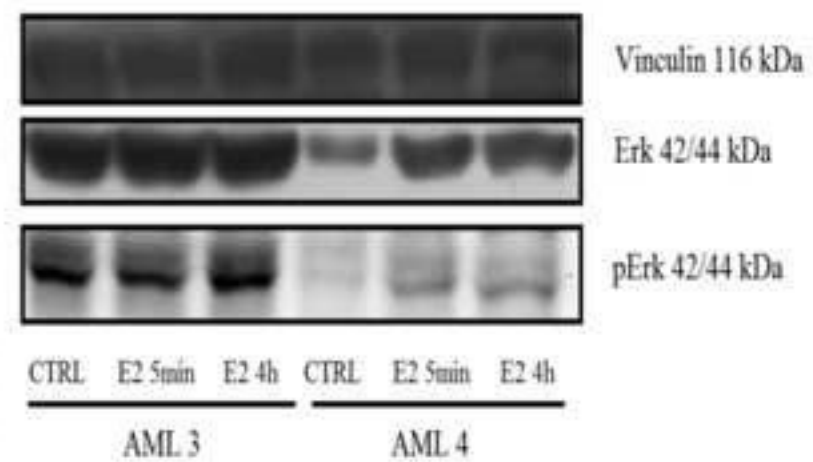
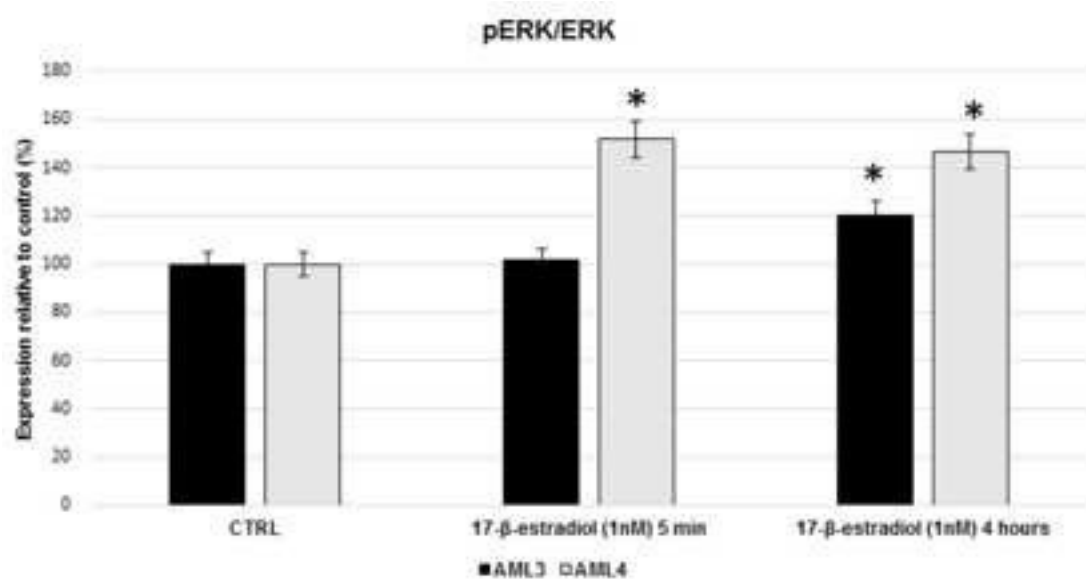
10. Gaston CL, Slavin J, Henderson M, Choong PF. Epithelioid angiomyolipoma with skeletal and pulmonary metastasis on 8 year follow-up. *Pathology*. 2010; 42:591–4.
11. Baldi BG, Pimenta SP, Kawassaki Ade M, Bernardi Fdel C, Dolhnikoff M, Carvalho CR. Pulmonary arterial involvement leading to alveolar hemorrhage in lymphangiomyomatosis. *Clinics*. 2011; 66:1301–1303.
12. Martignoni G, Pea M, Reghellin D, Zamboni G, Bonetti F. PEComas: the past, the present and the future. *Virchows Arch*. 2008; 452:119-32.
13. Carsillo T, Astrinidis A, Henske EP. Mutations in the tuberous sclerosis complex gene TSC2 are a cause of sporadic pulmonary lymphangiomyomatosis. *Proceedings of the National Academy of Sciences of the United States of America*. 2000; 97:6085–6090.
14. Hoon V, Thung SN, Kaneko M, Unger PD. HMB-45 reactivity in renal angiomyolipoma and Lymphangiomyomatosis. *Arch Pathol Lab Med*. 1994; 118:732-4.
15. Lesma E, Sirchia SM, Ancona S, Carelli S, Bosari S, Ghelma F, et al. The methylation of the TSC2 promoter underlies the abnormal growth of TSC2 angiomyolipoma-derived smooth muscle cells. *Am J Pathol*. 2009; 174:2150-9.
16. Logginidou H, Ao X, Russo I, Henske EP. Frequent estrogen and progesterone receptor immunoreactivity in renal angiomyolipomas from women with pulmonary lymphangiomyomatosis. *Chest*. 2000; 117:25–30.
17. Johnson SR, Tattersfield AE. Decline in Lung Function in Lymphangiomyomatosis. *American Journal of Respiratory and Critical Care Medicine*. 1999; 160:628-633.
18. Yu J, Astrinidis A, Henske EP. Chromosome 16 loss of heterozygosity in tuberous sclerosis and sporadic lymphangiomyomatosis. *American Journal of Respiratory and Critical Care Medicine*. 2001; 164:1537-1540.
19. Flavin RJ, Cook J, Fiorentino M, Bailey D, Brown M, Loda MF.  $\beta$ -Catenin is a useful adjunct immunohistochemical marker for the diagnosis of pulmonary lymphangiomyomatosis. *Am J Clin Pathol*. 2011; 135:776-782.

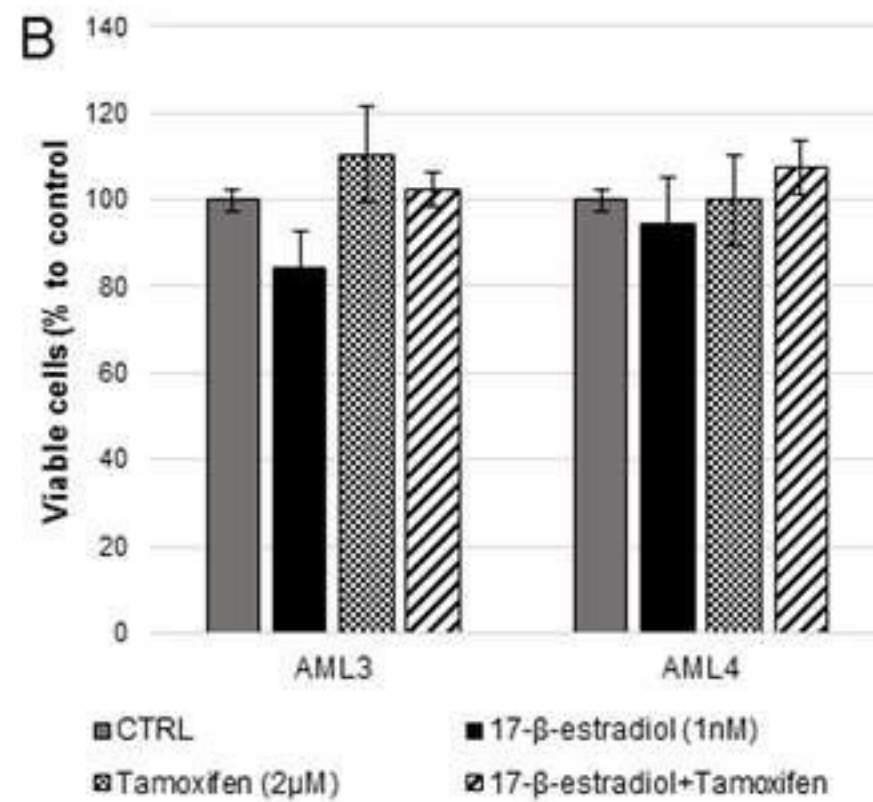
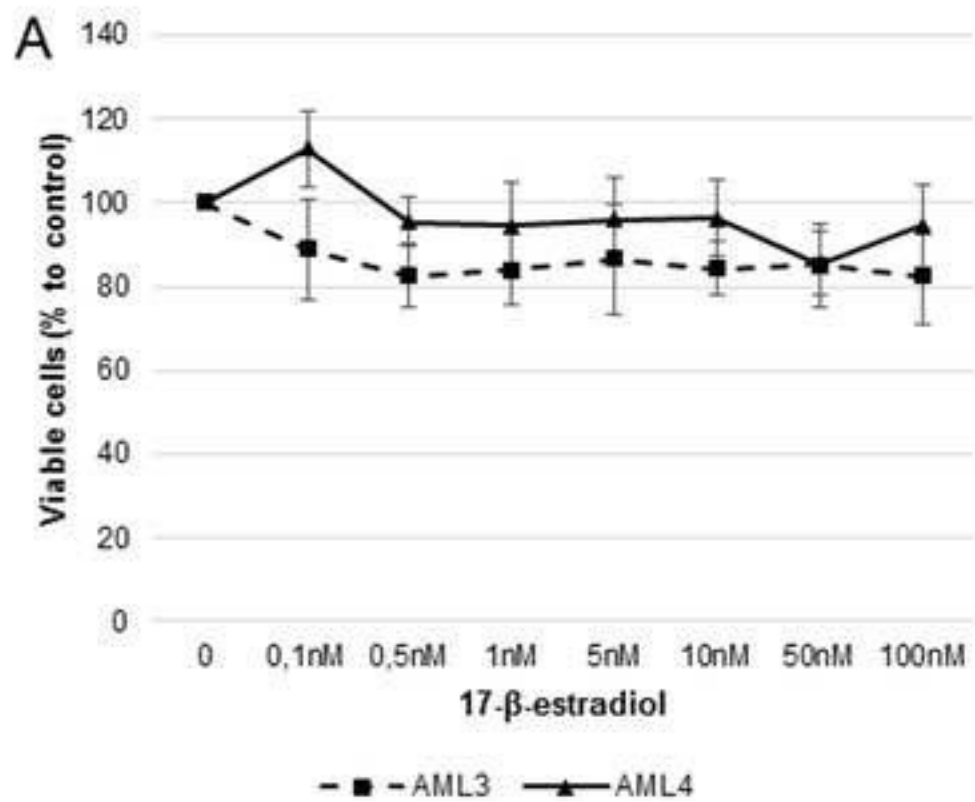
- 466 20. Henske EP. Metastasis of benign tumor cells in tuberous sclerosis complex. *Genes Chromosomes Cancer*.  
467 2003; 38:376–81.
- 468 21. Mognetti B, La Montagna G, Perrelli MG, Pagliaro P, Penna C. Bone marrow mesenchymal stem cells  
469 increase motility of prostate cancer cells via production of stromal cell-derived factor-1 $\alpha$ . *J Cell Mol Med*.  
470 2013; 17:287-92.
- 471 22. Matsui K, Takeda K, Yu ZX, Travis WD, Moss J, Ferrans VJ. Role for activation of matrix  
472 metalloproteinases in the pathogenesis of pulmonary lymphangiomyomatosis. *Arch Pathol Lab Med*.  
473 2000; 124:267–275.
- 474 23. Hayashi T, Fleming MV, Stetler-Stevenson WG, Liotta LA, Moss J, Ferrans VJ, Travis WD.  
475 Immunohistochemical study of matrix metalloproteinases (MMPs) and their Tissue inhibitors (TIMPs) in  
476 pulmonary lymphangiomyomatosis (LAM). *Hum Pathol*. 1997; 28:1071-8.
- 477 24. Lesma E, Grande V, Carelli S, Brancaccio D, Canevini MP, Alfano RM, et al. Isolation and Growth of  
478 Smooth Muscle-Like Cells Derived from Tuberous Sclerosis Complex-2 Human Renal Angiomyolipoma:  
479 Epidermal Growth Factor Is the Required Growth Factor. *The American Journal of Pathology*. 2005;  
480 167:1093–1103.
- 481 25. Muratori L, Ronchi G, Raimondo S, Geuna S, Giacobini-Robecchi MG, Fornaro M. Generation  
482 of new neurons in dorsal root Ganglia in adult rats after peripheral nerve crush injury. *Neural Plast*. 2015;  
483 2015:860546.
- 484 26. Mognetti B, La Montagna G, Perrelli MG, Marino S, Pagliaro P, Cracco CM, Penna C. Zoledronic Acid  
485 and Leuprorelin Acetate, Alone or in Combination, Similarly Reduce Proliferation and Migration of  
486 Prostate Cancer Cells In Vitro. *International Journal of Medical Biology*. 2014; 1:1–7.
- 487 27. Gambarotta G, Garzotto D, Destro E, Mautino B, Giampietro C, Cutrupi S, et al. ErbB4 expression in  
488 neural progenitor cells (ST14A) is necessary to mediate neuregulin-1 $\beta$ -induced migration. *The Journal*  
489 *of Biological Chemistry*. 2004; 279:48808–16.

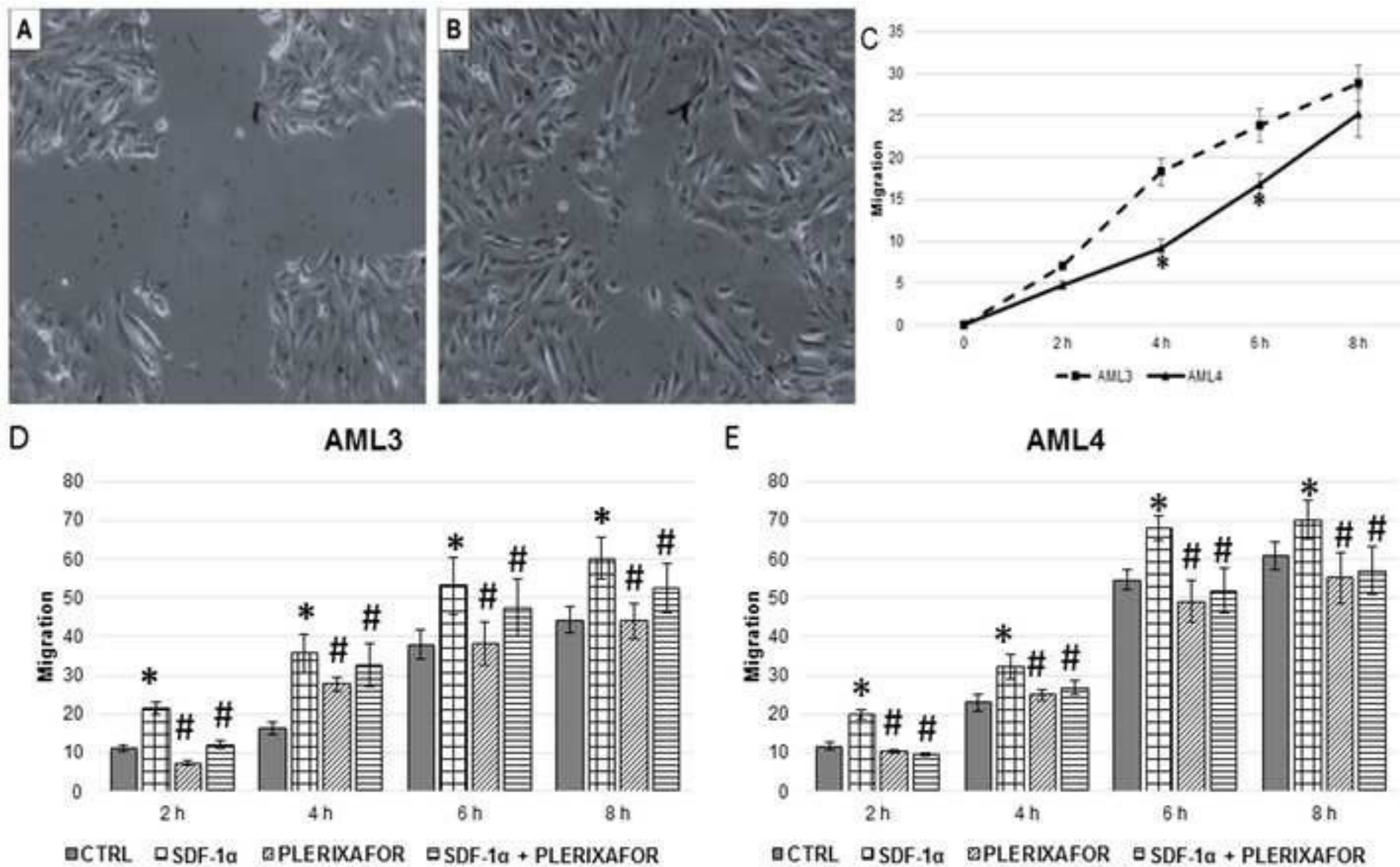
- 490 28. Mognetti B, Barberis A, Marino S, Di Carlo F, Lysenko V, Marty O, G elo en A. Preferential Killing of  
491 Cancer Cells Using Silicon Carbide Quantum Dots. *Journal of Nanoscience and Nanotechnology*.2010;  
492 10:7971–7975.
- 493 29. Yu J, Astrinidis A, Howard S, Hensk EP. Estradiol and tamoxifen stimulate LAM-associated  
494 angiomyolipoma cell growth and activate both genomic and nongenomic signaling pathways. *Am J Physiol*  
495 *Lung Cell Mol Physiol*. 2003; 286:694-700.
- 496 30. Vonesh EF, Chinchilli VG. *Linear and Nonlinear Models for the Analysis of Repeated Measurements*.  
497 Chapman and Hall; 1996.
- 498 31. Kucia M, Jankowski K, Reza R, Wysoczynski M, Bandura L, Allendorf DJ, et al. CXCR4-SDF-1  
499 signalling, locomotion, chemotaxis and adhesion, *J Mol Histol*. 2004; 35:233-45.
- 500 32. Zaitseva L, Murray MY, Shafat MS, Lawes MJ, MacEwan DJ, Bowles KM, Rushworth SA. Ibrutinib  
501 inhibits SDF1/CXCR4 mediated migration in AML. *Oncotarget*, 2014; 5:9930-8.
- 502 33. Filardo EJ, Quinn JA, Bland KI, Frackelton AR Jr. Estrogen-induced activation of Erk-1 and Erk-2  
503 requires the G protein-coupled receptor homolog, GPR30, and occurs via trans-activation of the epidermal  
504 growth factor receptor through release of HB-EGF. *Mol Endocrinol*. 2000; 14:1649-60.
- 505 34. Simoncini T, Hafezi-Moghadam A, Brazil DP, Ley K, Chin WW, Liao JK. Interaction of oestrogen  
506 receptor with the regulatory subunit of phosphatidylinositol-3-OH kinase. *Nature*. 2000; 407:538-41.
- 507 35. Song RX, Zhang Z, Chen Y, Bao Y, Santen RJ. Estrogen signaling via a linear pathway involving insulin-  
508 like growth factor I receptor, matrix metalloproteinases, and epidermal growth factor receptor to activate  
509 mitogen-activated protein kinase in MCF-7 breast cancer cells. *Endocrinology*. 2007; 148:4091-101.
- 510 36. Yu JJ, Robb VA, Morrison TA, Ariazi EA, Karbowniczek M, Astrinidis A, et al. Estrogen promotes the  
511 survival and pulmonary metastasis of tuberin-null cells. *Proc Natl Acad Sci U S A*. 2009; 106:2635-40.
- 512 37. Yu T, Liu M, Luo H, Wu C, Tang X, Tang S, et al. GPER mediates enhanced cell viability and motility via  
513 non-genomic signaling induced by 17 $\beta$ -estradiol in triple-negative breast cancer cells. *J Steroid Biochem*  
514 *Mol Biol*. 2014; 143:392-403.



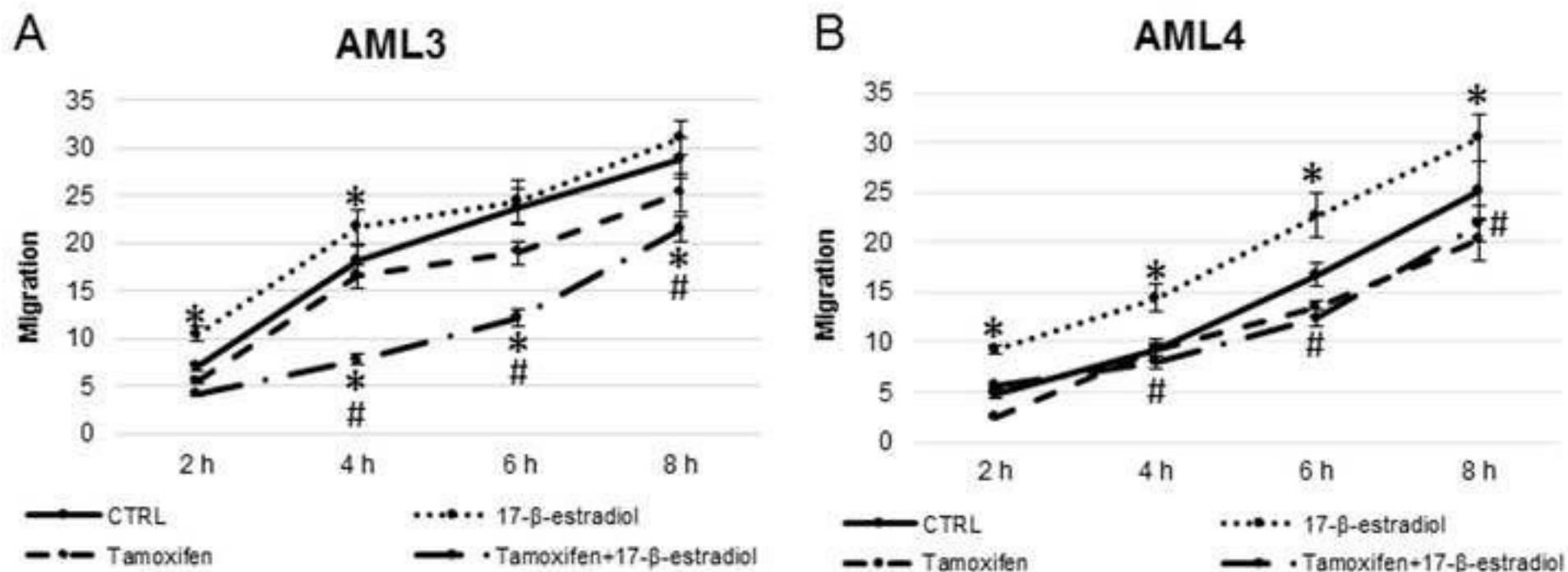


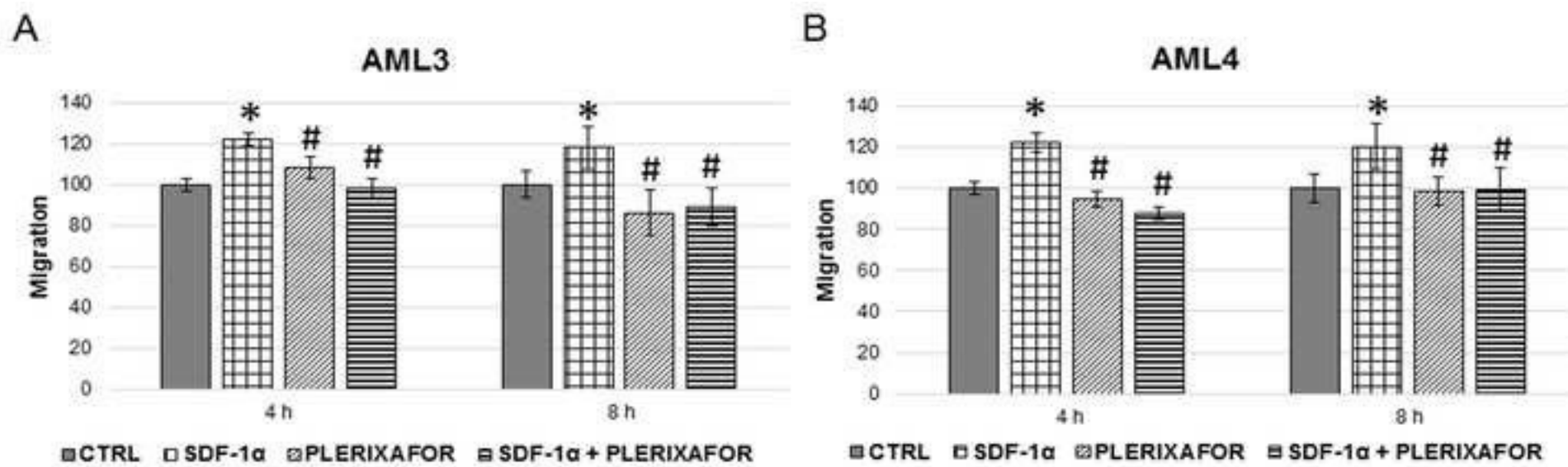


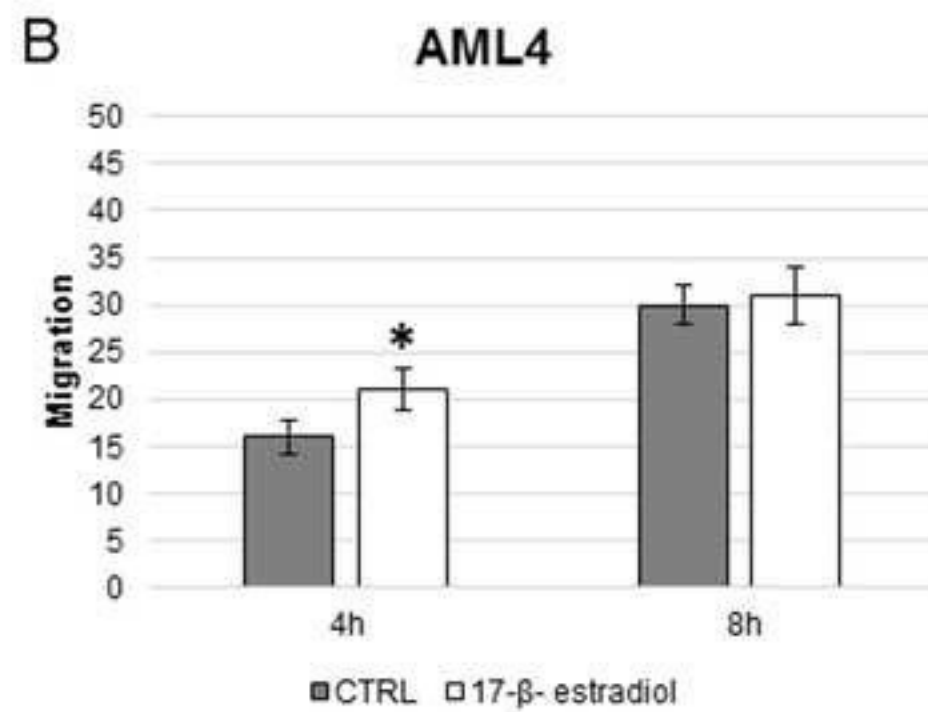
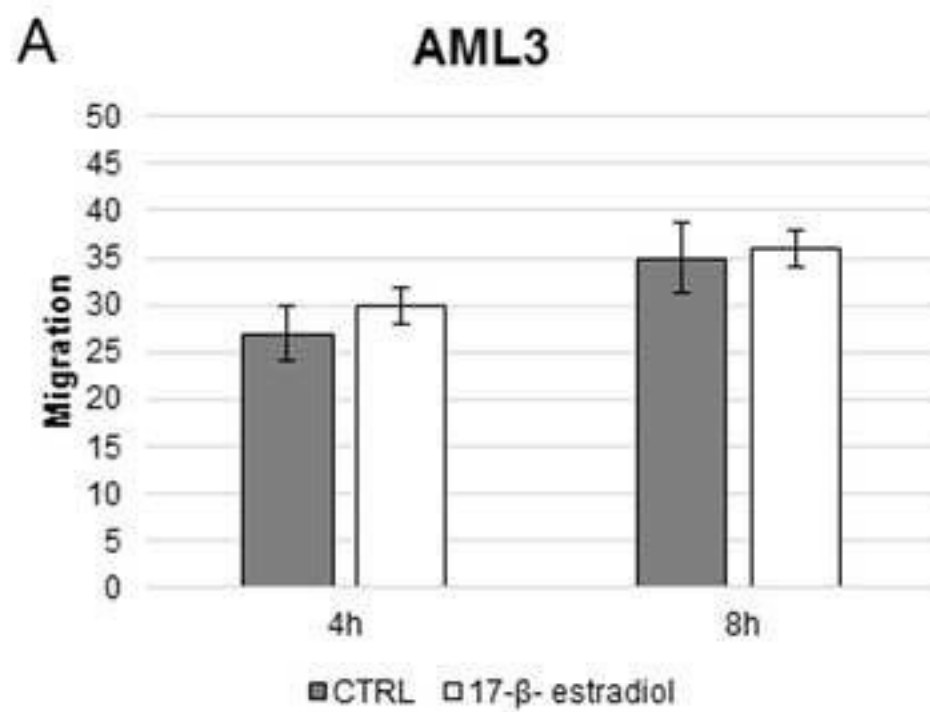


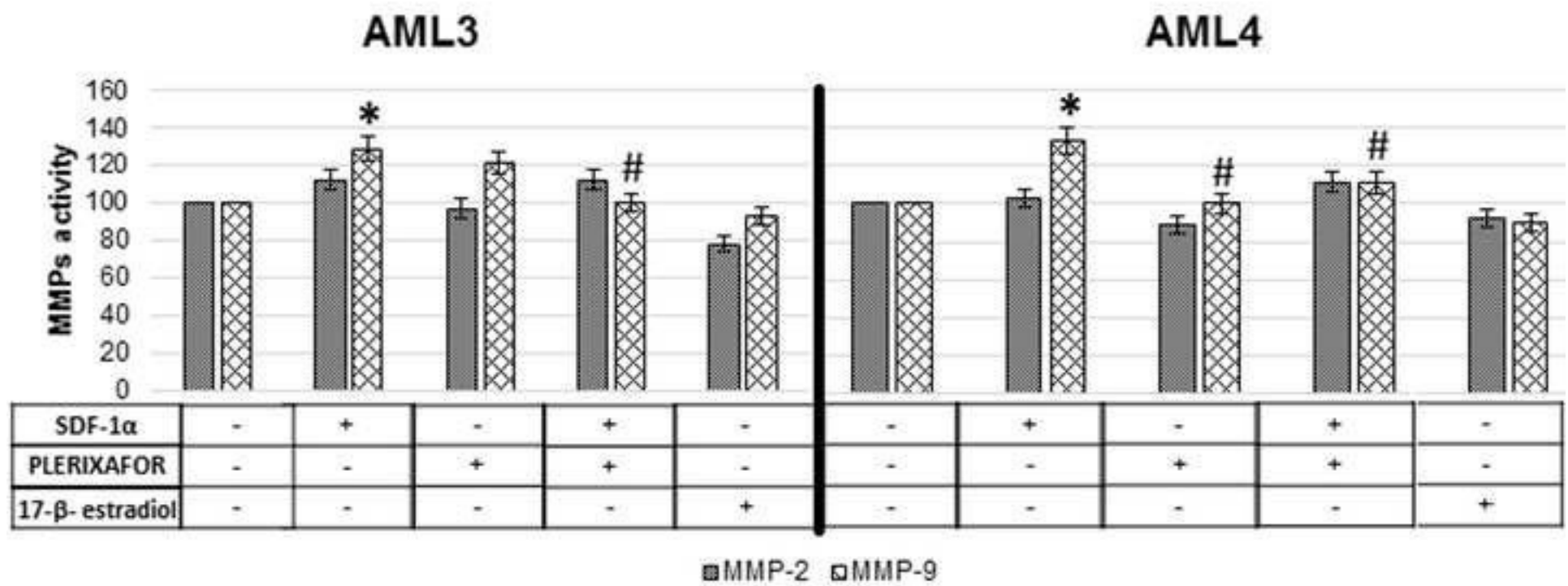


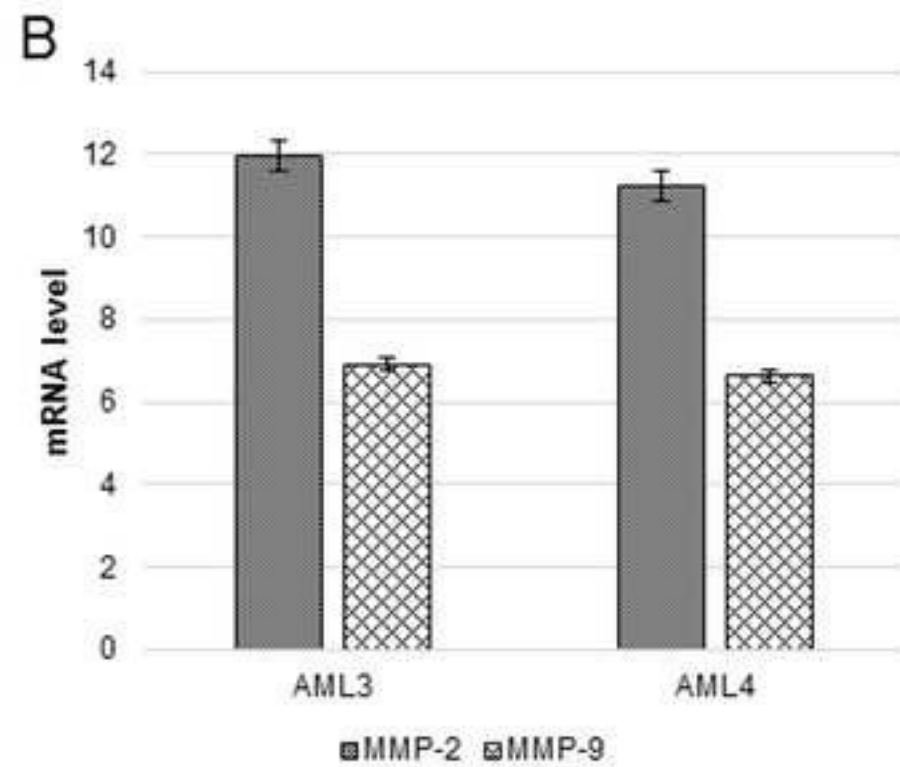
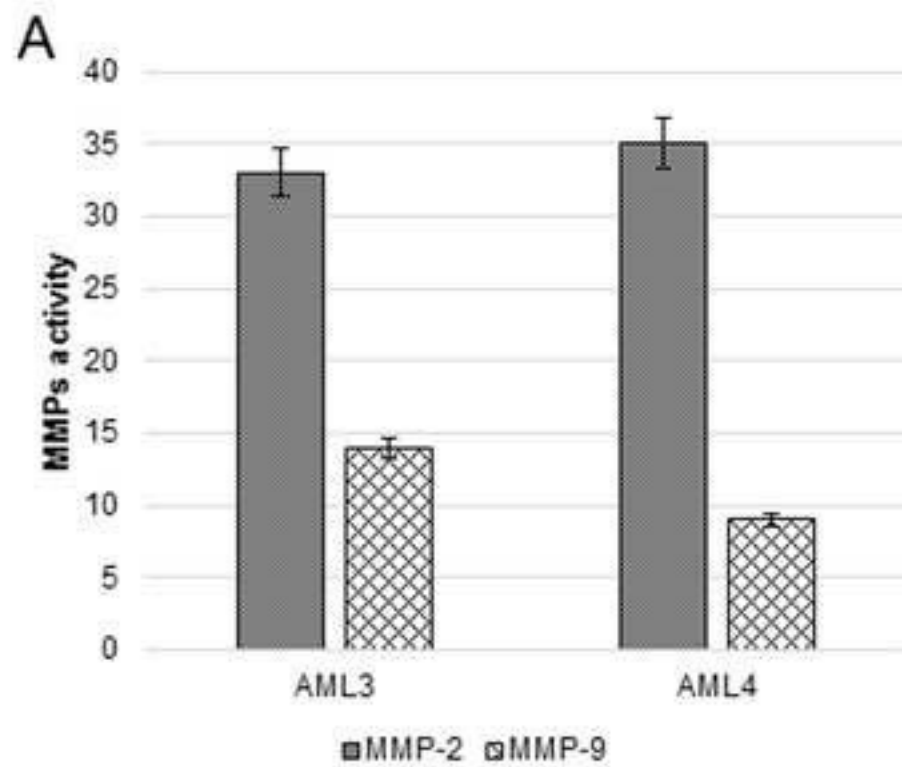














**Zoledronic acid and leuprorelide acetate affect DU-145  
migration towards stem cell conditioned medium**

Journal:	<i>The Prostate</i>
Manuscript ID	Draft
Wiley - Manuscript type:	Original Article
Date Submitted by the Author:	n/a
Complete List of Authors:	La Montagna, Giuseppe; Scienze Cliniche e Biologiche Bertolini, Francesca; Università degli Studi di Torino, Scienze Cliniche e Biologiche Mognetti, Barbara; Università degli Studi di Torino, Scienze Cliniche e Biologiche
Key Words:	prostate cancer, bisphosphonate, cytotoxicity, metastasis, GnRH analogues

SCHOLARONE™  
Manuscripts

view

1  
2  
3 1 **Title: Zoledronic acid and leuprorelide acetate affect DU-145 migration towards stem**  
4 2 **cell conditioned medium.**

5  
6 3  
7  
8 4 G. La Montagna<sup>1</sup>, F. Bertolini<sup>1</sup>, B. Mognetti<sup>1\*</sup>

9  
10 5 <sup>1</sup>Department of Clinical and Biological Science, University of Turin, Regione Gonzole 10,  
11 6 10043, Orbassano, Italy

12  
13  
14 7  
15  
16 8 Correspondence to: Barbara Mognetti, Department of Clinical and Biological Science,  
17 9 University of Turin, Regione Gonzole 10, 10043, Orbassano (TO).

18  
19  
20 11  
21 12 Corresponding author: Barbara Mognetti

22 13 Tel.: +39 0116705439

23 14 Fax: +39 0119038639

24 15 E-mail: [barbara.mognetti@unito.it](mailto:barbara.mognetti@unito.it)

25  
26 16 First author: Giuseppe La Montagna

27 17 Tel.: +39 0116705439

28 18 Fax: +39 0119038639

29 19 E-mail: [285103@edu.unito.it](mailto:285103@edu.unito.it)

30  
31 20 Second author: Francesca Bertolini

32  
33 21 Tel.: +39 0116705439

34 22 Fax: +39 0119038639

35 23 E-mail: [francesca.bertolini@unito.it](mailto:francesca.bertolini@unito.it)

36  
37  
38  
39  
40 26 **Short title:** DU-145 migration toward conditioned medium

41  
42  
43  
44  
45  
46 29 **Keywords:** prostate cancer; bisphosphonate; cytotoxicity; metastasis; GnRH analogues.

47  
48  
49  
50  
51 32 **Conflict of interest**

52  
53  
54 33 The authors confirm that there are no conflicts of interest.

55  
56 34

1  
2  
3 35 **Abstract**  
4

5  
6 36 Background: To study the effect of GnRH analogues (leuprolide acetate, LA) and  
7  
8 37 bisphosphonates (zoledronic acid, ZA), alone or in combination, on human prostate cancer  
9  
10 38 (PCa) cells proliferation and migration, in vitro.

11  
12 39 Methods: Cell proliferation (MTT assay) and three-dimensional (transwell assay) migration  
13  
14 40 were analyzed on human PCa cell line (DU-145) in basal condition, under drug treatment or  
15  
16 41 in MSC-CM (mesenchymal stem cells conditioned medium), whose cytokines content was  
17  
18 42 previously measured by Milliplex bead immunoassay; finally, we observed by western blot  
19  
20 43 analysis how these LA and ZA modify Akt phosphorylation.

21  
22 44 Results: ZA (5  $\mu$ M) cytotoxicity appears after 48-hours incubation, while LA cytotoxicity  
23  
24 45 only after 72-hours at 100  $\mu$ M. Both subcytotoxic ZA and LA concentrations decrease 3D  
25  
26 46 PCa cell migration rate. pAkt/Akt ratio is diminished by LA and, though less strikingly, by  
27  
28 47 ZA, in agreement with the respective inhibition migration ratios. MSC-CM significantly  
29  
30 48 increases PCa cell migration (210% $\pm$  2.2; P<0.05), but this phenomenon is quenched both by  
31  
32 49 ZA and LA.  
33

34  
35  
36 50 Conclusions: Our results suggest that LA and, mostly, ZA have a direct toxic effect on cancer  
37  
38 51 cells. Furthermore, they inhibit cellular migration even under attractive stimuli exerted by  
39  
40 52 MSC; this might contribute to explain their effect in limiting metastatization.  
41

42 53

43 54

44 55

45 56

46 57

47 58

48 59



1  
2  
3 60 ***Introduction***  
4  
5 61

6  
7 62 Prostate cancer is the most frequent genitourinary tumor, representing 11% of the male  
8  
9 63 malignancies in Europe, and is one of the leading causes of morbidity and mortality in the  
10  
11 64 world [1].

12  
13 65 Administration of GnRH agonist or other analogues (such as leuprolide acetate, buserelin,  
14  
15 66 deslorelin, goserelin and istreterelin) is a well-established treatment of prostate cancer inducing  
16  
17 67 a pharmacological castration [2] and resulting in cancer regression. Despite pharmacological  
18  
19 68 treatment, the onset of metastatic dissemination represents, together with the development of  
20  
21 69 androgen-independent growth, a critical progression step of human prostate cancer that  
22  
23 70 largely determines the clinical course of the disease and survival of the patients [3]. Bone is a  
24  
25 71 preferential site of metastases [4], which produce a crucial impact on patients' functional  
26  
27 72 status and quality of life due to significant pain and high risk of skeletal-related events,  
28  
29 73 including pathologic bone fractures (both vertebral and non-vertebral), spinal cord  
30  
31 74 compression, surgery and radiotherapy to bone [5]. The burden of metastatic disease can be  
32  
33 75 treated by administering a potent inhibitor of osteoclast activity such as zoledronic acid (ZA),  
34  
35 76 a bisphosphonate widely used to treat skeletal complications of malignancy and considered  
36  
37 77 the drug of choice for both the prevention and the treatment of bone mass loss. In vivo, it  
38  
39 78 inhibits the release of growth factors from osteoblasts and bone marrow stromal cells [6].  
40  
41 79 Moreover, bisphosphonates modulate many other cellular and physiologic processes relevant  
42  
43 80 to bone metabolism and tumor initiation and progression [7].

44  
45  
46  
47  
48 81 Prostate cancer cells tropism for the bone is the result of a sequential series of molecular  
49  
50 82 events: bone metastases arise as a result of a crosstalk between metastatic cells, bone matrix,  
51  
52 83 osteoblasts and osteoclasts, and cellular components of the bone marrow microenvironment.  
53  
54 84 Among these, bone marrow mesenchymal stem cells (BM-MSCs) play a paramount role in  
55  
56  
57  
58  
59  
60

1  
2  
3 85 the so-called metastatic niche [8, 9]. Prostate cancer cells migration can be influenced by  
4  
5 86 MSC-CM soluble factors [8], and drugs normally used for prostate cancer treatment, such as  
6  
7 87 zoledronic acid and leuprolide acetate, interact with this process [10]. We aimed at examining  
8  
9 88 the effect of such molecules on the behavior of the human prostate cancer cell line DU-145 in  
10  
11 89 an in vitro cell co-culture model of invasion assay. Cells were exposed to the drugs, alone or  
12  
13 90 in combination, prior and/or during the migration test. We previously demonstrated that an  
14  
15 91 up-regulation of Akt phosphorylation may exert a crucial role in DU-145 cell migration under  
16  
17 92 conditioned medium stimulus [9]. Knowing that PI3-K/Akt signaling pathway plays a critical  
18  
19 93 role in cell invasion and in modulation of cell migration [11], we also examined if zoledronic  
20  
21 94 acid and leuprolide acetate modulate AKT level.  
22  
23  
24  
25  
26

## 27 **Materials and Methods**

### 28 29 30 31 **Materials**

32  
33 99 All reagents were purchased from Sigma (St. Louis, MO, USA) unless otherwise stated.  
34  
35 100 Tissue culture plasticware was from Falcon (Franklin Lakes, NJ, USA).  
36  
37 101 Zoledronic acid (ZA) [1-hydroxy-2-(1H-imidazol-1-yl)ethane-1,1-diyl]bis(phosphonic acid)  
38  
39 102 was generously provided by Novartis (Surrey, UK) and leuprolide acetate (LA) (N-[1-[[1-[[1-  
40  
41 103 [[1-[[1-[[1-[[5-(diaminomethylideneamino)-1-[2-(ethylcarbamoyl)pyrrolidin-1-yl]-1-oxo-  
42  
43 104 pentan-2-yl]carbamoyl]-3-methyl-butyl]carbamoyl]-3-methylbutyl]carbamoyl]-2-(4-  
44  
45 105 hydroxyphenyl)ethyl]carbamoyl]-2-hydroxy-ethyl]carbamoyl]-2-(1H-indol-3-  
46  
47 106 yl)ethyl]carbamoyl]-2-(3H-imidazol-4-yl)ethyl]-5-oxopyrrolidine-2-carboxamide) was from  
48  
49 107 Takeda (Osaka, Japan).  
50  
51  
52  
53  
54  
55  
56  
57  
58  
59  
60

**110 Prostate cancer cell culture**

111 Human androgen independent DU-145 prostate cancer cells were purchased from ATCC  
112 (Rockville, MD, USA). Cells were maintained at 37°C in a humidified 5% CO<sub>2</sub> atmosphere  
113 in RPMI 1640 containing 10 mL/L penicillin and streptomycin solution, NaHCO<sub>3</sub> 2 g/L  
114 (7.5% w/v), 10% Fetal Bovine Serum (FBS).

**116 Proliferation assay**

117 DU-145 cells were seeded into flat-bottomed 96-well microplates (1,000/100 µL culture  
118 medium/well) and allowed to attach overnight in complete medium before drugs addition.  
119 Drugs were added to culture medium, alone or in combination, testing various concentrations  
120 from 2.5 µM to 50 µM (ZA) [12] and from 0.5 µM to 100 µM (LA) [13] for 24–96 hours,  
121 according to protocols. The MTT (3-(4,5-dimethylthiazol-2-yl)-2,5-diphenyltetrazolium  
122 bromide) assay was performed as previously described [14]. Data (mean ± standard  
123 deviation) were the average values of 8 replicates. Each experiment was repeated thrice. Cell  
124 viability was expressed as percentage of living cells with respect to controls.

**126 Mesenchymal stem cells isolation and MSC-CM collection**

127 Bone marrow cells were obtained from femurs of adult rats as described in Mognetti et al,  
128 2013. They were grown in complete αMEM containing 10% FBS, 2 mM L-glutamine, 100  
129 U/ml penicillin and 100 µg /mL streptomycin at 37 °C and 5% CO<sub>2</sub> for 3 days as previously  
130 described [9].

131 For migration assay, conditioned medium was collected after three days of culture,  
132 centrifuged at 4000 rpm for 5 minutes at 4°C in order to eliminate cells and cellular debris,  
133 and used for migration assays or frozen.

134

135

1  
2  
3 136 ***Three-dimensional migration assay***  
4

5 137 Three-dimensional (3D) migration assay was used to measure the invasiveness of DU-145  
6  
7 138 cells in response of various stimuli. Migration assays were performed in transwells (BD  
8  
9 139 Falcon cell culture inserts incorporating polyethylene terephthalate – PET – membrane with  
10  
11 140 8.0  $\mu\text{M}$  pores,  $6\pm 2*10^4$  pores / $\text{cm}^2$ ) as previously described [9].

12  
13 141 Briefly,  $10^5$  cells were resuspended in 200  $\mu\text{L}$  of RPMI containing 2% FBS with or without  
14  
15 142 drugs (zoledronic acid 20  $\mu\text{M}$ , leuprolide acetate 100  $\mu\text{M}$  or both, representing non-toxic  
16  
17 143 concentration at 24 hours as per the described viability assay) and then seeded in the upper  
18  
19 144 chamber of a transwell; in the lower chamber we added RPMI or MSC-CM as detailed in  
20  
21 145 Table I. In some cases, before seeding cells were grown for 18 hours in presence of  
22  
23 146 zoledronic acid 20  $\mu\text{M}$ , leuprolide acetate 100  $\mu\text{M}$  or both (Table I).

24  
25 147 Transwells were placed in the incubator at 37 °C and 5%  $\text{CO}_2$  for 6 hours and finally treated  
26  
27 148 as detailed by Mognetti et al. [9].

28  
29 149 Wells were photographed using a BRESSER MikroCam 3 Mpx camera, with an optical  
30  
31 150 microscope (Leica DC 100) at 100x. Five pictures were randomly chosen per well, and used  
32  
33 151 to count the migrated cells with ImageJ software using cell-counter plug-in. Results from  
34  
35 152 different experiments (performed at least three times in duplicate) were expressed as mean  $\pm$   
36  
37 153 standard deviation. In order to avoid any cytotoxic effect of potentially confounding  
38  
39 154 migration results, we performed a cytotoxicity test at the same time and same conditions of  
40  
41 155 every migration test.  
42  
43

44  
45 156

46  
47  
48 157 ***Immunoassay to detect cytokine content in MSC-CM***  
49

50 158 Cytokine profiles in MSC-CM were determined using the Human Cytokine/ Chemokine  
51  
52 159 Magnetic Bead Panel protocol from the “Milliplex<sup>®</sup> Human Cytokine 5 Plex” kit (Billerica,  
53  
54 160 MA). The procedure was conducted according to the manufacturer’s protocol.  
55  
56  
57  
58  
59  
60

1  
2  
3 161 Briefly, the assay plates were washed with washing buffer, and shaken on an orbital plate  
4  
5 162 shaker for 10 minutes at room temperature. The washing buffer was decanted and the  
6  
7 163 standards, assay buffer, or samples/controls were mixed with serum matrix in each well,  
8  
9 164 incubated overnight at 4°C on an orbital shaker with specific antibody to detect GM-CSF,  
10  
11 165 MCP1/CCL2, IL-10, IFN $\gamma$ , TNF $\alpha$ ; well contents were then removed and wells washed.  
12  
13 166 Biotinylated detection antibodies were then added and incubated for 1 hour at room  
14  
15 167 temperature while shaking. After incubation, well contents were removed and streptavidin-  
16  
17 168 phycoerythrin was added and incubated for 30 minutes at room temperature, then washed and  
18  
19 169 resuspended in Sheath Fluid. Plates were read on the Luminex MagPix<sup>®</sup> machine and data  
20  
21 170 were collected using the Luminex xPONENT<sup>®</sup> software (v. 4.2); data analysis was performed  
22  
23 171 using the Milliplex<sup>®</sup> Analyst software (v. 5.1).  
24  
25  
26  
27 172

### 28 173 ***Western blotting***

29  
30  
31 174 Cells were seeded in 10 cm diameter Petri dishes, cultured until sub-confluence and then  
32  
33 175 drugs were added (ZA 20  $\mu$ M and LA 100  $\mu$ M, to reproduce the same conditions of migration  
34  
35 176 assay). After 6 hours incubation, cells were collected, treated and immunoblotted as detailed  
36  
37 177 according to Mognetti et al. [9].  
38

39  
40 178 Blots were probed with primary polyclonal antibody (Cell Signaling Technology, Danvers,  
41  
42 179 MA, USA) suspended in TBS Tween 0.1% as follows: anti-Akt (mouse, 1:800), anti-pAkt  
43  
44 180 (Ser473, rabbit, 1:500), and anti-vinculin (developed in rabbit, Sigma). Vinculin was used as  
45  
46 181 an internal control.

47  
48 182 HRP-conjugated anti-mouse (Amersham-GE Healthcare, Buckinghamshire, UK) and anti-  
49  
50 183 rabbit (Santa Cruz Biotechnology) were diluted (1:6000 and 1:8000, resp.) in TBS Tween  
51  
52 184 0.025%. Bands were quantified using the ImageJ software.  
53  
54  
55  
56  
57  
58  
59  
60

1  
2  
3 185 Phosphorylation levels of Akt were expressed as ratio pAkt/Akt. All data were expressed as  
4  
5 186 percentage modification relative to control conditions.  
6

7 187

8  
9 188 ***Statistical analysis***

10  
11 189 All the data in this study were shown as the mean  $\pm$  standard deviation. Statistical analyses  
12  
13 190 were performed by One-way ANOVA, with Dunnett's post tests, or two-way ANOVA using  
14  
15 191 GraphPad Prism version 5.00 for Windows (GraphPad Software, San Diego California USA).  
16  
17 192 Coefficient of Drug Interaction (CDI) was used to define the type of interactions between the  
18  
19 193 employed drugs. CDI was calculated by means of the equation:  $CDI = AB/(A \times B)$ , where AB  
20  
21 194 is the relative cell migration of the combination; A or B, relative cell migration of the single  
22  
23 195 agent.  $CDI < 1$  indicates a synergistic effect;  $CDI = 1$  indicates an additive effect;  $CDI > 1$   
24  
25 196 indicates an antagonistic effect.  
26  
27  
28  
29  
30  
31  
32  
33  
34

35  
36 200 **Results**

37  
38 201 ***Effect of zoledronic acid, leuprolide acetate and combination of both on cell proliferation***

39  
40 202

41 203 Incubation up to 24 hours with 20 and 40  $\mu$ M zoledronic acid induced a weak cytotoxic effect  
42  
43 204 on DU-145 (Figure 1A). A statistically significant cytotoxicity appears after 48 hours of  
44  
45 205 incubation, already at the 5  $\mu$ M concentration.  
46

47  
48 206 Leuprolide acetate displayed no cytotoxicity on DU-145 cells (Figure 1B), within the  
49  
50 207 concentration range tested, after 24 and 48 hours of incubation.  
51

52 208 A significant toxicity is appreciable only after 72 hours of incubation from 5  $\mu$ M on.  
53  
54  
55  
56  
57  
58  
59  
60

209 Addition of leuprolide acetate 100  $\mu$ M did not increase zoledronic acid cytotoxicity at any  
210 concentration after 48 hours incubation (Figure 1C).

211

### 212 ***3D migration assay***

213

214 Both drugs (ZA and LA) decreased migration rate of DU-145 cells when compared to control  
215 conditions (Figure 2). At these conditions, leuprolide acetate was significantly more effective  
216 than ZA in inhibiting cell migration. The simultaneous presence of the two drugs influenced  
217 migration less than each single drug; association decreased the efficiency of leuprolide  
218 acetate alone and did not seem to differ from incubation with zoledronic acid alone.

219 Single drug pre-incubation did not potentiate the effect of simple incubation, in any case  
220 (Figure 2). The effects of any single drug were not significantly potentiated by any pre-  
221 incubation, even, in some cases, abolished (pre-incubation with ZA or LA and pre-incubation  
222 with ZA following by migration with ZA).

223 When cells were pre-incubated with the single drugs before migration test performed in  
224 control medium, migration was not inhibited at all. On the other hand, when cells were pre-  
225 incubated with both drugs, migration, even if occurring in RPMI, was inhibited as much as  
226 when cells were not pretreated but incubated with both drugs simultaneously. MSC-CM  
227 significantly increases the rate of migration towards control medium, and the addition of both  
228 drugs quenched the attractive effect of conditioned medium (Figure 2).

229

### 230 ***Drug interaction***

231 CDI results suggest an antagonistic effect in the incubation LA + ZA, slightly additive for  
232 Pre-incubation ZA + incubation LA and synergistic for Pre-incubation LA + incubation ZA  
233 as reported in Table II.

234

1  
2  
3 235 ***Cytokines content in MSC- CM***

4  
5 236 Cytokines were detected in MSC-CM as follows:

- 6  
7 237 • GM-CSF: 93.40 pg/ml  
8  
9 238 • MCP1/CCL2: 12.95 µg/ml  
10  
11 239 • IL-10: 1.81 pg/ml  
12  
13 240 • IFN $\gamma$ : 30.75 pg/ml  
14  
15 241 • TNF $\alpha$ : 40.34 pg/ml  
16  
17

18 242

19  
20 243 ***pAkt/Akt ratio after drugs incubation***

21 244

22  
23 245 Both drugs inhibit Akt phosphorylation compared to control (Figure 3) after 3 hours  
24  
25 246 incubation. This effect was completely lost after 6 hours of treatment.  
26  
27

28 247

29  
30 248

31  
32 249 ***Discussion***

33  
34  
35 250 In this work, we have demonstrated that ZA and LA inhibits, in vitro, the proliferation of  
36  
37 251 human prostate cancer cells: this is particularly true for ZA, whose cytotoxicity appears  
38  
39 252 already after 48- hours incubation and at lower concentrations than those necessary to  
40  
41 253 observe a LA-induced cytotoxic effect. Since patients often receive both drugs, we searched  
42  
43 254 for eventual interactions between the two drugs in vitro. Therefore, we incubated DU-145  
44  
45 255 cells with both drugs simultaneously (at variable concentrations of ZA). No synergistic effect  
46  
47 256 was induced by the simultaneous incubation with ZA and LA on cells.

48  
49  
50 257 Besides cytotoxicity, we wondered if ZA and LA could have other effects on prostate cancer  
51  
52 258 cells in vitro. Therefore, because of its relevance on metastasis phenomenon, we decided to  
53  
54  
55  
56  
57  
58  
59  
60



1  
2  
3 259 investigate migration by means of the transwell assay and the evaluation of Akt  
4  
5 260 phosphorylation level.

6  
7 261 Both ZA and LA provoke a significant decrease in Akt phosphorylation in 3 hours, but after  
8  
9 262 6-hours it returns to the control levels; this observation suggests that their inhibitory effect  
10  
11 263 occurs early, the timing being in agreement with that observed in inhibition of cell migration  
12  
13 264 (Figure 2). Furthermore, no synergistic effect is provoked by ZA and LA co-incubation  
14  
15 265 (Table II); even, LA effect seems to be significantly reduced by the presence of ZA. On the  
16  
17 266 other hand, pre-incubation with LA (but not with ZA) significantly potentiate inhibitory  
18  
19 267 migration properties of both LA and ZA in a synergistic manner. Nevertheless, the  
20  
21 268 simultaneous presence of the drugs has to induce some effect on cell migratory properties,  
22  
23 269 since when cells were pre-incubated with the single drugs their migration in culture medium  
24  
25 270 was not inhibited at all, while 18-hours pre-incubation with ZA and LA significantly  
26  
27 271 decreased their migration, even in RPMI. This may suggest that incubation with each drug  
28  
29 272 singularly can cause not relevant/reversible changes, which cells are able to repair, while  
30  
31 273 specific pre-incubation and/or specific drugs sequences (in particularly pre-incubation with  
32  
33 274 LA followed by incubation with ZA) could lead to hard reversible changes affecting cell  
34  
35 275 migration. We do not know, at present, how to explain this phenomenon, but a durable effect  
36  
37 276 of the simultaneous presence of ZA and LA is probably worth further investigations.

38  
39  
40  
41  
42 277 About the ability to migrate more towards MSC-CM, it has been shown that migration and  
43  
44 278 formation of metastases by prostate cancer cells in vivo is largely influenced by several  
45  
46 279 factors produced by bone cells [15-19]. We observed a massive migratory increase under  
47  
48 280 MSC-CM stimulus. It is interesting to note that both ZA and LA inhibit DU-145 3D-  
49  
50 281 migration at the same magnitude also when cells undergo MSC-CM stimuli (Figure 2).  
51  
52 282 According to the literature, we found that the MSC-CM contains several factors involved in  
53  
54 283 cancer cell survival and migration, such as  $TNF\alpha$ , MCP1/CCL2 [15, 16, 17] and GM-CSF

1  
2  
3 284 [20]. Aggressive cancer cell lines such as DU-145 and PC3 express a higher amount of  
4  
5 285 CCL2-specific receptor CCR2 compared with the less aggressive cancer cells such as LNCaP  
6  
7 286 or non-neoplastic PrEC and RWPE-1 cells [21]; a positive correlation has also been  
8  
9 287 established between CCR2 expression and prostate cancer progression [17]. Furthermore,  
10  
11 288 Rivas and coll. [20] shown that prostate cancer cells express functional high-affinity GM-  
12  
13 289 CSF receptors and therefore this hematopoietic growth factor may have an effect on prostate  
14  
15 290 carcinoma cells. The increased expression of GM-CSF receptors in prostatic hypertrophy and  
16  
17 291 neoplastic prostate epithelium suggests a relationship between prostatic epithelial cell growth  
18  
19 292 and GM-CSF [20]. At least, as shown by Gao and coll. [22], TNF $\alpha$  factor in endothelial cells  
20  
21 293 may increase the activation and ligation of  $\alpha v \beta 3$  integrins [22] to facilitate cell migration, and  
22  
23 294 regarding prostate cancer activation have a central role in prostate cancer metastatization  
24  
25 295 [23].

26  
27  
28 296 As previously reported in literature, most of these factors are affected by action of ZA and  
29  
30 297 LA [24-29]. In particular, a direct correlation between GM-CSF and MCP-1 decreased levels  
31  
32 298 and cell invasiveness has been demonstrated [24, 27]. On the basis of these observations, we  
33  
34 299 could speculate that, as demonstrated in other systems, it can be confirmed in our own that  
35  
36 300 the action of ZA and LA in decreasing migration could be both directed to the tumor cells  
37  
38 301 and indirectly on potential metastatic niche.  
39  
40

41 302

42 303

#### 43 304 **Conclusion**

44  
45  
46  
47  
48 305 Our results suggest that: (i) drugs in use in vivo for prostate cancer treatment have a direct  
49  
50 306 effect on prostate cancer cells proliferation, and this could contribute to justify the results  
51  
52 307 obtained in vivo; (ii) effect of drugs overlapping is difficult to predict a priori; we are unable,  
53  
54 308 with data at our disposal, to identify a regimen that clearly enhances the effect of the two  
55  
56  
57  
58  
59  
60

1  
2  
3 309 drugs. However, we have shown that specific co-incubation prolongs inhibitory effect on  
4  
5 310 prostate cancer cells migration; (iii) drugs affect migratory ability of prostate cancer cells,  
6  
7 311 and this could contribute to justify their limiting effect of in vivo metastases (mostly LA);  
8  
9 312 (iv) in the same way ZA and LA diminish the chemoattractive effect of the bone marrow  
10  
11 313 mesenchymal stem cells and, hence, the potential role that they can play in the phenomenon  
12  
13 314 of metastasis; (v) both ZA and LA are also able to decrease cell migration, and this probably  
14  
15 315 by acting on the PI3K/Akt pathway [30].  
16  
17  
18  
19 316  
20  
21 317  
22  
23  
24 318 **Acknowledgments**  
25  
26  
27 319 This study was supported by University of Turin (ex 60%). Authors thank Prof.ssa Biasi for  
28  
29 320 sharing her experience in cytochines quantification.  
30  
31  
32 321  
33  
34  
35 322  
36  
37  
38 323  
39  
40  
41 324  
42  
43  
44  
45 325  
46  
47  
48 326  
49  
50  
51 327  
52  
53  
54 328  
55  
56  
57  
58  
59  
60

329

330 **References**

331 1. Torre LA, Bray F, Siegel RL, Ferlay J, Lortet-Tieulent J, Jemal A. Global Cancer  
332 Statistics, 2012. *CA cancer J Clin.* 2015; 65:87–108.

333

334 2. Magnan S, Zarychanski R, Pilote L, Bernier L, Shemilt M, Vigneault E, Fradet V, Turgeon  
335 AF. Intermittent vs Continuous Androgen Deprivation Therapy for Prostate Cancer: A  
336 Systematic Review and Meta-analysis. *JAMA Oncol.* 2015; 1:1261-9.

337

338 3. Hyytinen ER, Thalmann GN, Zhau HE, Karhu R, Kallioniemi OP, Chung LW, Visakorpi  
339 T. Genetics changes associated with the acquisition of androgen-independent growth,  
340 tumorigenicity and metastatic potential in a prostate cancer model. *Cancer.* 1997; 75:190-195.

341

342 4. Costa L, Badia X, Chow E, Lipton A, Wardley A. Impact of skeletal complications on  
343 patients' quality of life, mobility, and functional independence. *Support Care Cancer.* 2008;  
344 16:879–889.

345

346 5. Broder MS, Gutierrez B, Cherepanov D, Linhares Y. Burden of skeletal-related events in  
347 prostate cancer: unmet need in pain improvement. *Support Care Cancer.* 2015; 23:237–247.

348

349 6. Weinfurt KP, Li Y, Castel LD, Saad F, Timbie JW, Glendenning GA, Schulman KA. The  
350 significance of skeletal-related events for the health-related quality of life of patients with  
351 metastatic prostate cancer. *Annals of Oncology.* 2005; 16: 579–584.

352

- 1  
2  
3 353 7. Green J and Clézardin, P. The molecular basis of bisphosphonates activity: a preclinical  
4  
5 354 prospective. *Semin Oncol.* 2010; 37:s3-s11.  
6  
7 355 8. Joseph J, Shiozawa Y, Jung Y, Kim JK, Pedersen E, Mishra A, et al. Disseminated  
8  
9 356 prostate cancer cells can instruct hematopoietic stem and progenitor cells to regulate bone  
10  
11 357 phenotype. *Mol Cancer Res.* 2012; 10: 282–292.  
12  
13 358  
14  
15 359 9. Mognetti B, La Montagna G, Perrelli MG, Pagliaro P, Penna C. Bone marrow  
16  
17 360 mesenchymal stem cells increase motility of prostate cancer cells via production of stromal  
18  
19 361 cell-derived factor-1 $\alpha$ . *J Cell Mol Med.* 2013; 17: 287-92.  
20  
21 362  
22  
23 363 10. Mognetti B, La Montagna G, Perrelli MG, Marino S, Pagliaro P, Cracco CM, Penna C.  
24  
25 364 Zoledronic Acid and Leuprorelin Acetate, Alone or in Combination, Similarly Reduce  
26  
27 365 Proliferation and Migration of Prostate Cancer Cells In Vitro. *International Journal of*  
28  
29 366 *Medical Biology.* 2014; 1:1–7.  
30  
31 367  
32  
33 368 11. Kim D, Kim S, Koh H, Yoon S, Chung A, Cho KS, Chung J. Akt/PKB promotes cancer  
34  
35 369 cell invasion via increased motility and metalloproteinase production. *FASEB J.* 2001;  
36  
37 370 15:1953-1962.  
38  
39 371  
40  
41 372 12. Mani J, Vallo S, Barth K, Makarevic J, Juengel E, Bartsch G, et al. Zoledronic acid  
42  
43 373 influences growth, migration and invasive activity of prostate cancer cells in vitro. *Prostate*  
44  
45 374 *Cancer Prostatic Dis.* 2012; 15: 250–255.  
46  
47 375  
48  
49 376 13. Montagnani Marelli M, Moretti RM, Mai S, Procacci P, Limonta P. Gonadotropin-  
50  
51 377 releasing hormone agonists reduce the migratory and the invasive behavior of androgen-  
52  
53  
54  
55  
56  
57  
58  
59  
60

1  
2  
3 378 independent prostate cancer cells by interfering with the activity of IGF-I. *Int J Oncol.* 2007;  
4  
5 379 30: 261–271.

6  
7 380 14. Mognetti B, Barberis A, Marino S, Di Carlo F, Lysenko V, Marty O, Geloën A.  
8  
9 381 Preferential Killing of Cancer Cells Using Silicon Carbide Quantum Dots. *Journal of*  
10  
11 382 *Nanoscience and Nanotechnology.* 2010; 10: 7971–7975.

12  
13 383

14  
15 384 15. Ashida N, Arai H, Yamasaki M, Kita T. Distinct signaling pathways for MCP-1-  
16  
17 385 dependent integrin activation and chemotaxis. *J Biol Chem.* 2001; 276:16555-16560

18  
19 386

20  
21 387 16. Lu Y, Cai Z, Galson DL. Monocyte chemotactic protein-1 (MCP-1) act as a paracrine and  
22  
23 388 autocrine factor for prostate cancer growth and invasion. *Prostate.* 2006; 66:1311-1318

24  
25 389

26  
27 390 17. Lu Y, Xiao G, Galson DL. PTHrP-induced MCP-1 production by human bone marrow  
28  
29 391 endothelial cells and osteoblasts promotes osteoclast differentiation and prostate cancer cell  
30  
31 392 proliferation and invasion in vitro. *Int J Cancer.* 2007; 121:724-733

32  
33 393

34  
35 394 18. Schiller KR, Zillhardt MR, Alley J, Borjesson DL, Beitz AJ, Mauro LJ. Secretion of  
36  
37 395 MCP-1 and other paracrine factors in a novel tumor-bone coculture model. *BMC Cancer.*  
38  
39 396 2009; 9:45.

40  
41 397

42  
43 398 19. Zhang J, Lu Y, Pienta KJ. Multiple roles of chemokine (C-C motif) ligand 2 in promoting  
44  
45 399 prostate cancer growth. *JNCI.* 2010; 102:522-528.

46  
47 400

- 1  
2  
3 401 20. Rivas CI, Vera JC, Delgado-López F, Heaney ML, Guaiquil VH, Zhang RH, et al.  
4  
5 402 Expression of granulocyte-macrophage colony-stimulating factor receptors in human prostate  
6  
7 403 cancer. *Blood*. 1998; 91:1037-43.  
8  
9 404  
10  
11 405 21. Lu Y, Cai Z, Xiao G. CCR2 expression correlates with prostate cancer progression. *J Cell*  
12  
13 406 *Biochem*. 2007; 101:676-685  
14  
15 407  
16  
17 408 22. Gao B, Saba TM, Tsan MF. Role of alpha(v)beta(3)-integrin in TNF-alpha-induced  
18  
19 409 endothelial cell migration. *Am J Physiol Cell Physiol*. 2002; 283:c1196-c1205.  
20  
21 410  
22  
23 411 23. Pécheur I, Peyruchaud O, Serre CM, Guglielmi J, Voland C, Bourre F, et al. Integrin  
24  
25 412 alpha(v)beta3 expression confers on tumor cells a greater propensity to metastasize to bone.  
26  
27 413 *FASEB J*. 2002; 16:1266-8.  
28  
29 414  
30  
31 415 24. Dai J, Lu Y, Yu C, Keller JM, Mizokami A, Zhang J, Keller ET.  
32  
33 416 Reversal of chemotherapy-induced leukopenia using granulocyte macrophage colony-  
34  
35 417 stimulating factor promotes bone metastasis that can be blocked with osteoclast inhibitors.  
36  
37 418 *Cancer Res*. 2010; 70:5014-23.  
38  
39 419  
40  
41 420 25. Tseng HC, Kanayama K, Kaur K, Park SH, Park S, Kozłowska A, et al. Bisphosphonate-  
42  
43 421 induced differential modulation of immune cell function in gingiva and bone marrow in vivo:  
44  
45 422 role in osteoclast-mediated NK cell activation. *Oncotarget*. 2015; 6:20002-25.  
46  
47  
48  
49  
50 423  
51  
52  
53  
54  
55  
56  
57  
58  
59  
60

1  
2  
3 424 26. Khan KN, Kitajima M, Hiraki K, Fujishita A, Sekine I, Ishimaru T, Masuzaki H. Changes  
4  
5 425 in tissue inflammation, angiogenesis and apoptosis in endometriosis, adenomyosis and  
6  
7 426 uterine myoma after GnRH agonist therapy. *Hum Reprod.* 2010; 25:642-53.

8  
9 427 DOI: <https://doi.org/10.1093/humrep/dep437>  
10

11 428

12  
13 429 27. Jia XH, Du Y, Mao D, Wang ZL, He ZQ, Qiu JD, et al. Zoledronic acid prevents the  
14  
15 430 tumor-promoting effects of mesenchymal stem cells via MCP-1 dependent recruitment of  
16  
17 431 macrophages. *Oncotarget.* 2015; 6:26018-28.

18  
19 432

20  
21 433 28. Guzmán-Soto I, Salinas E, Quintanar JL. Leuprolide Acetate Inhibits Spinal Cord  
22  
23 434 Inflammatory Response in Experimental Autoimmune Encephalomyelitis by Suppressing  
24  
25 435 NF- $\kappa$ B Activation. *Neuroimmunomodulation.* 2016; 23:33-40.

26  
27 436

28  
29 437 29. Kondo W, dal Lago EA, Noronha Ld, Olandoski M, Kotze PG, Amaral VF. Effect of  
30  
31 438 anti-TNF- $\alpha$  on peritoneal endometrial implants of rats. *Rev Col Bras Cir.* 2011;38:266-73.

32  
33 439

34  
35 440 30. Hong K, Kim J, Hong J, Yoon H, Lee J, Hong S, Hong S. Inhibition of Akt activity  
36  
37 441 induces the mesenchymal-to-epithelial reverting transition with restoring E-cadherin  
38  
39 442 expression in KB and KOSCC-25B oral squamous cell carcinoma cells. *J Exp Clin Canc Res.*

40  
41 443 2009; 28:28

42  
43 444

44  
45 445

46  
47 446

48  
49 447



448

449

450

451

452

**453 Figure legend**

454

455 **Figure 1.** Effect of zoledronic acid and leuprolide acetate on DU-145 growth.

456 (A) Proliferation assay after 24, 48 and 72 hours culture in presence of increasing  
457 concentration of zoledronic acid (2.5-50  $\mu\text{M}$ ). (B) Proliferation assay after 24, 48 and 72  
458 hours culture in presence of increasing concentration of leuprolide acetate (0.5-100  $\mu\text{M}$ ). (C)  
459 Effect of LA 100  $\mu\text{M}$  and ZA (0-40  $\mu\text{M}$ ), alone or in combination, on DU-145 cell after 48  
460 hours incubation.

461 \*= $P < 0.05$  vs control.

462

463 **Figure 2.** Three-dimensional migration.

464 Migration rate after incubation or pre-incubation with drugs and/or in conditioned media  
465 (CM) compared to control. Migration is expressed in arbitrary units.

466 \*= $P < 0.05$  vs control; \*\*\* =  $P < 0.001$  vs control; •= $P < 0.001$  vs ZA; #= $P < 0.001$  vs LA+ZA.

467

468 **Figure 3.** Western blotting

469 Drugs effect on pAkt/Akt in DU-145 cell line after 3 and 6 hours of incubation with LA 100  
470  $\mu\text{M}$  or ZA 20  $\mu\text{M}$ . Vinculin as internal control.

1  
2  
3 471  
4

5 472 **Table I.** Experimental conditions for migration assay. LA= leuprolide acetate 100  $\mu$ M;

6  
7 473 ZA= zoledronic acid 20  $\mu$ M; MSC-CM= Mesenchymal stem cells conditioned medium.  
8

9 474

10 475  
11

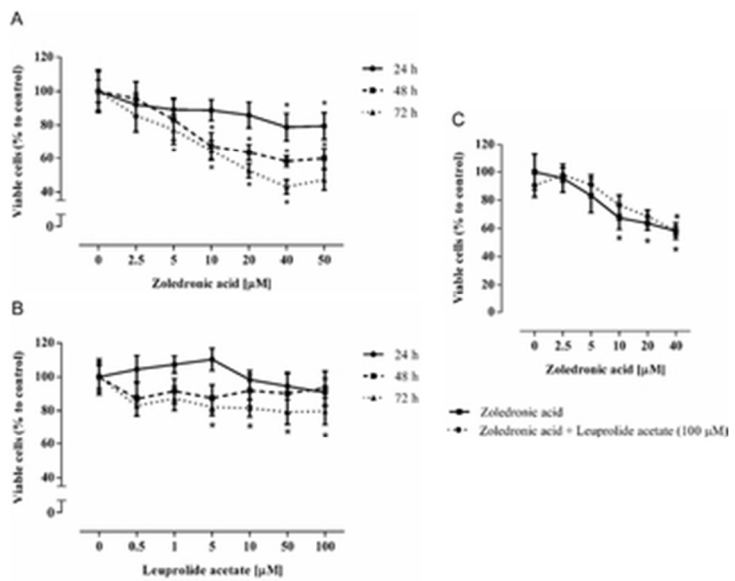
12  
13 476 **Table II.** Drug interactions.  $CDI < 1$  indicates a synergistic effect;  $CDI = 1$  indicates an

14  
15 477 additive effect;  $CDI > 1$  indicates an antagonistic effect.  
16

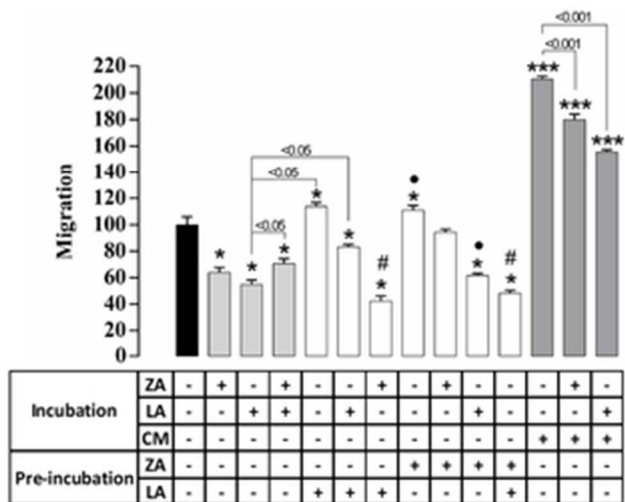
17 478  
18  
19  
20  
21  
22  
23  
24  
25  
26  
27  
28  
29  
30  
31  
32  
33  
34  
35  
36  
37  
38  
39  
40  
41  
42  
43  
44  
45  
46  
47  
48  
49  
50  
51  
52  
53  
54  
55  
56  
57  
58  
59  
60

For Peer Review

1  
2  
3  
4  
5  
6  
7  
8  
9  
10  
11  
12  
13  
14  
15  
16  
17  
18  
19  
20  
21  
22  
23  
24  
25  
26  
27  
28  
29  
30  
31  
32  
33  
34  
35  
36  
37  
38  
39  
40  
41  
42  
43  
44  
45  
46  
47  
48  
49  
50  
51  
52  
53  
54  
55  
56  
57  
58  
59  
60

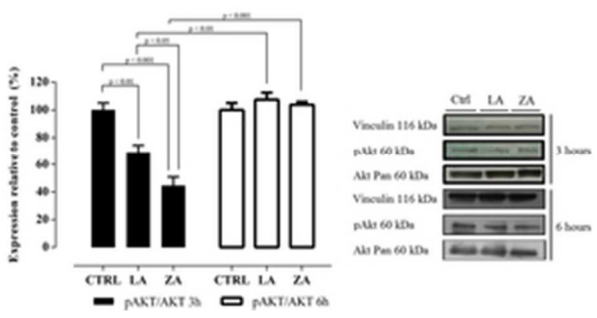


15x12mm (600 x 600 DPI)



13x10mm (600 x 600 DPI)

1  
2  
3  
4  
5  
6  
7  
8  
9  
10  
11  
12  
13  
14  
15  
16  
17  
18  
19  
20  
21  
22  
23  
24  
25  
26  
27  
28  
29  
30  
31  
32  
33  
34  
35  
36  
37  
38  
39  
40  
41  
42  
43  
44  
45  
46  
47  
48  
49  
50  
51  
52  
53  
54  
55  
56  
57  
58  
59  
60



12x6mm (600 x 600 DPI)

Or Peer Review

Pre-incubation 18 hours	Migration test 6 hours
none	RPMI
	ZA
	LA
LA	RPMI
	LA
	ZA
ZA	RPMI
	ZA
	LA
ZA + LA	RPMI
none	MSC-CM
	MSC-CM + ZA
	MSC-CM + LA

1  
2  
3  
4  
5  
6  
7  
8  
9  
10  
11  
12  
13  
14  
15  
16  
17  
18  
19  
20  
21  
22  
23  
24  
25  
26  
27  
28  
29  
30  
31  
32  
33  
34  
35  
36  
37  
38  
39  
40  
41  
42  
43  
44  
45  
46  
47  
48  
49  
50  
51  
52  
53  
54  
55  
56  
57  
58  
59  
60

<b>AB</b>	<b>A</b>	<b>B</b>	<b>CDI</b>
<i>Incubation LA + ZA</i>	Incubation ZA	Incubation LA	2,02
<i>Pre-incubation ZA + incubation LA</i>	Pre- incubation ZA	Incubation LA	1,02
<i>Pre-incubation LA + incubation ZA</i>	Pre-incubation LA	Incubation ZA	0,58

For Peer Review